



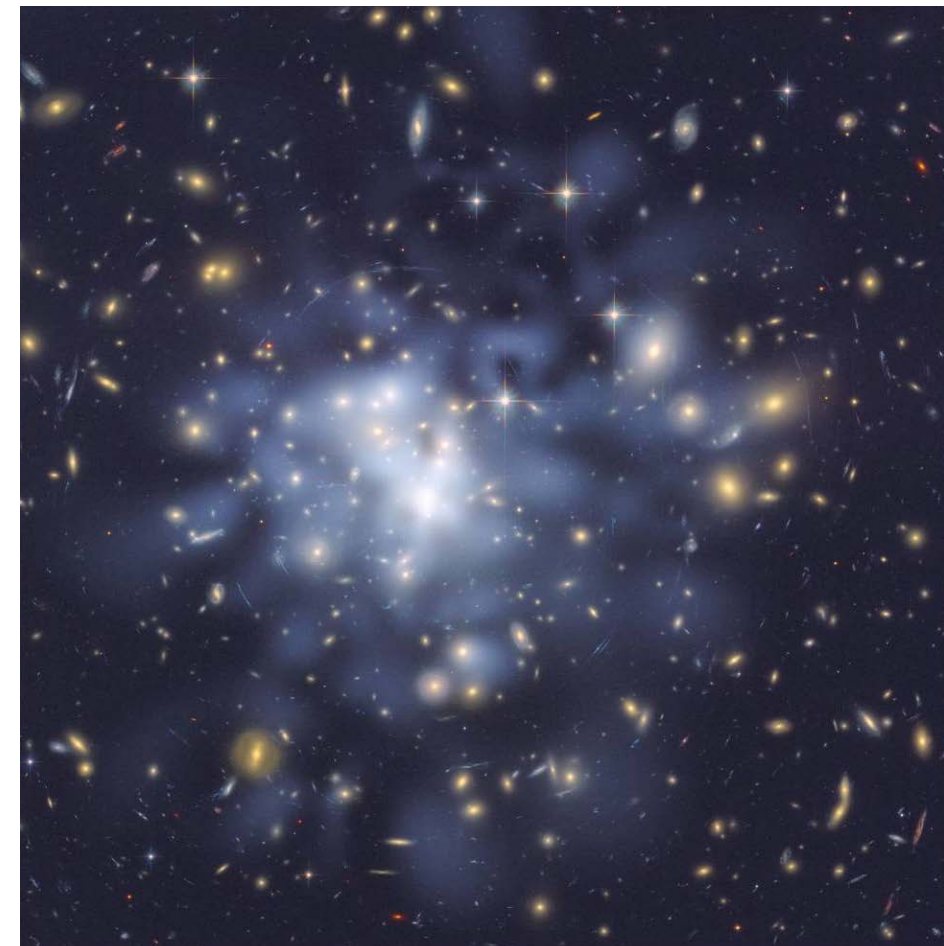
**Universität
Zürich**^{UZH}

Dark Matter Detection II: Experiments

August 16, 2016

PSI Summer School Exothiggs
Lyceum Alpinum, Zuoz

Laura Baudis, Universität Zürich



Content part II

- **Overview:** experimental techniques and the WIMP landscape
- **Liquid Noble Element Experiments**

Principles

The scintillation and ionisation process in noble liquids

Challenges for dark matter detectors

The double phase detector concept

Concrete examples

- **Cryogenic experiments at mK temperatures**

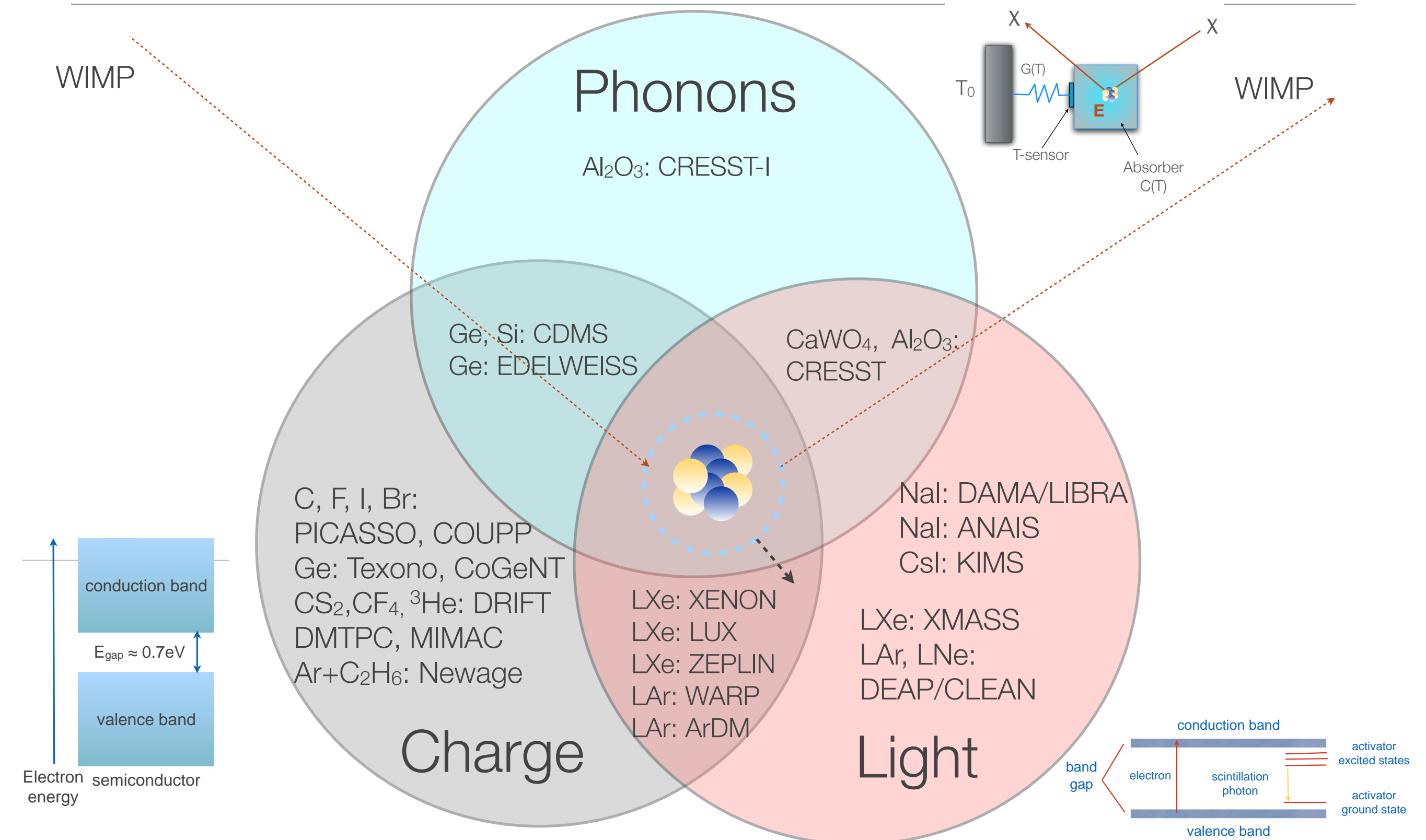
Principles of phonon mediated detectors

Detection of fast and thermalised phonons

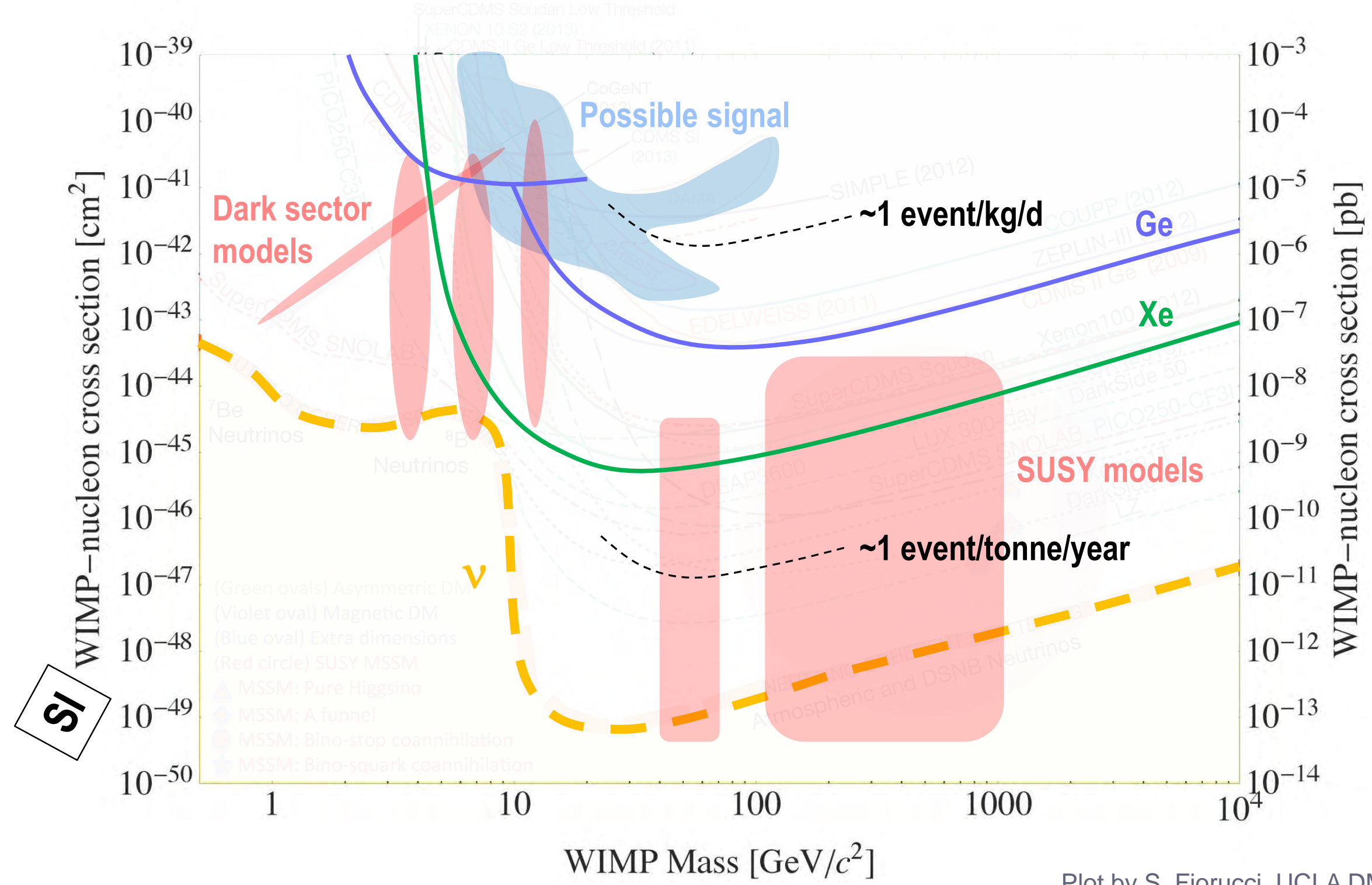
Temperature measurements: thermistors, SC transition sensors (SPT, TES)

Concrete examples: CDMS, EDELWEISS, CRESST

Direct Detection Techniques



The WIMP landscape



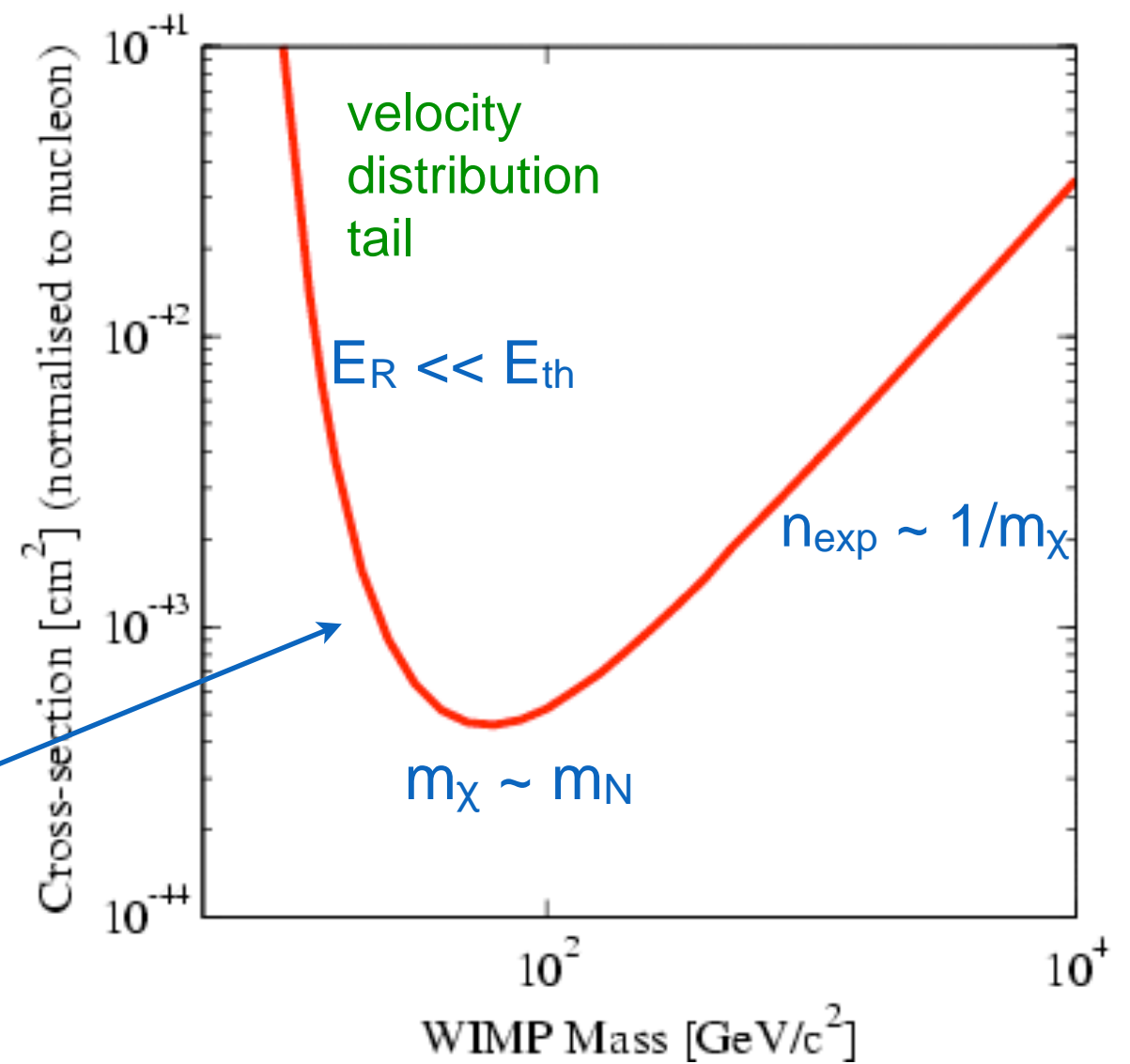
Vanilla Exclusion Plot

- Assume we have detector of mass M , taking data for a period of time t
- The total exposure will be $\epsilon = M \times t$ [kg days]; nuclear recoils are detected above an energy threshold E_{th} , up to a chosen energy E_{max} . The expected number of events n_{exp} will be:

$$n_{exp} = \epsilon \int_{E_{th}}^{E_{max}} \frac{dR}{dE_R} dE_R$$

⇒ cross sections for which $n_{exp} \geq 1$
can be probed by the experiment

- If ZERO events are observed, Poisson statistics implies that $n_{exp} \leq 2.3$ at 90% CL
=> exclusion plot in the cross section versus mass parameter space
(assuming known local density)

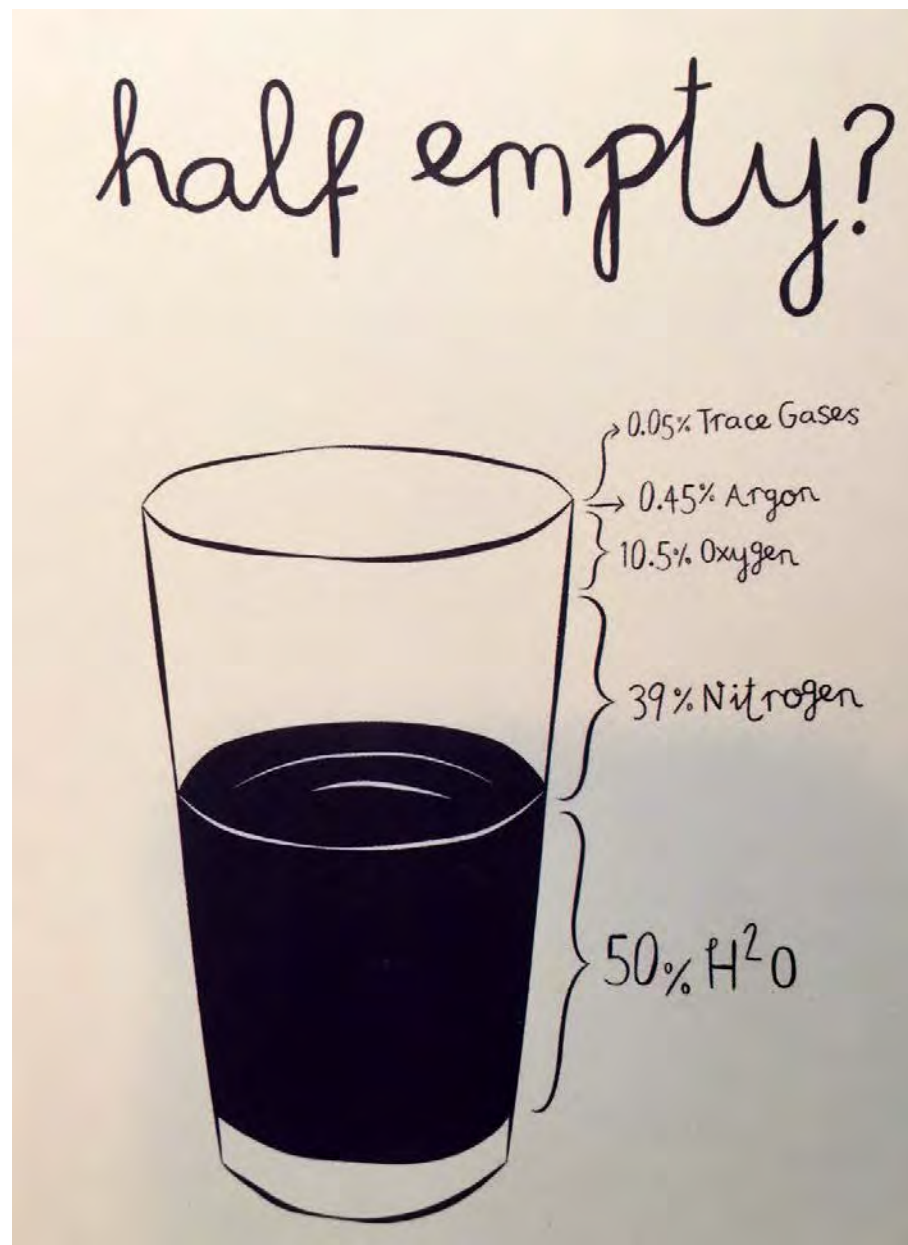


Liquefied noble gases

Noble gases

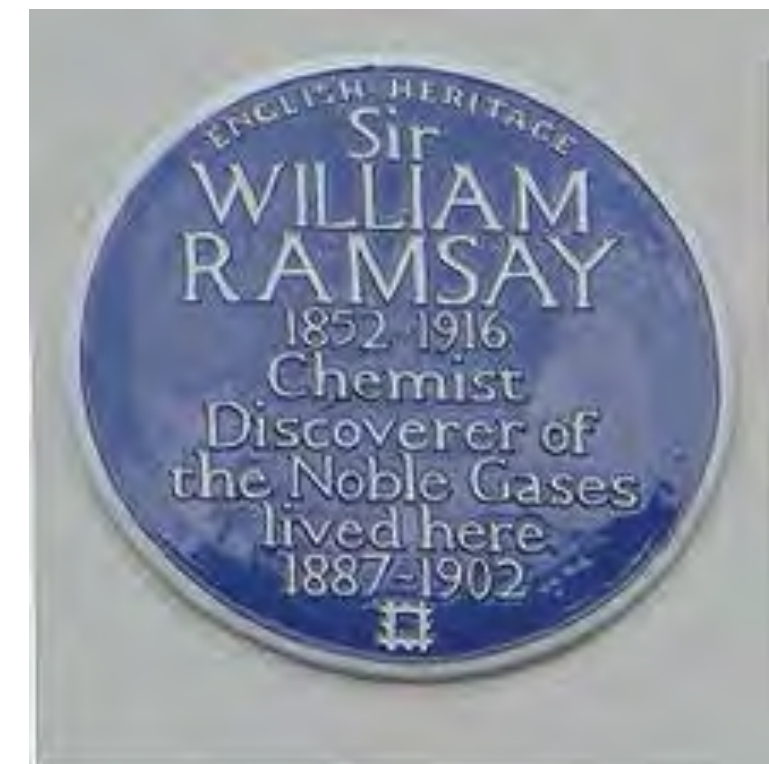
W. Ramsay: "These gases occur in the air but sparingly as a rule, for while argon forms nearly 1 hundredth of the volume of the air, neon occurs only as 1 to 2 hundred-thousandth, helium as 1 to 2 millionth, krypton as 1 millionth and xenon only as about 1 twenty-millionth part per volume.

- Xenon ("the strange one") and argon ("the inactive one")



Noble gases: discovered by William Ramsay, student of Bunsen and professor at UC London

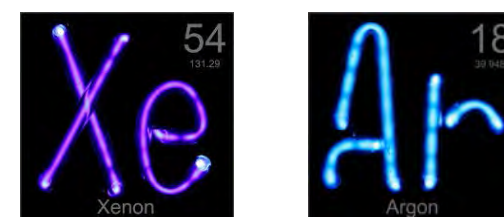
1904 Nobel Prize in Chemistry



Why noble gases for direct dark matter detection?

- Dense, homogeneous target with self-shielding; fiducialisation
- Large detector masses feasible at moderate costs
- High light (40 photons/keV) and charge ($W_{\text{LAr}} = 24 \text{ eV}$, $W_{\text{LXe}} = 15 \text{ eV}$) yields

Properties [unit]	Xe	Ar	Ne
Atomic number:	54	18	10
Mean relative atomic mass:	131.3	40.0	20.2
Boiling point T_b at 1 atm [K]	165.0	87.3	27.1
Melting point T_m at 1 atm [K]	161.4	83.8	24.6
Gas density at 1 atm & 298 K [g l^{-1}]	5.40	1.63	0.82
Gas density at 1 atm & T_b [g l^{-1}]	9.99	5.77	9.56
Liquid density at T_b [g cm^{-3}]	2.94	1.40	1.21
Dielectric constant of liquid	1.95	1.51	1.53
Volume fraction in Earth's atmosphere [ppm]	0.09	9340	18.2



Ionization in noble liquids

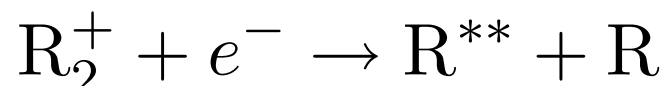
- The energy loss of an incident particle in noble liquids is shared between excitation, ionization and sub-excitation electrons liberated in the ionization process
- The average energy loss in ionization is slightly larger than the ionization potential or the gap energy, because it includes multiple ionization processes
- as a result, the ratio of the W-value (= average energy required to produce an electron-ion pair) to the ionization potential or gap energy = 1.6 - 1.7

Material	Ar	Kr	Xe
Gas			
Ionization potential I (eV)	15.75	14.00	12.13
W values (eV)	26.4 ^a	24.2 ^a	22.0 ^a
Liquid			
Gap energy (eV)	14.3	11.7	9.28
W value (eV)	23.6 ± 0.3^b	18.4 ± 0.3^c	15.6 ± 0.3^d

- the W-value in the liquid phase is smaller than in the gaseous phase
 - the W-value in xenon is smaller than the one in liquid argon, and krypton (and neon)
- => the ionization yield is highest in liquid xenon (of all noble liquids)

The Scintillation Process in Noble Liquids

- Scintillation in noble liquids arises in two distinct processes: excited atoms R^* (excitons) and ions R^+ , both produced by ionizing radiation:



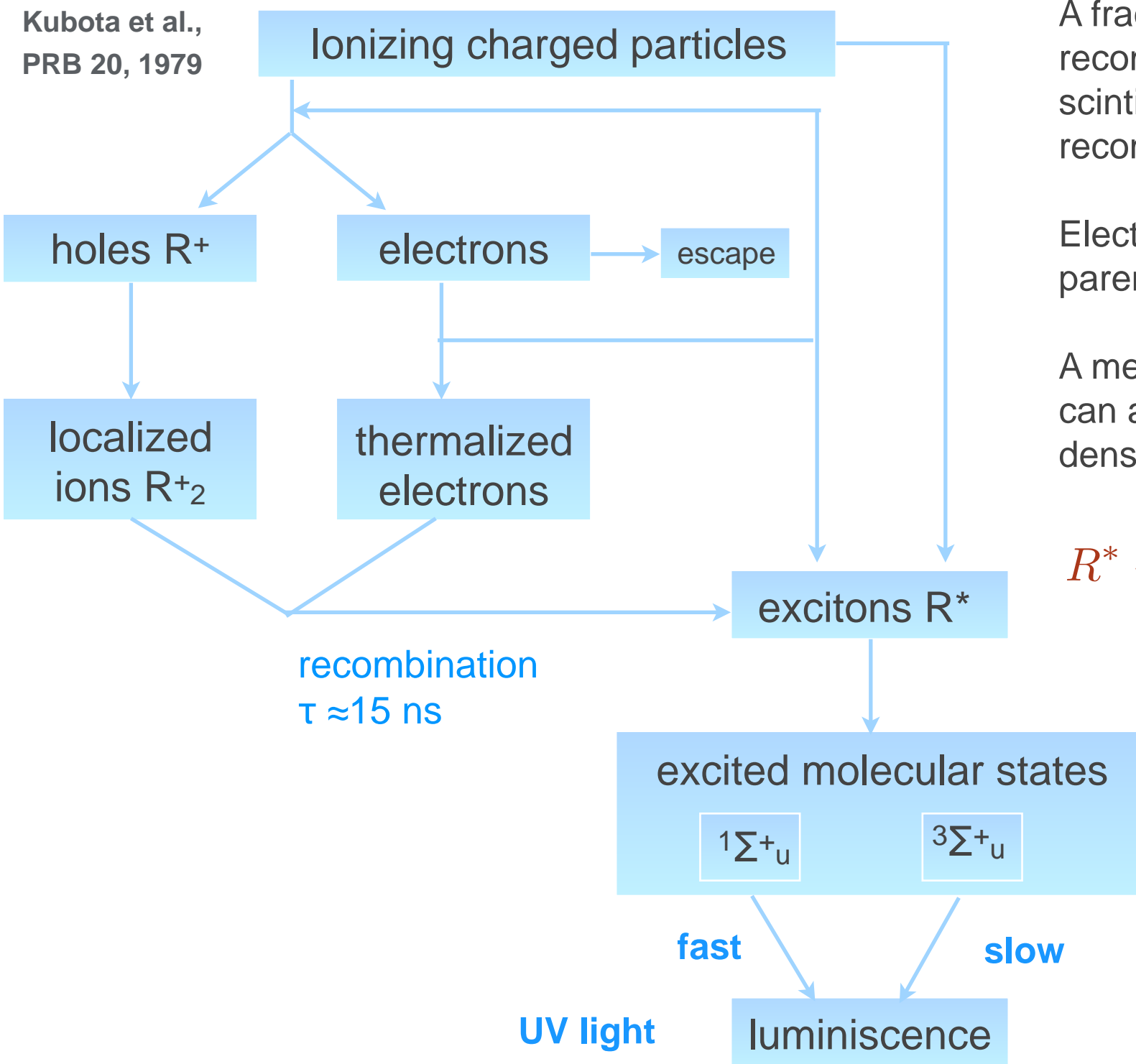
Excitons (R^*) will rapidly form excited dimers (R_2^*) with neighboring atoms

The excited dimer R_2^* , at its lowest excited level, is de-excited to the dissociative ground state by the *emission of a single UV photon*

This comes from the large energy gap between the lowest excitation and the ground level, forbidding other decay channels such as non-radiative transitions

$h\nu = \text{UV photon emitted in the process}$

The Scintillation Process in Noble Liquids



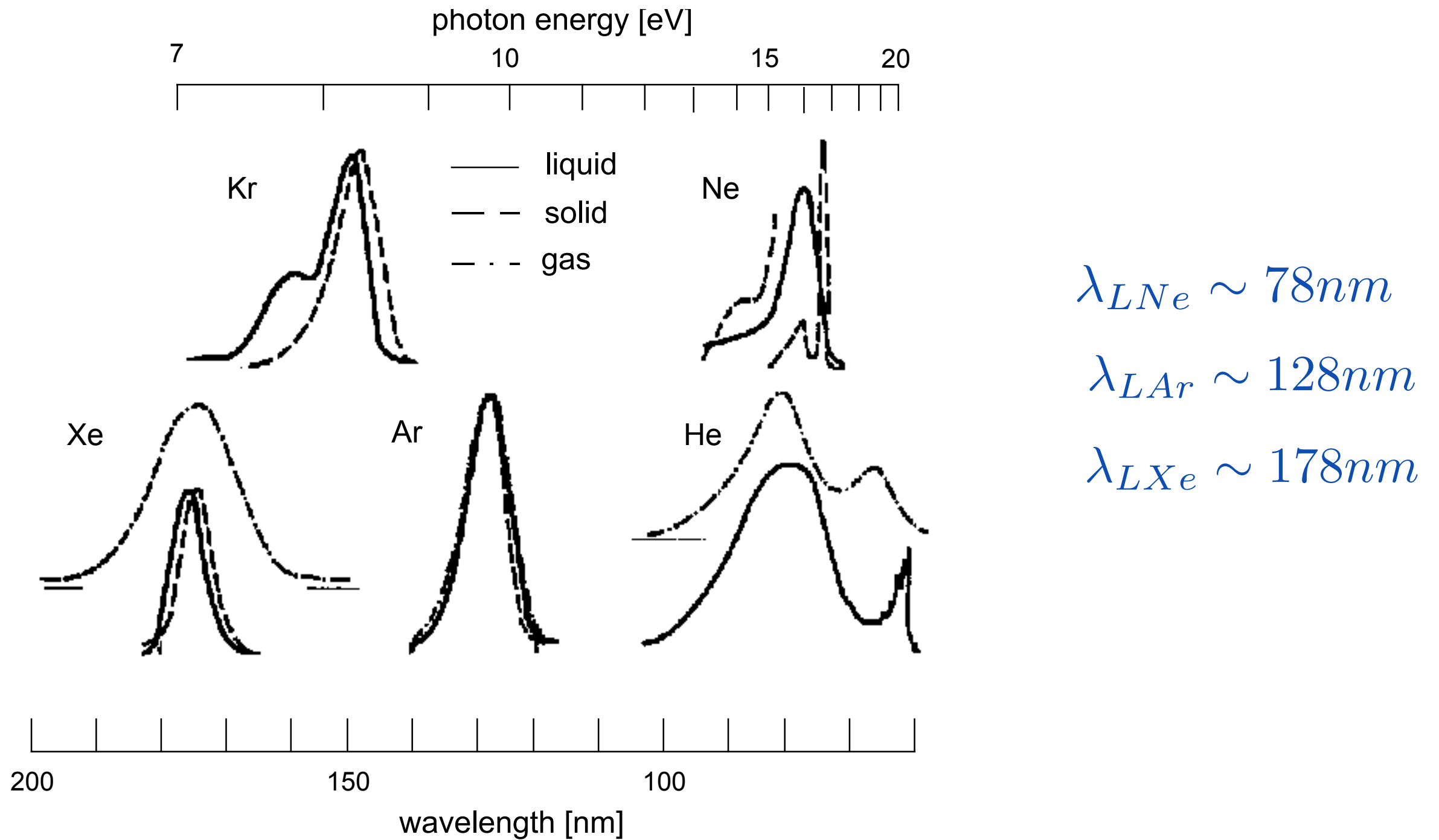
A fraction of the ionization electrons will recombine with ions and produce a scintillation photon in the process called recombination

Electrons that thermalize far from their parent ion may escape recombination

A mechanism called “bi-excitonic quenching” can also reduce the scintillation yield in very dense tracks:



The Energy of the UV Photons

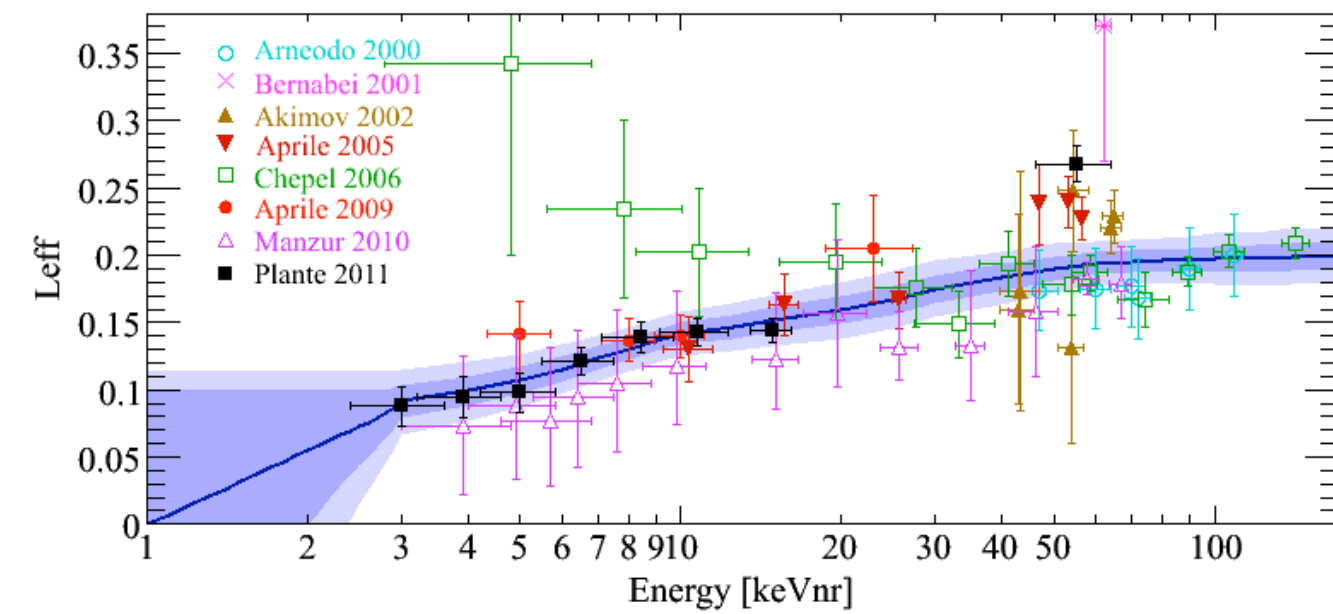


Light yield in noble liquids (nuclear recoils): xenon

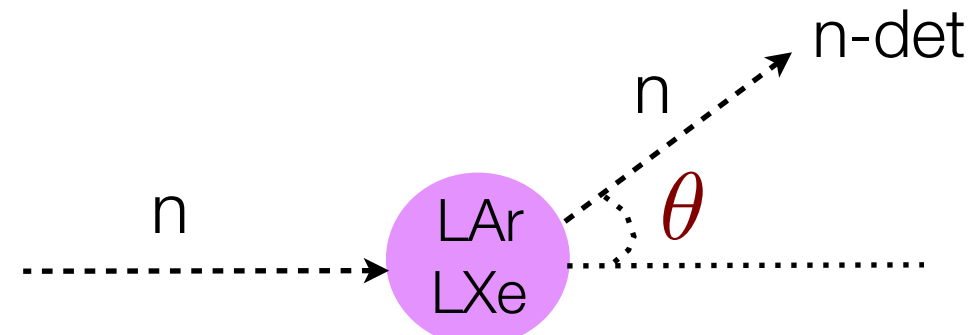
- Two methods:
 - direct: mono-energetic neutrons scatters which are tagged with a n-detector
 - indirect: measure energy spectra from n-sources, compare with MC predictions

$$\mathcal{L}_{\text{eff}}(E_{\text{nr}}) = \frac{L_{y,er}(E_{\text{nr}})}{L_{y,er}(E_{\text{ee}} = 122 \text{ keV})}$$

Plante *et al.*, Phys. Rev. C **84**, 045805, 2011



mean (solid) and 1-, 2-sigma uncertainties (blue bands)

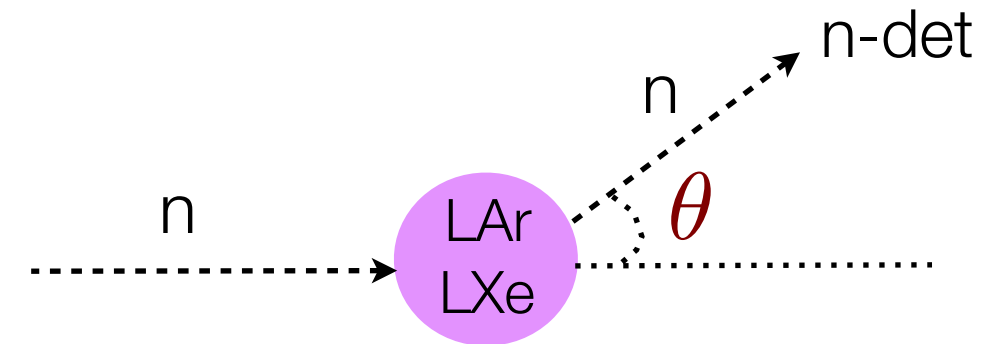
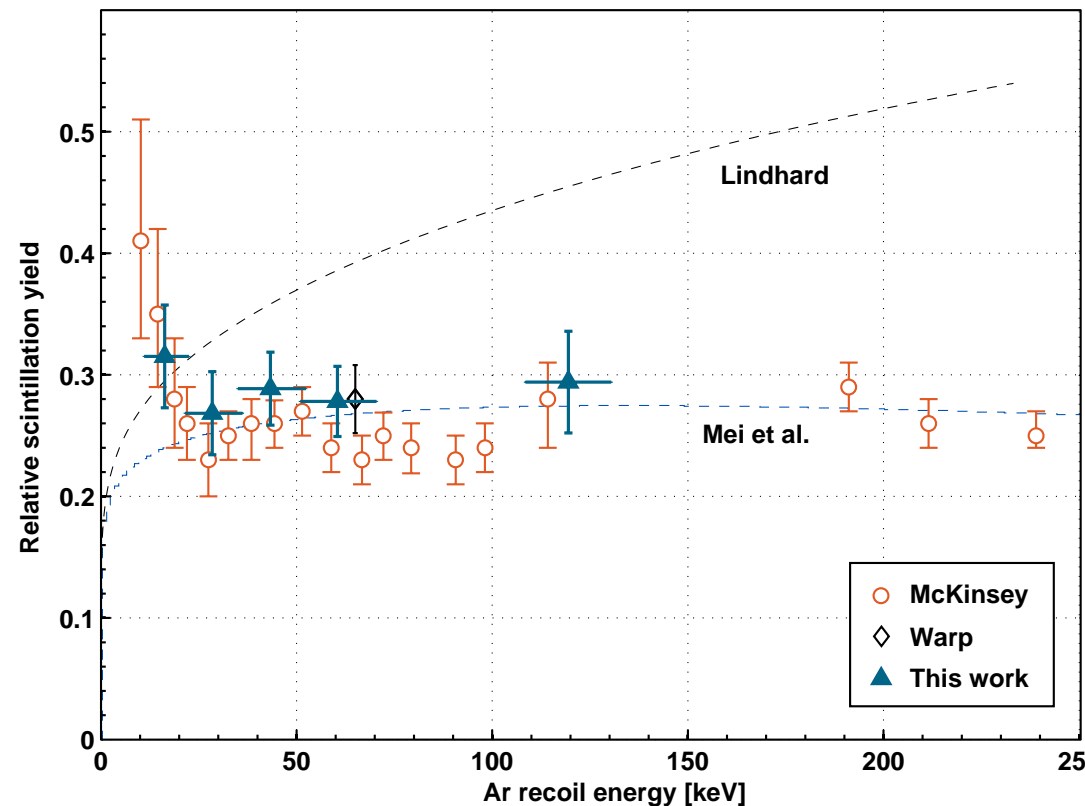


Light yield in noble liquids (nuclear recoils): argon

- Two methods:
 - direct: mono-energetic neutrons scatters which are tagged with a n-detector
 - indirect: measure energy spectra from n-sources, compare with MC predictions

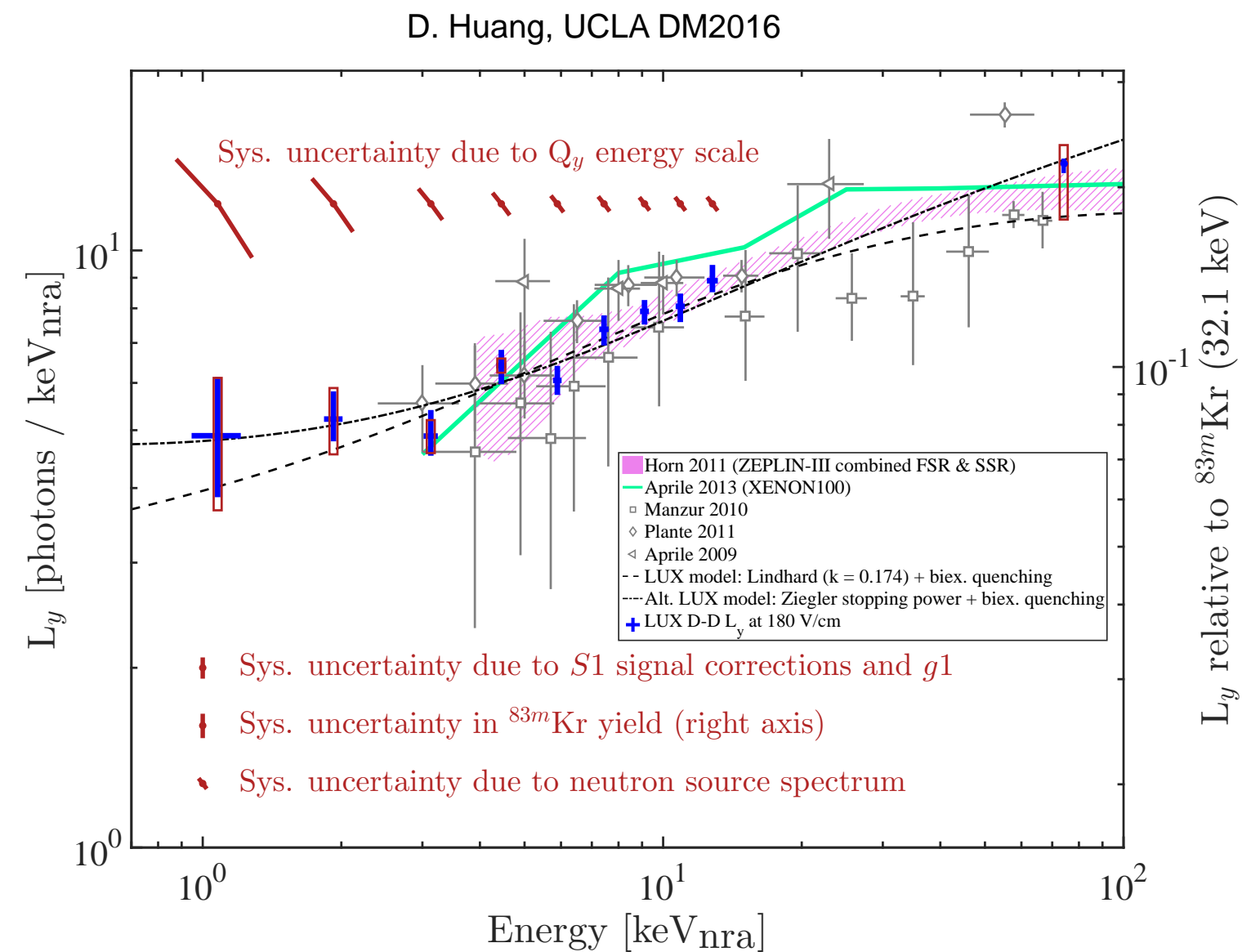
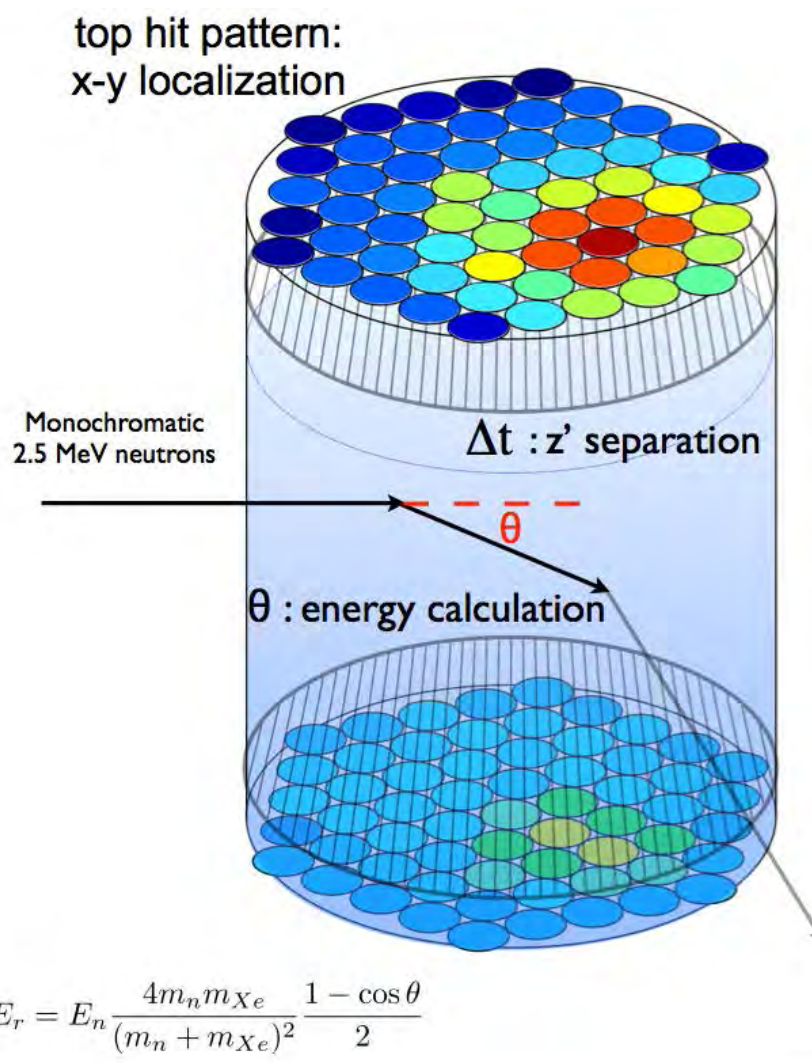
$$\mathcal{L}_{\text{eff}}(E_{\text{nr}}) = \frac{L_{y,er}(E_{\text{nr}})}{L_{y,er}(E_{\text{ee}} = 122 \text{ keV})}$$

D. Gastler *et al.*, Phys. Rev. C **85**, 065811, 2012



Light yield: new data from LUX

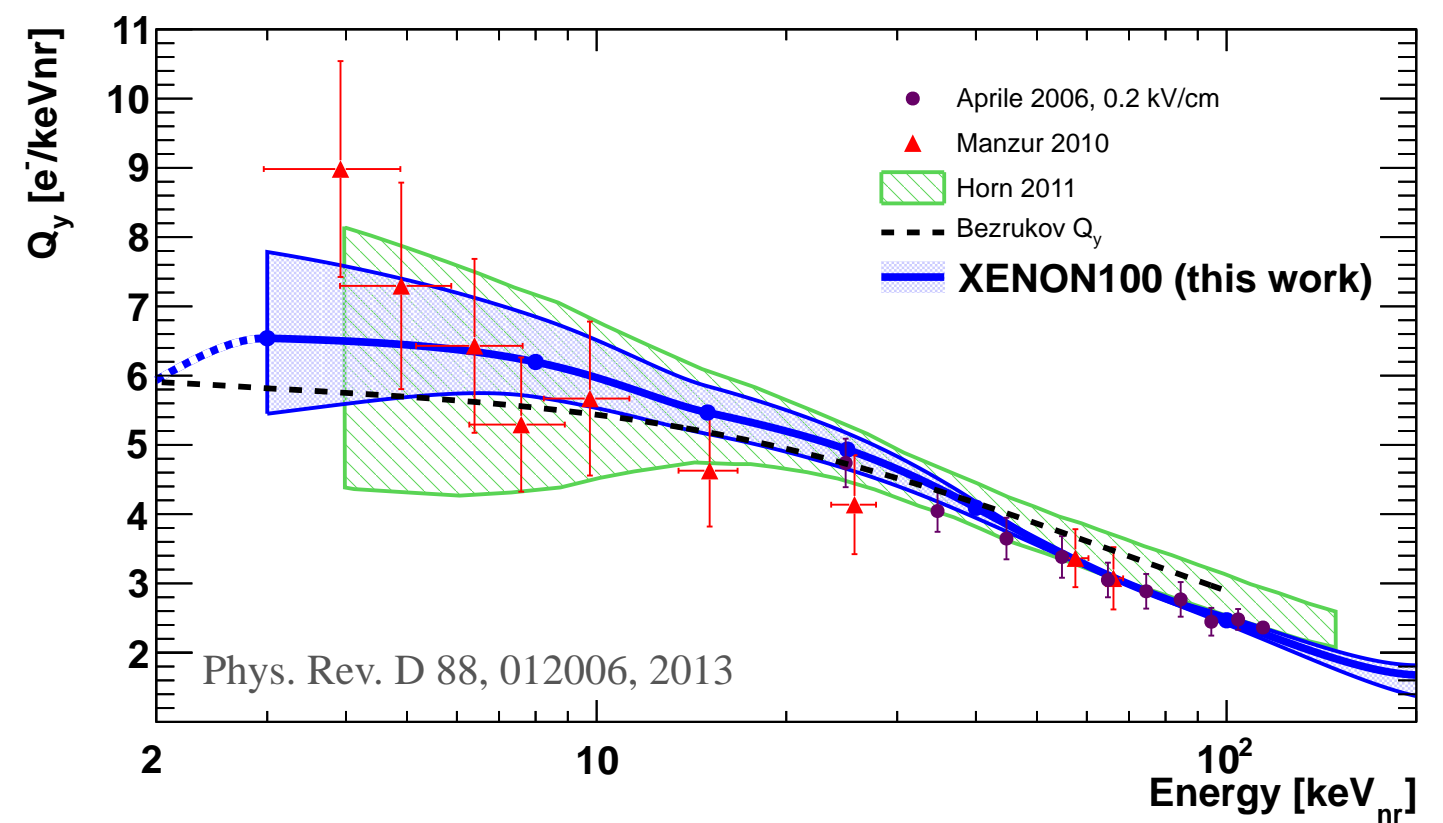
- Use data acquired *in situ* with monochromatic 2.5 MeV neutrons (D-D generator)
- Calculate energy (via angle θ) from x-y position and Δt (z separation)
- **Light yield measured down to 1 keV**



Charge yield in noble liquids (nuclear recoils): xenon

- Nuclear recoils: denser tracks, hence *larger electron-ion recombination than electronic recoils*
 - the collection of ionisation electrons becomes more difficult for nuclear than electronic recoils
- Ionisation yield of nuclear recoils: number of observed electrons per unit recoil energy

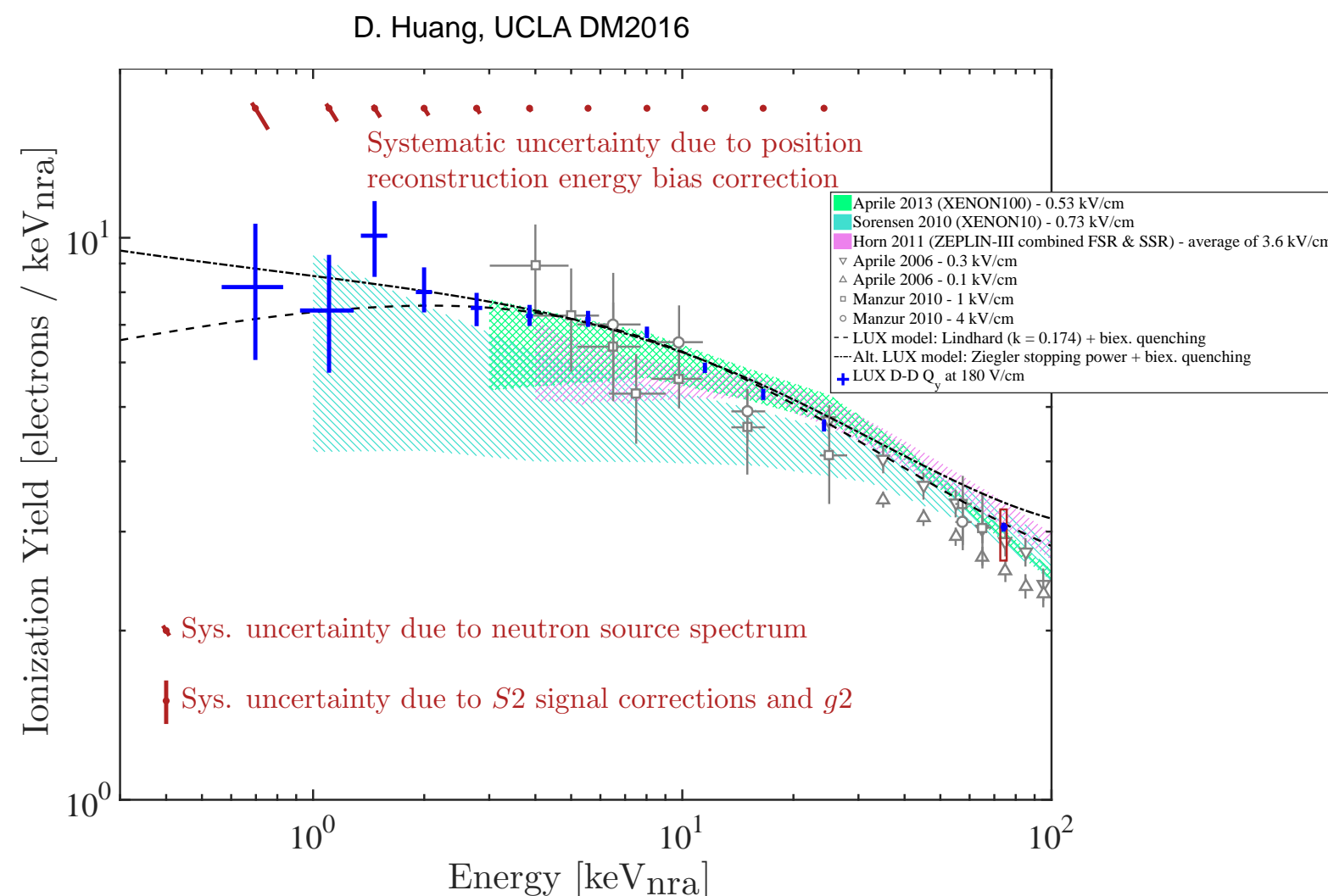
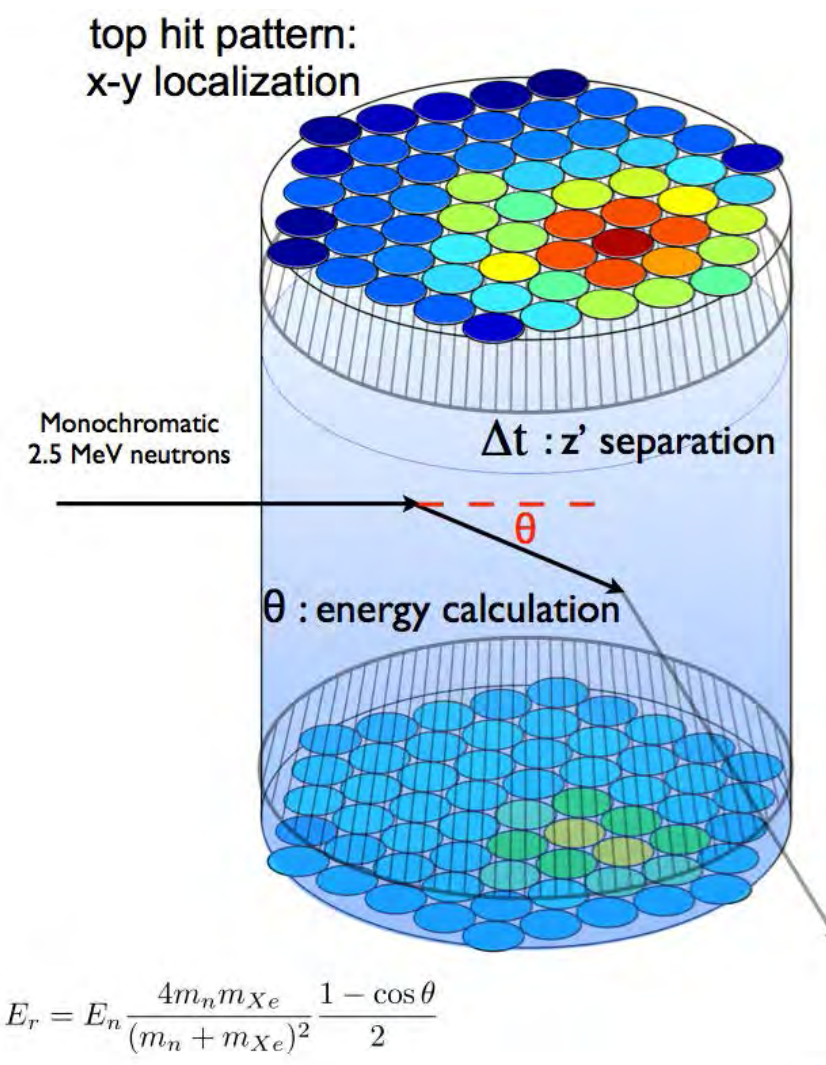
$$Q_{y,nr} = \frac{n_{e,nr}}{E_{nr}}$$



blue: indirect measurement, by data/MC
comparison of AmBe neutron calibration data

Charge yield: new data from LUX

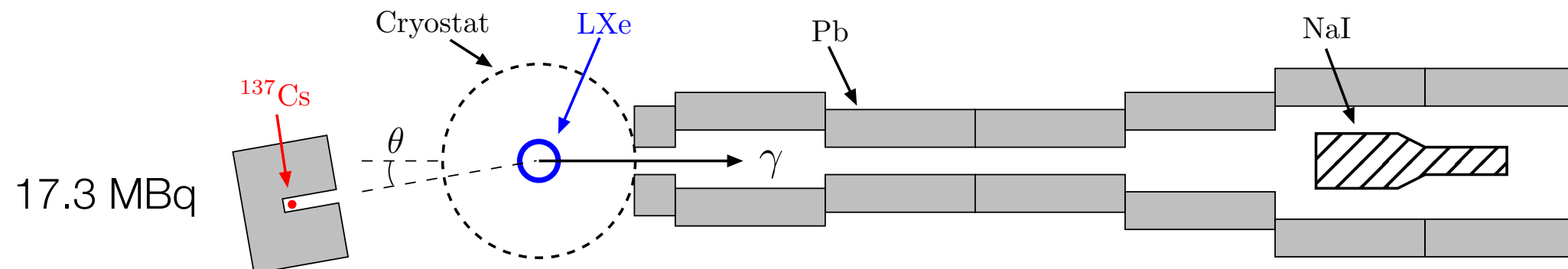
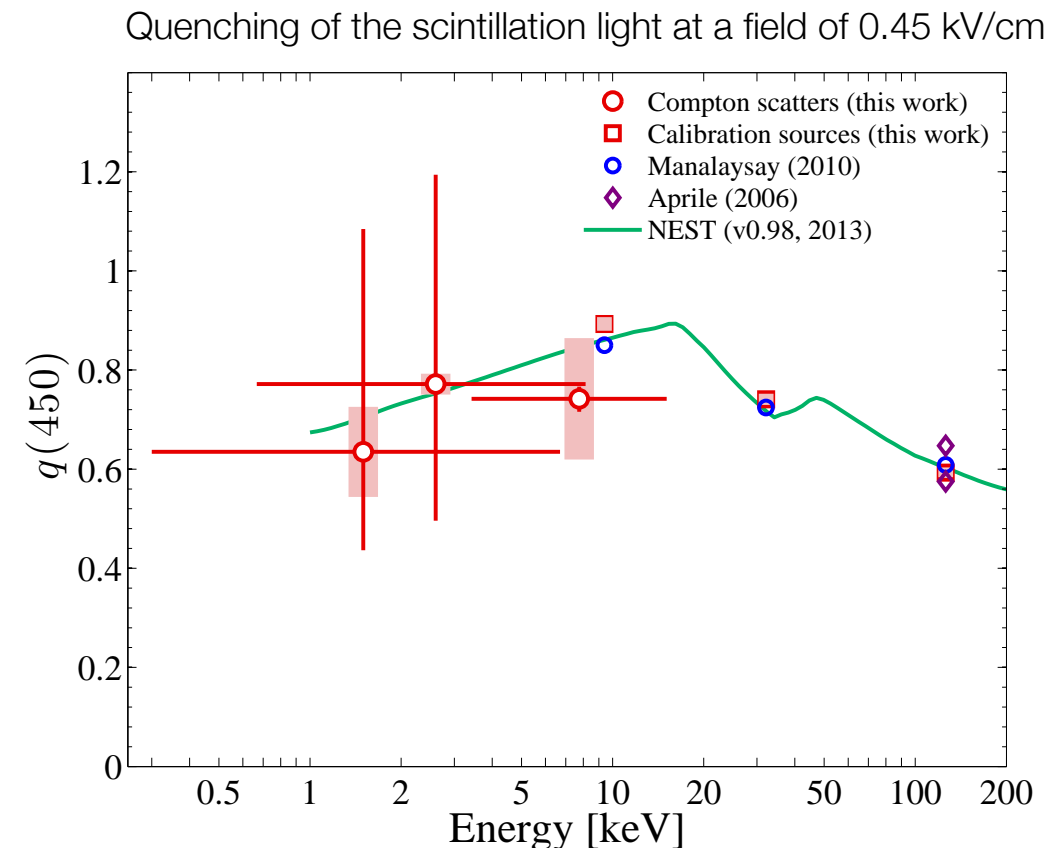
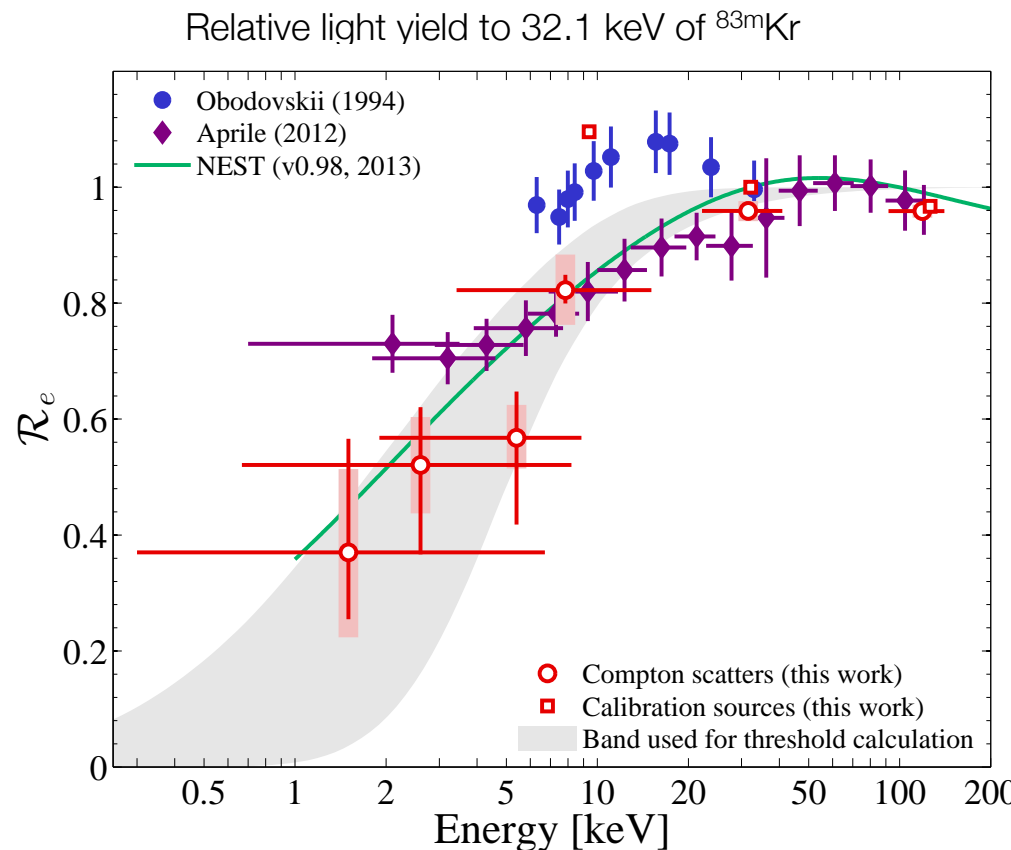
- Use data acquired *in situ* with monochromatic 2.5 MeV neutrons (D-D generator)
- Calculate energy (via angle) from x-y position and Δt (z separation)
- **Charge yield measured down to 0.7 keV**



Light yield in noble liquids (electronic recoils)

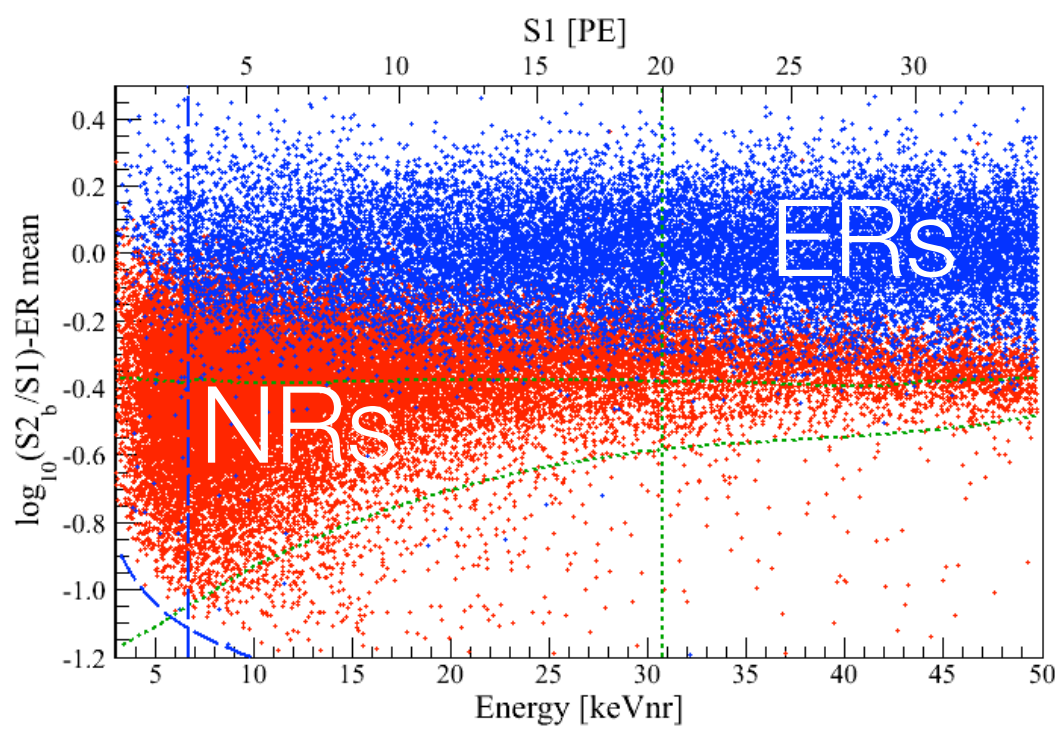
- Light yield decreases with lower deposited energies in the LXe
- Field quenching is $\sim 75\%$, only weak field-dependance

LB et al., PRD 87, 2013; arXiv:1303.6891

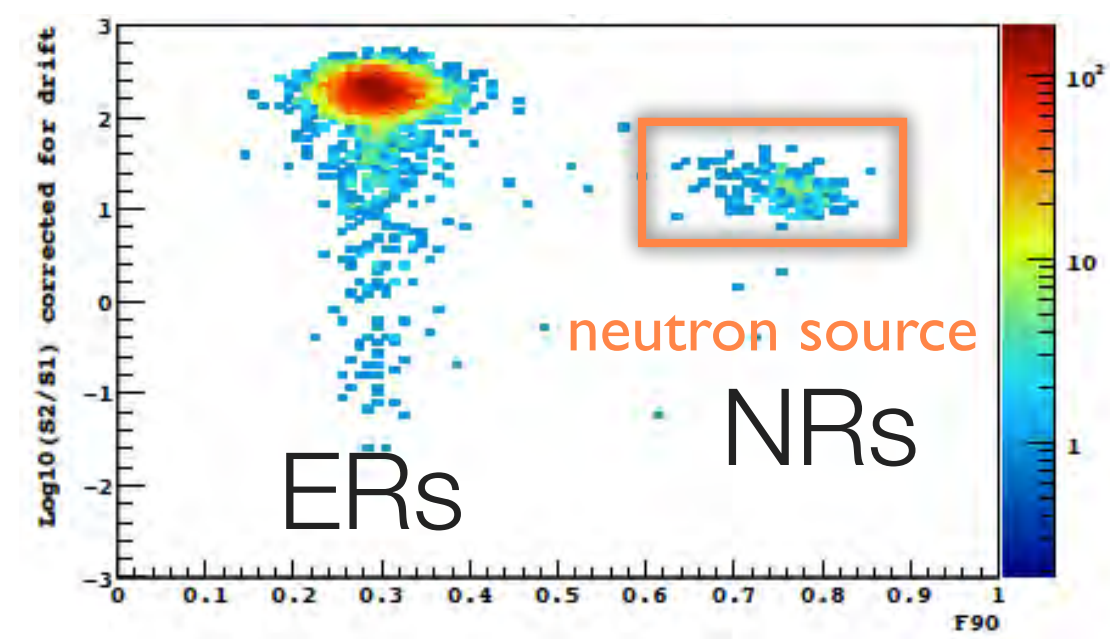


Particle discrimination

- Pulse shape of prompt scintillation signal (LAr)
 - the ratio of light from singlet and triplet depends on dE/dx ($\sim 10:1$ for NRs:ERs)
- Charge versus light (LAr and LXe)
 - the recombination probability, and thus the S2-to-S1 ratio depends on dE/dx



LXe (XENON100)

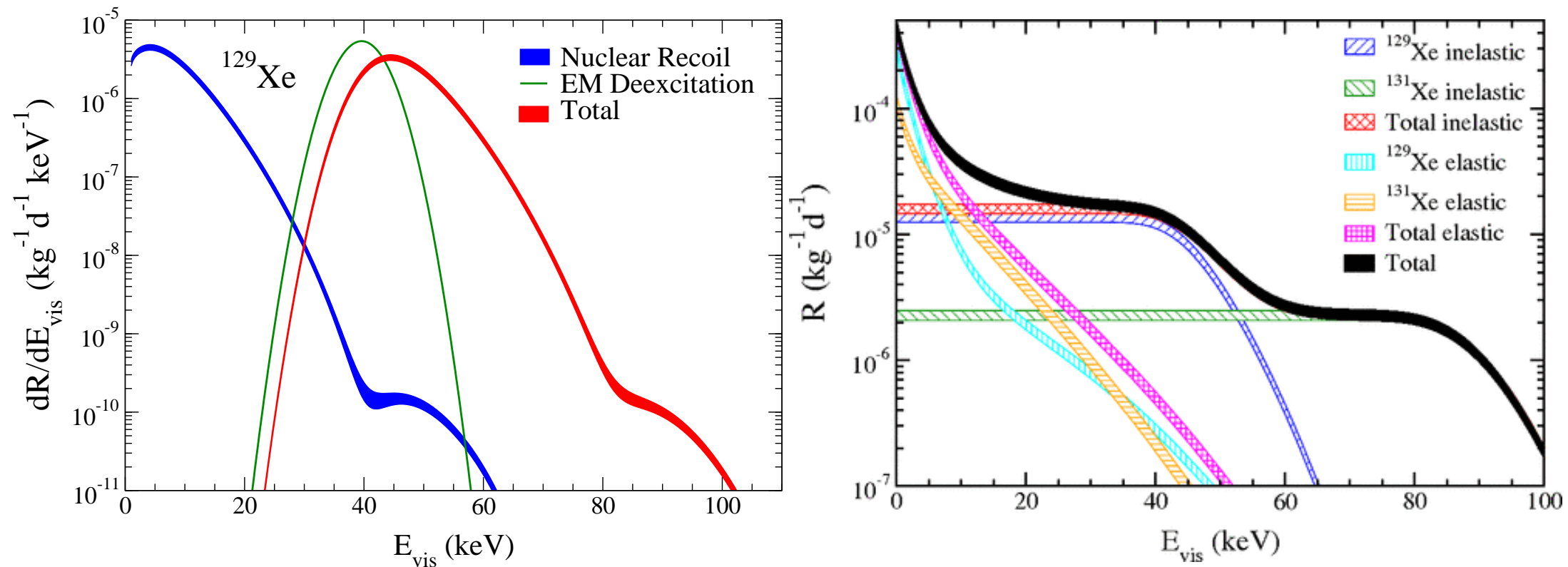


LAr (DarkSide-10)

Xenon: an additional WIMP channel

- Spin-dependent WIMP-nucleus *inelastic scattering*
 - shifts ROI to higher energies
 - integrated rate dominates at moderate energies, depending on the WIMP mass
 - probes the high-tail of the galactic WIMP velocity distribution

LB, G. Kessler, P. Klos, R. Lang, J. Menendez, S. Reichard, A. Schwenk, PRD 88 (2013)

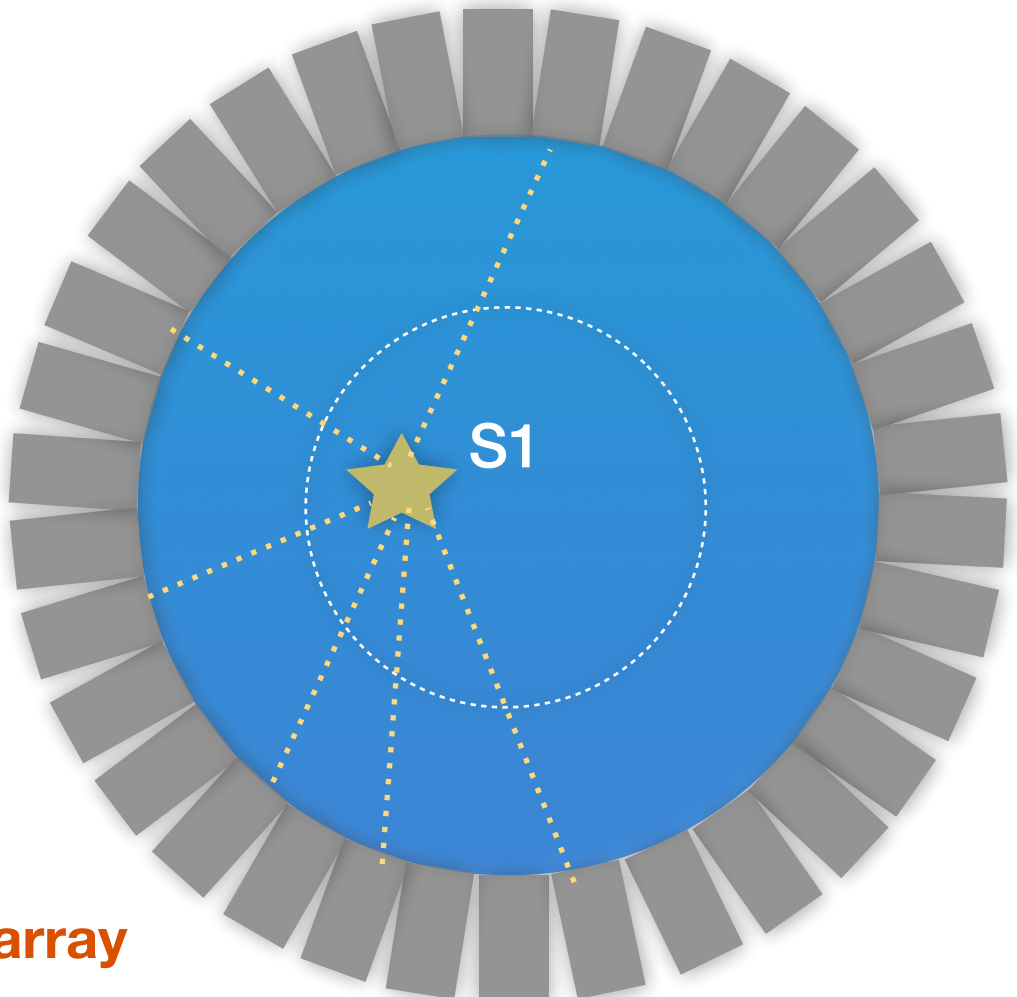


1 ns, 0.5 ns

40 keV, 80 keV

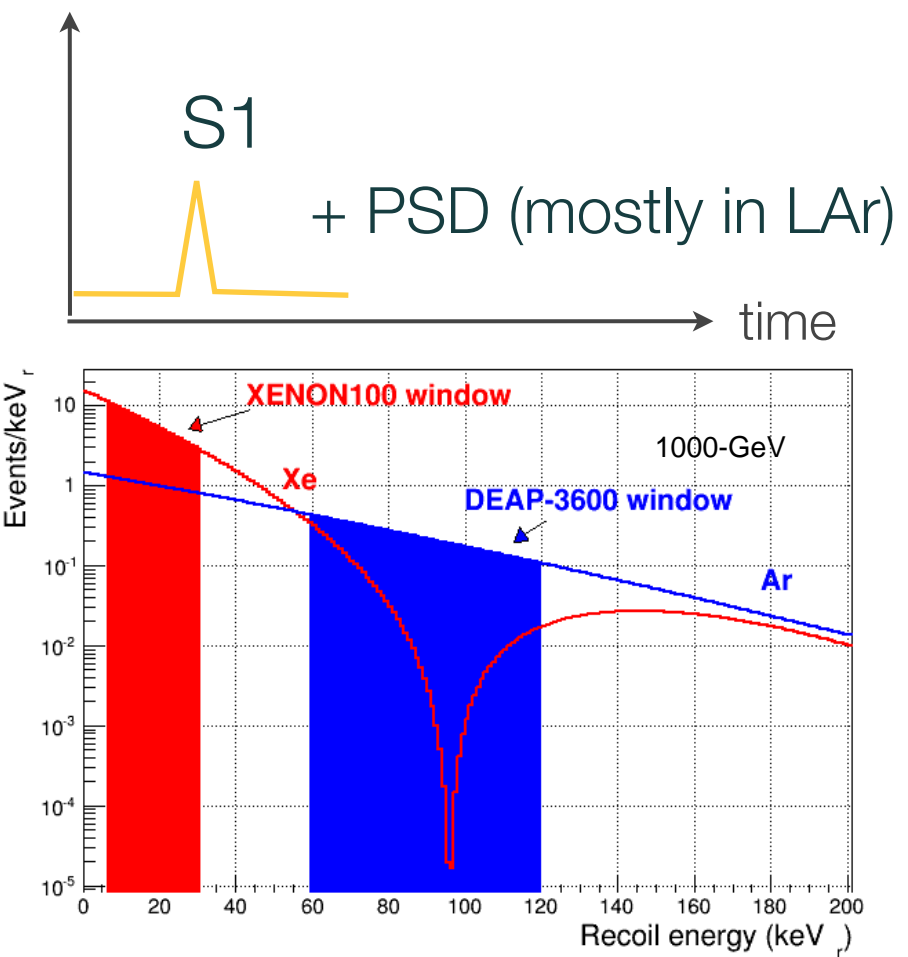
Single-phase noble liquid detectors

Instrumented LAr or LXe volume

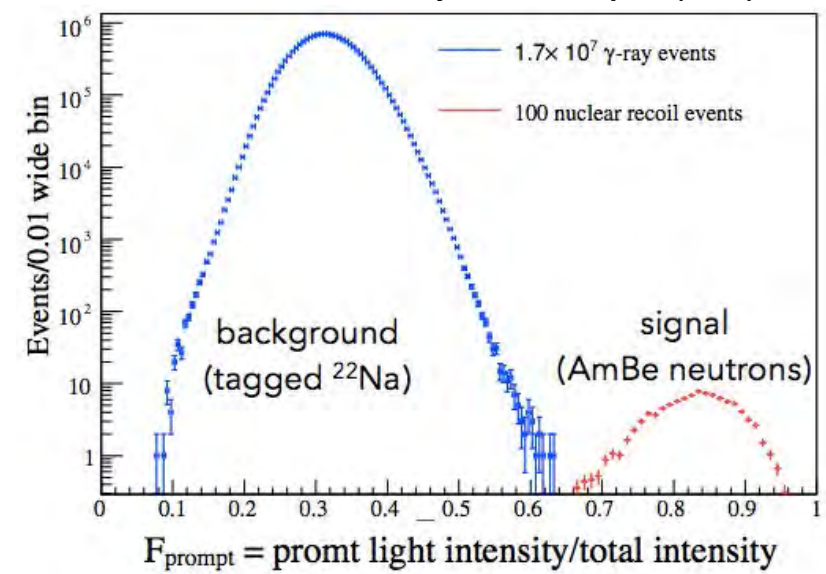


PMT array

position resolution: ~cm



M. Kuzniak et al., Nuc Phys B Proc Sup 00 (2014) 1–7



Single-phase detectors

- Challenge: ultra-low absolute backgrounds
- LAr: pulse shape discrimination, factor $10^9\text{-}10^{10}$ for gammas/betas



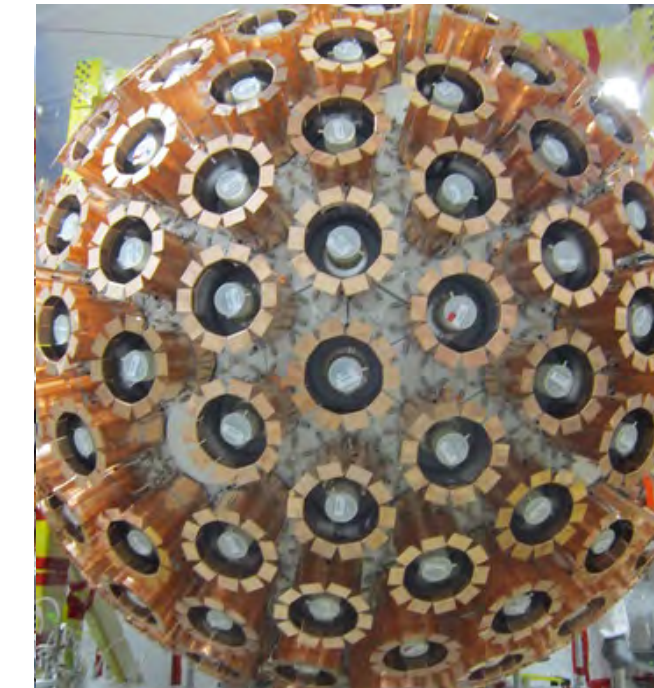
XMASS at Kamioka:

835 kg LXe (100 kg fiducial),
single-phase, 642 PMTs
new run since fall 2013
several results



CLEAN at SNOLab:

500 kg LAr (150 kg fiducial)
single-phase open volume
under commissioning
to run in 2016

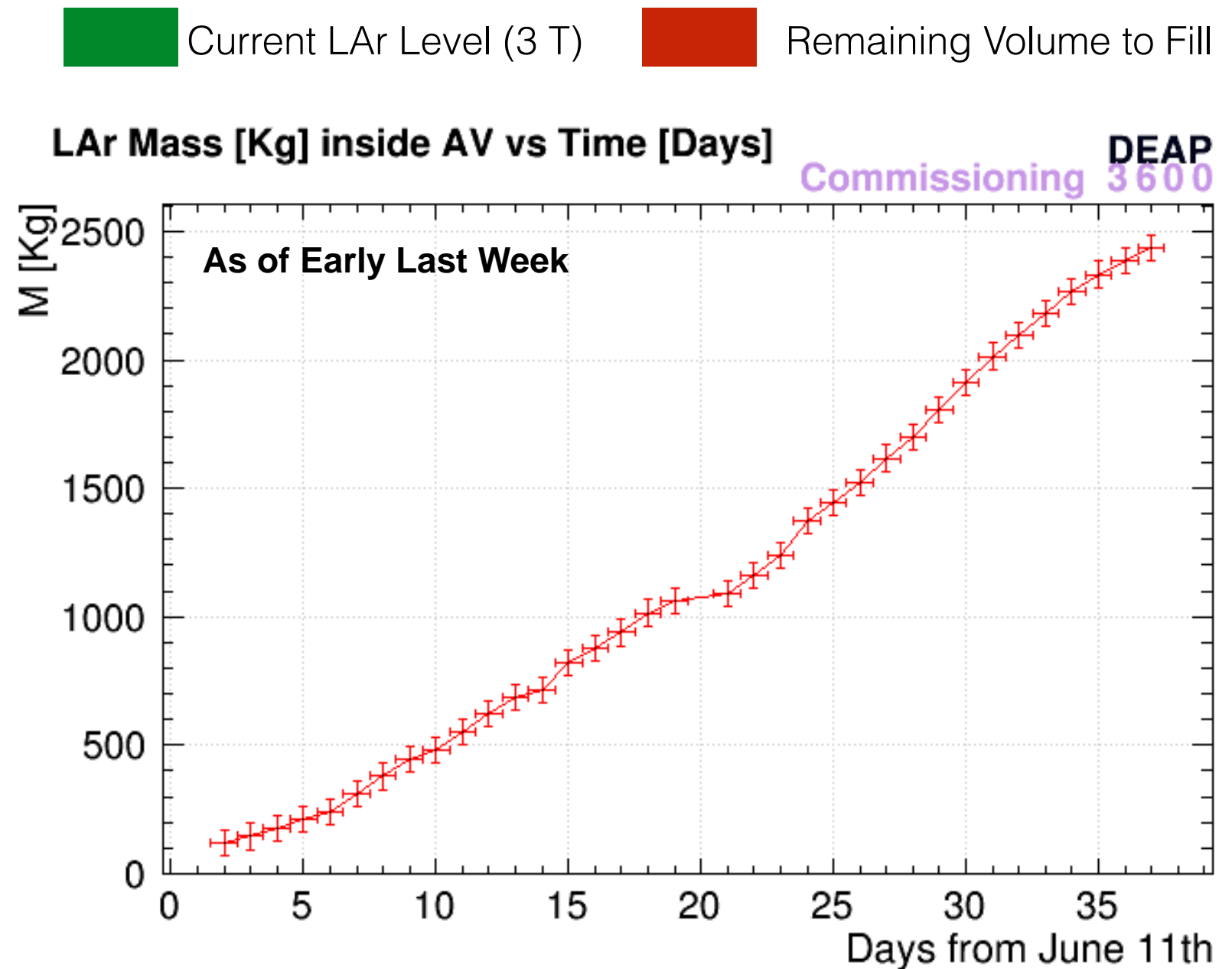
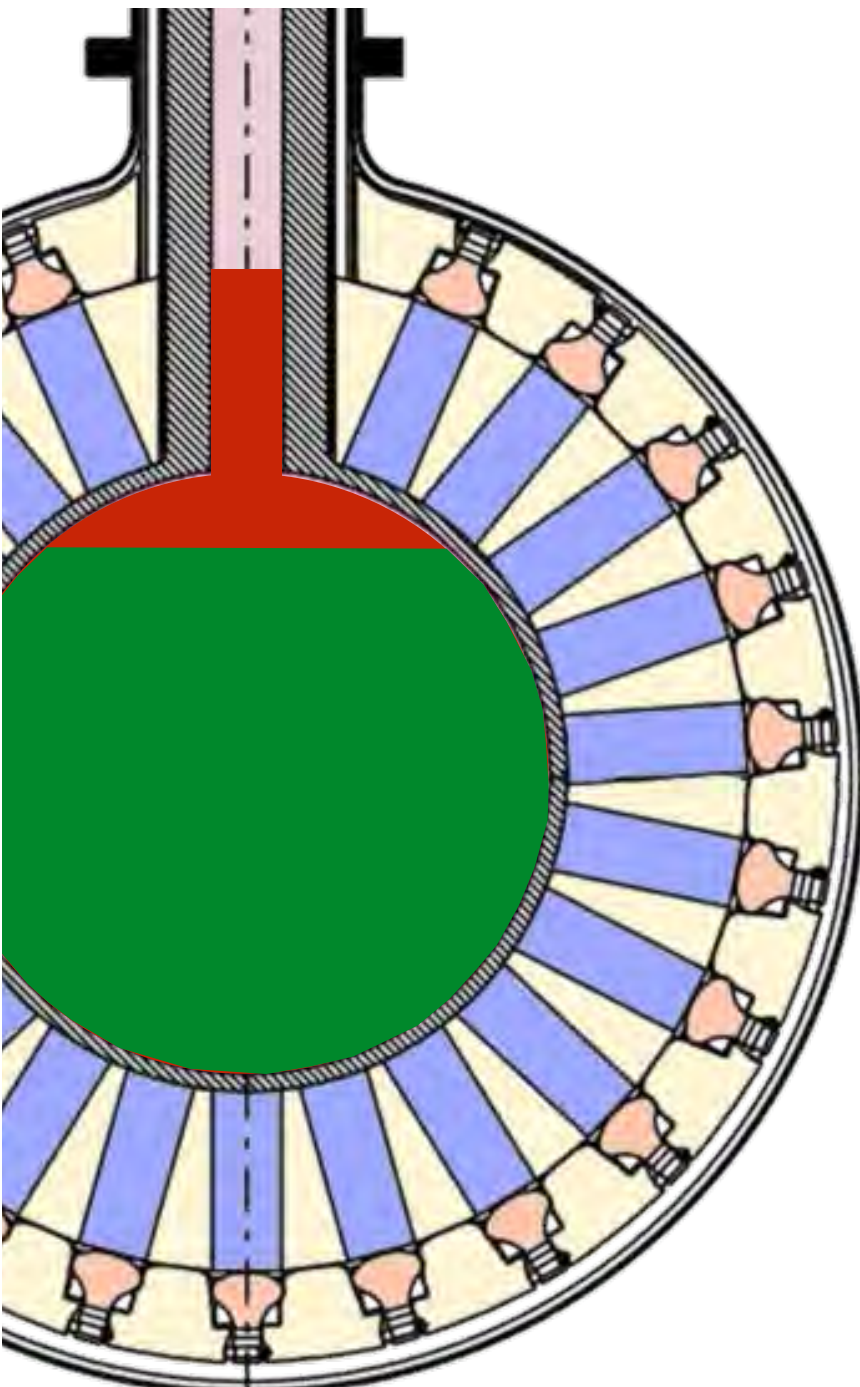


DEAP at SNOLab:

3600 kg LAr (1t fiducial)
single-phase detector
filling with LAr
dark matter run July 2016

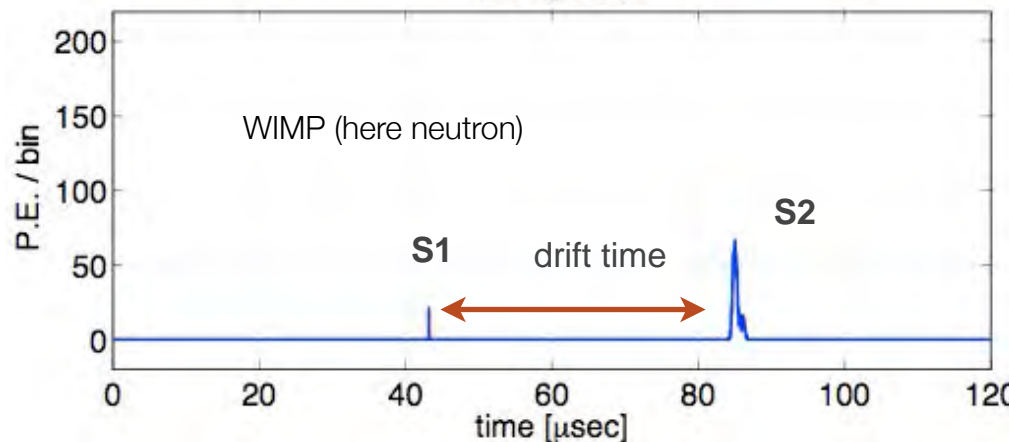
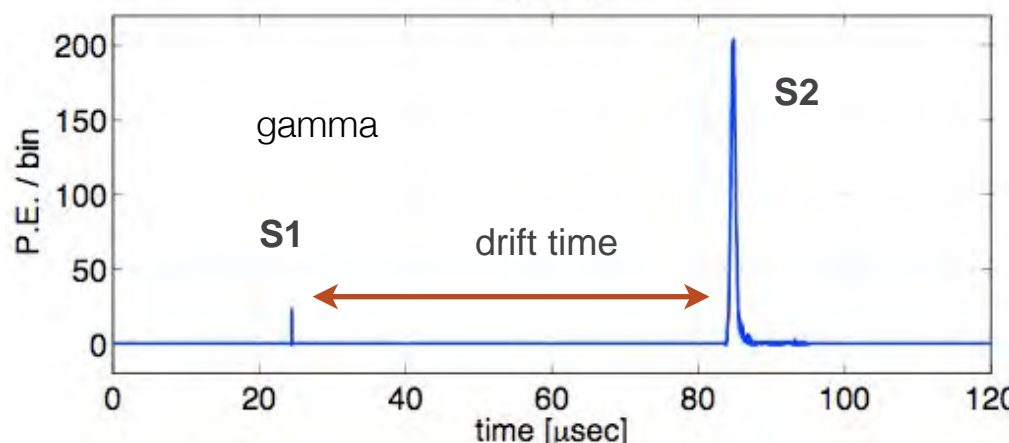
DEAP-3600: physics run to start in 2016

ICHEP2016

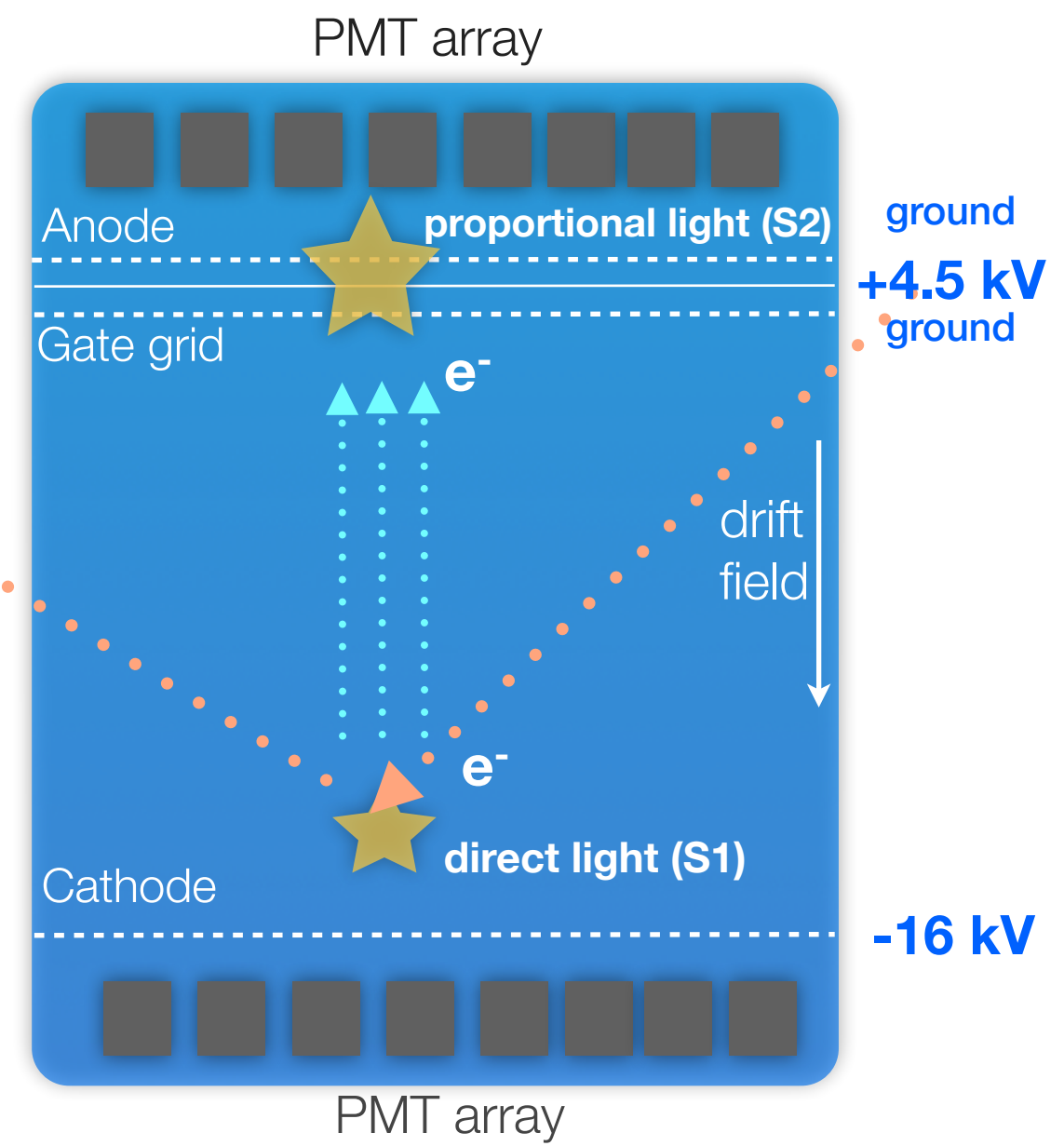


The Double-Phase Detector Concept

- Particle interaction in the active volume produces *prompt scintillation light (S1)* and ionisation electrons
- Electrons drift to interface ($E = 0.53 \text{ kV/cm}$) where they are extracted and amplified in the gas.
Detected as *proportional scintillation light (S2)*
 - $(S2/S1)_{\text{WIMP}} \ll (S2/S1)_{\text{Gamma}}$
 - 3-D position sensitive detector with particle ID

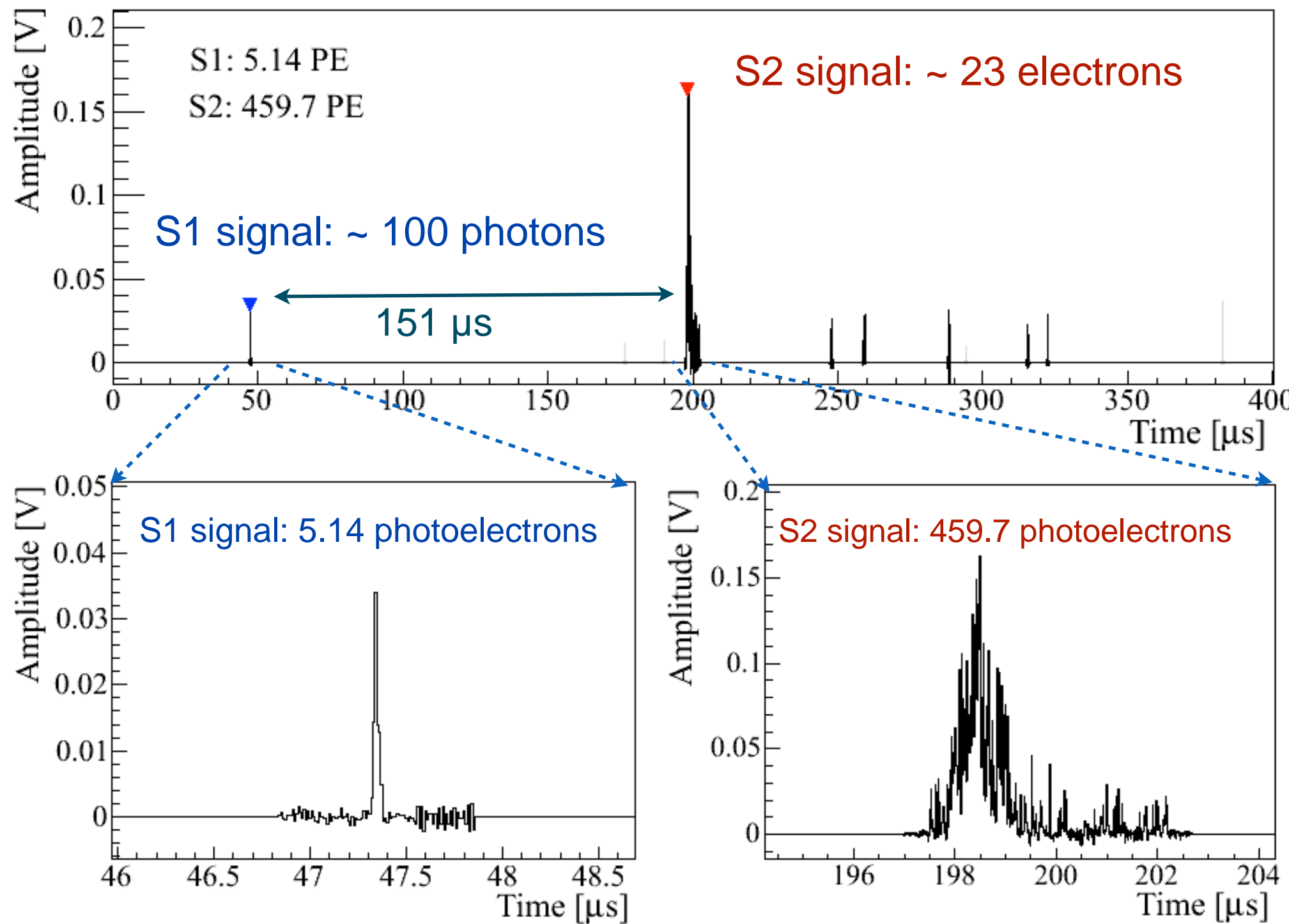


position resolution:
 $<3\text{mm in x-y}; < 0.3 \text{ mm in z}$



Example of a low-energy event in XENON100

The maximum electron drift time at 0.53 kV/cm is 176 μ s



Time projection chambers: argon



ArDM at Canfranc:

850 kg active LAr
(500 kg fiducial)

28 8-inch PMTs

completed first
physics run in single
phase mode (run I) in
2015
analysis ongoing

**preparing run II in
dual-phase,
scheduled for 2016**



DarkSide at LNGS

50 kg LAr (dep in ^{39}Ar)
(33 kg fiducial)

38 3-inch PMTs

started search with
underground argon in
2015 (April - Aug)

first results, PRD93,
2016



**continues to acquire
until ~1 y lifetime**

Time projection chambers: xenon



XENON100 at LNGS:

161 kg LXe
(~50 kg fiducial)

242 1-inch PMTs

results from run II

calibration data (YBe ,
 ^{83m}Kr , CH_3T , ^{220}Rn) etc



LUX at SURF:

350 kg LXe
(100 kg fiducial)

122 2-inch PMTs

re-analysis of 2013 data (run 3)
first result from run 4



PandaX at Jinping:

500 kg LXe
(306 kg fiducial)

110 3-inch PMTs

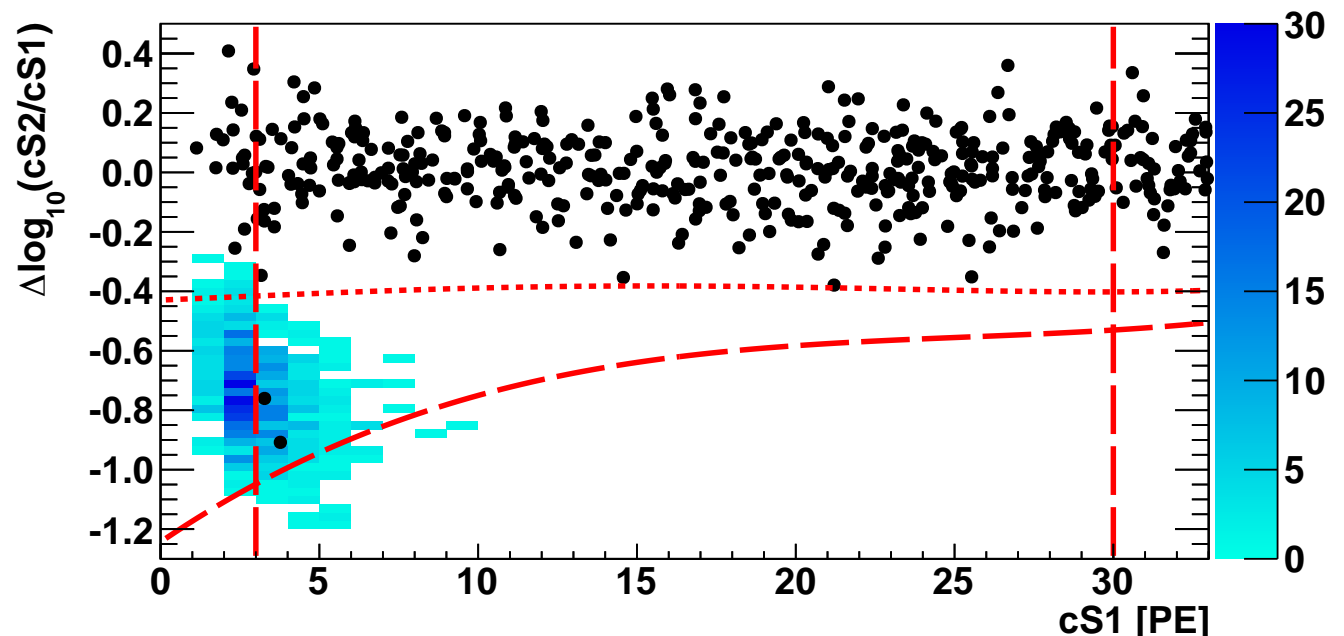
first commissioning run

**science data since
spring 2016, first
results**

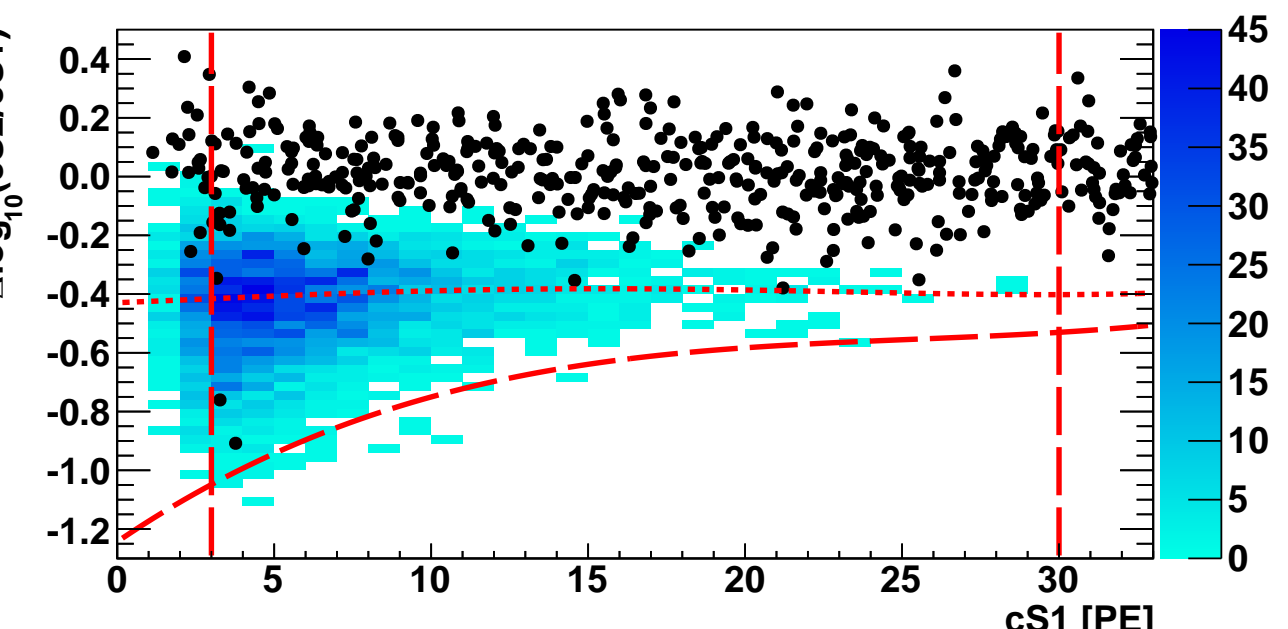
Predictions for light WIMPs

- How would WIMP signals look like in XENON100's Run10 data?

WIMP with $m_W = 8 \text{ GeV}$



WIMP with $m_W = 25 \text{ GeV}$



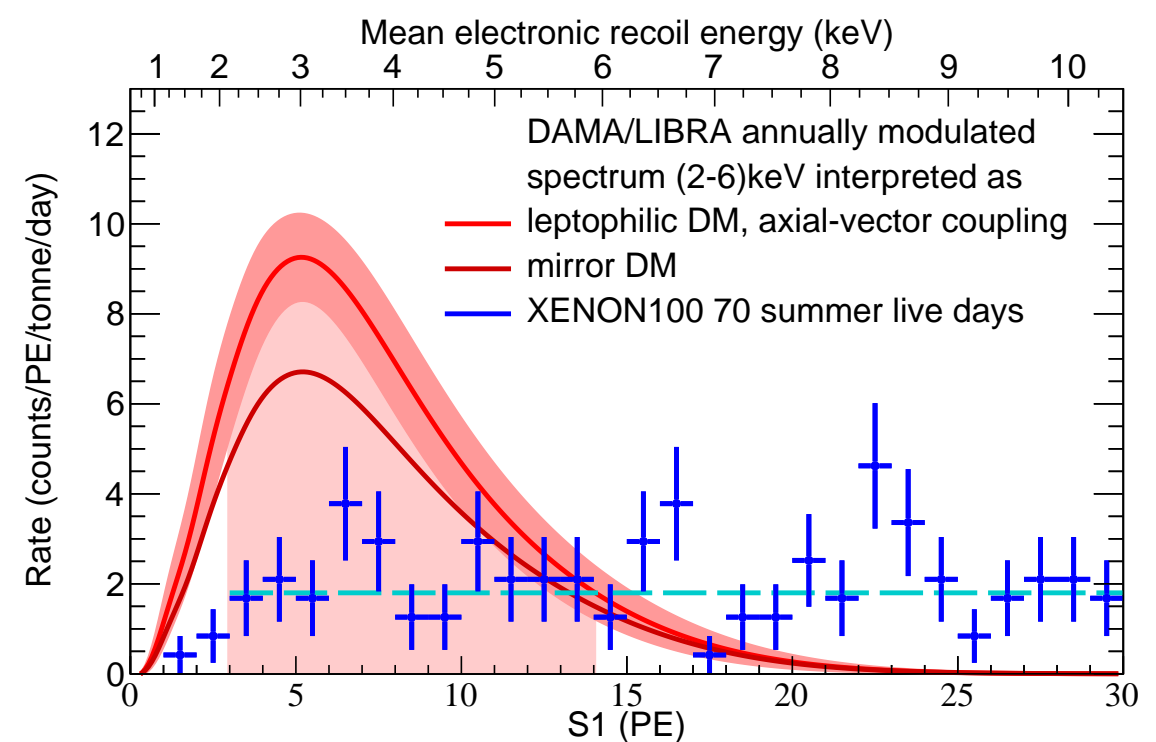
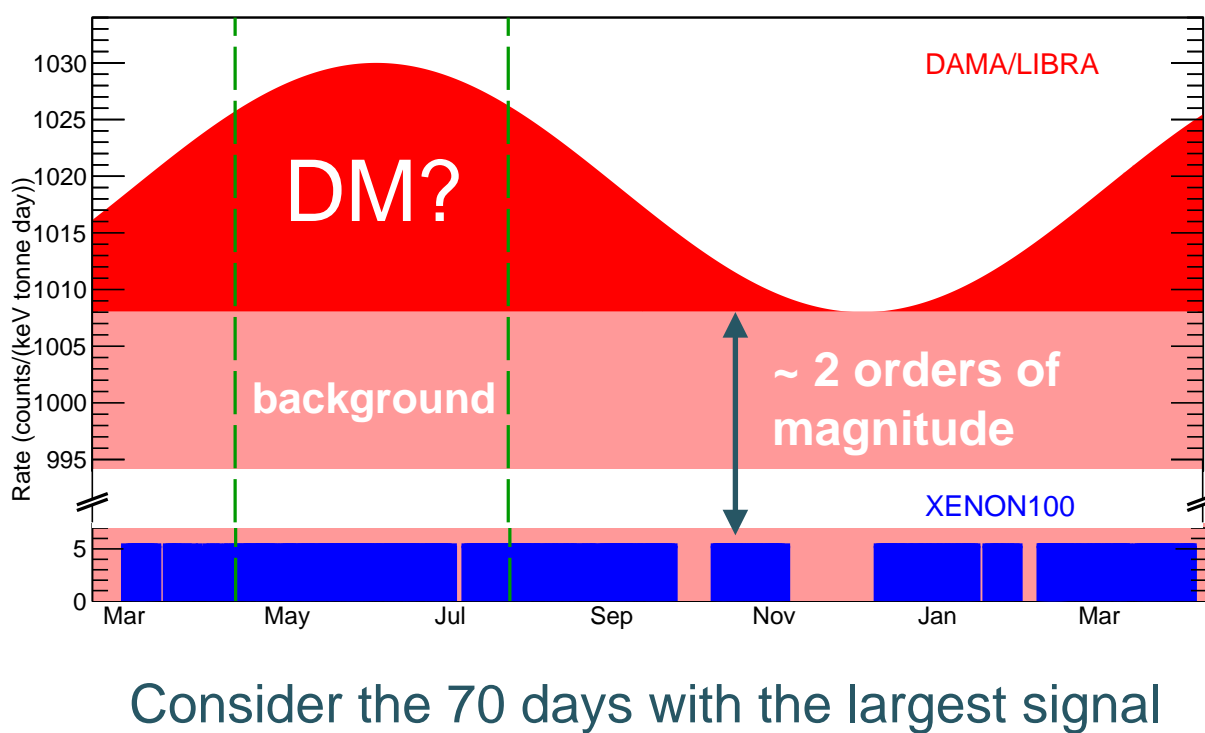
WIMP-nucleon cross
section : $3 \times 10^{-41} \text{ cm}^2$

WIMP-nucleon cross
section : $1.6 \times 10^{-40} \text{ cm}^2$

Recent XENON100 results

- Dark matter particles interacting with e^-
 - XENON100's ER background lower than DAMA modulation amplitude
→ search for a signal above background in the ER spectrum

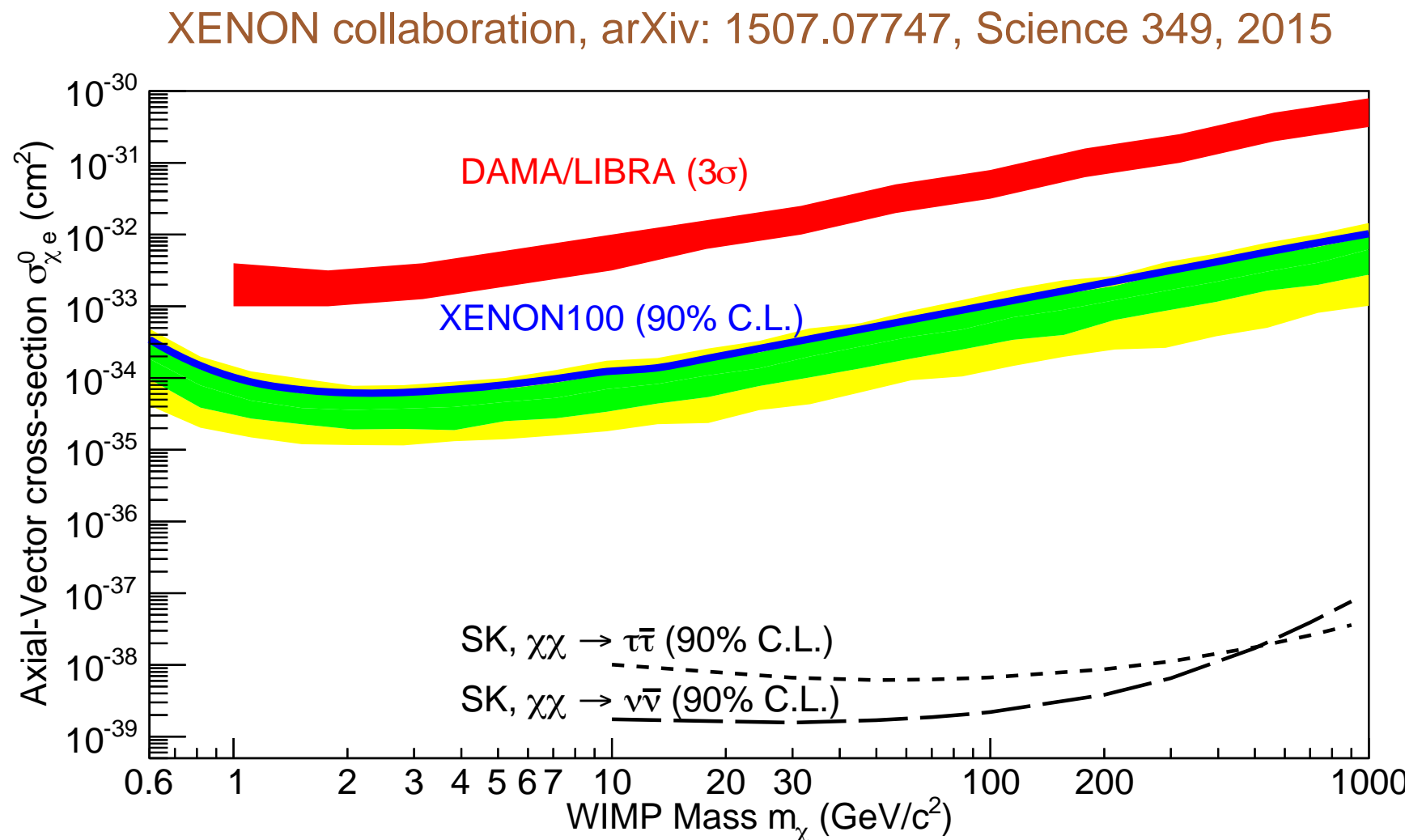
XENON collaboration, arXiv: 1507.07747, Science 349, 2015



DAMA/LIBRA modulated spectrum as would be seen in XENON100 (for axial-vector WIMP- e^- scattering)

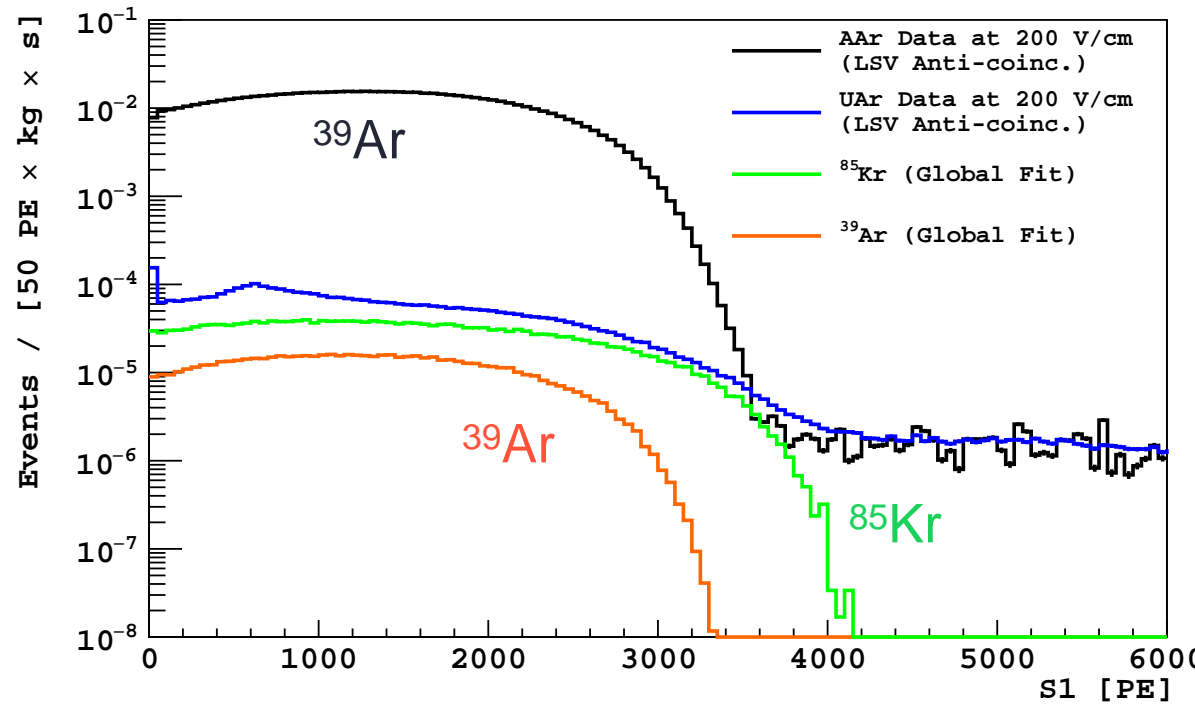
XENON100 excludes leptophilic models

- Dark matter particles interacting with e^-
 1. No evidence for a signal
 2. Exclude various leptophilic models as explanation for DAMA/LIBRA

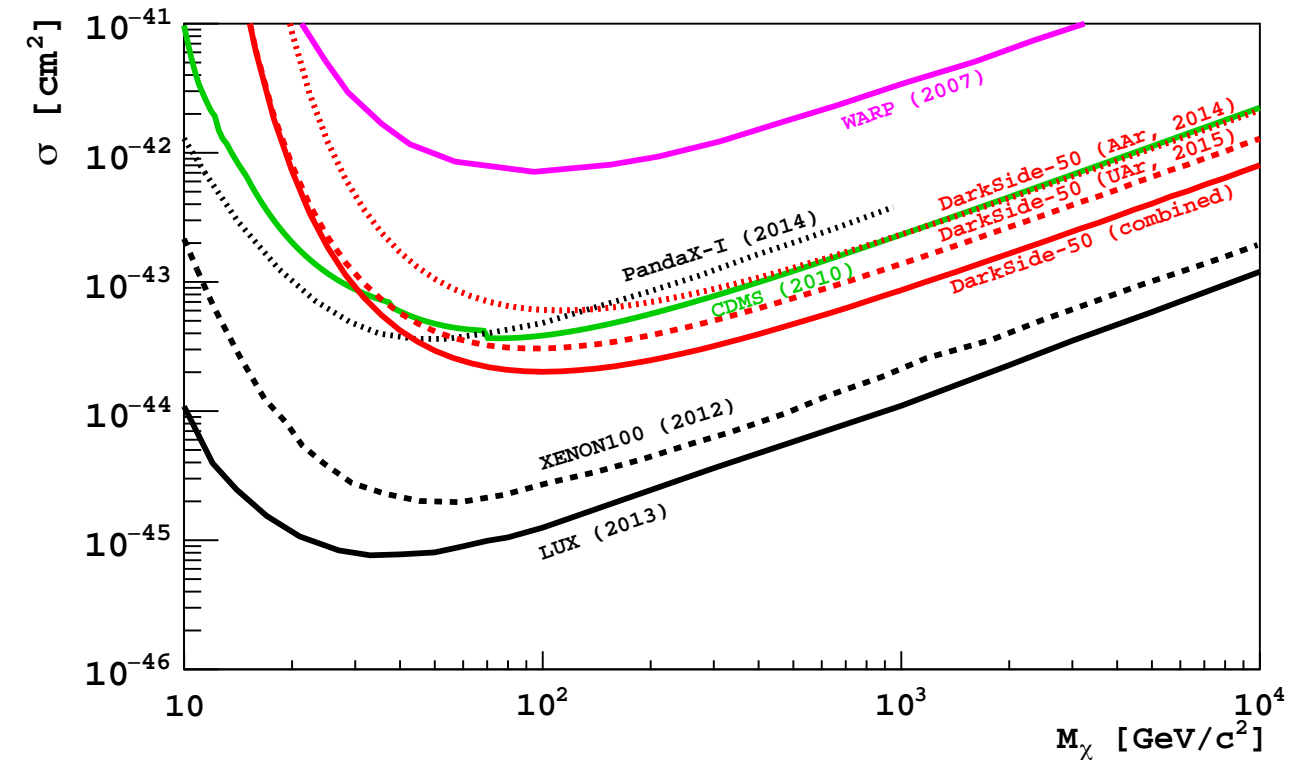


Liquefied noble gases recent results: argon

DarkSide-50: factor 1.4×10^3 depletion of ^{39}Ar

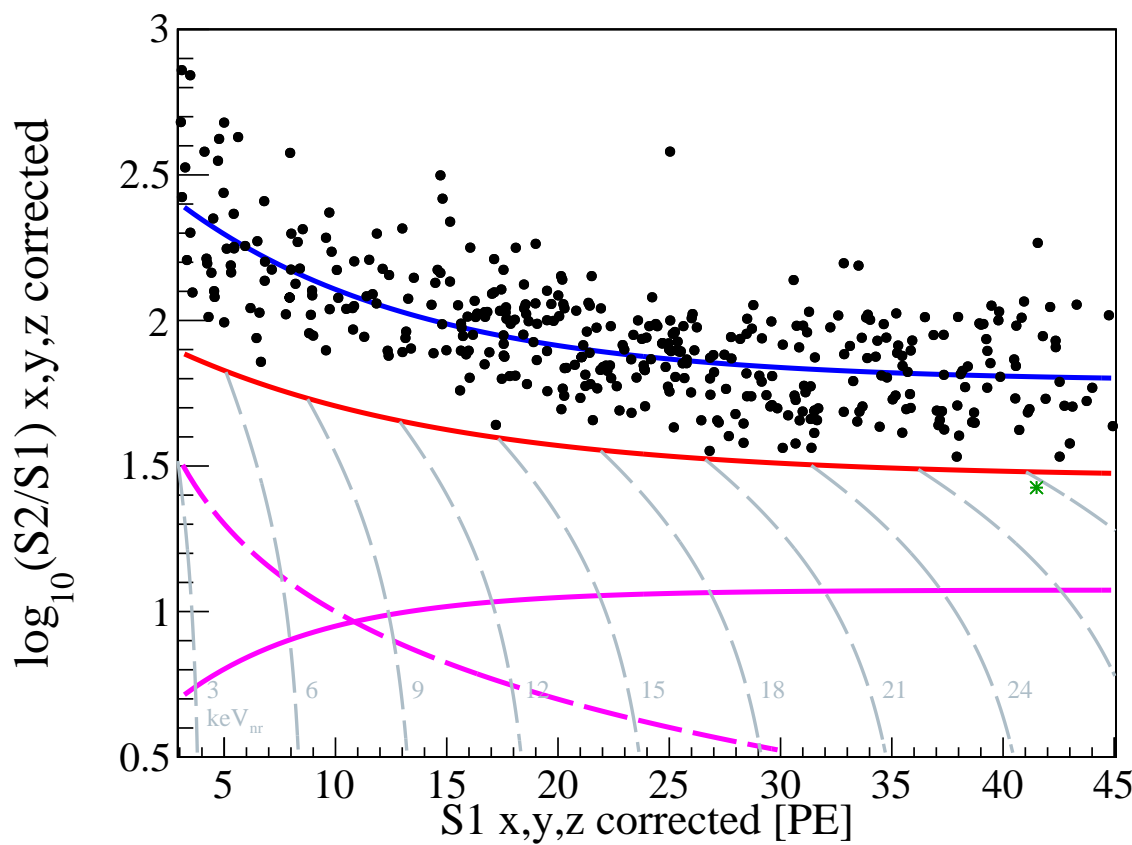


DarkSide-50, 70.9 live days, arXiv:1510.00702



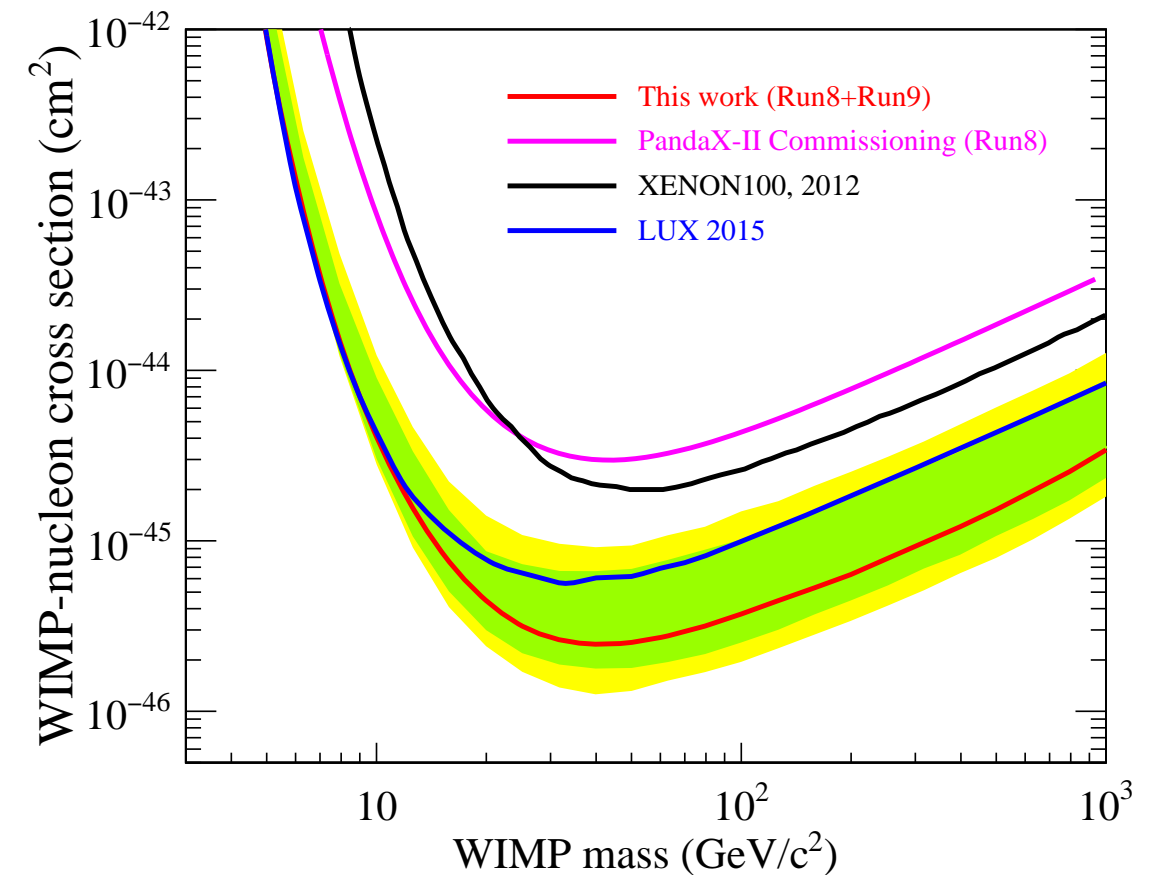
Liquefied noble gases recent results: xenon

PandaX: dark matter data



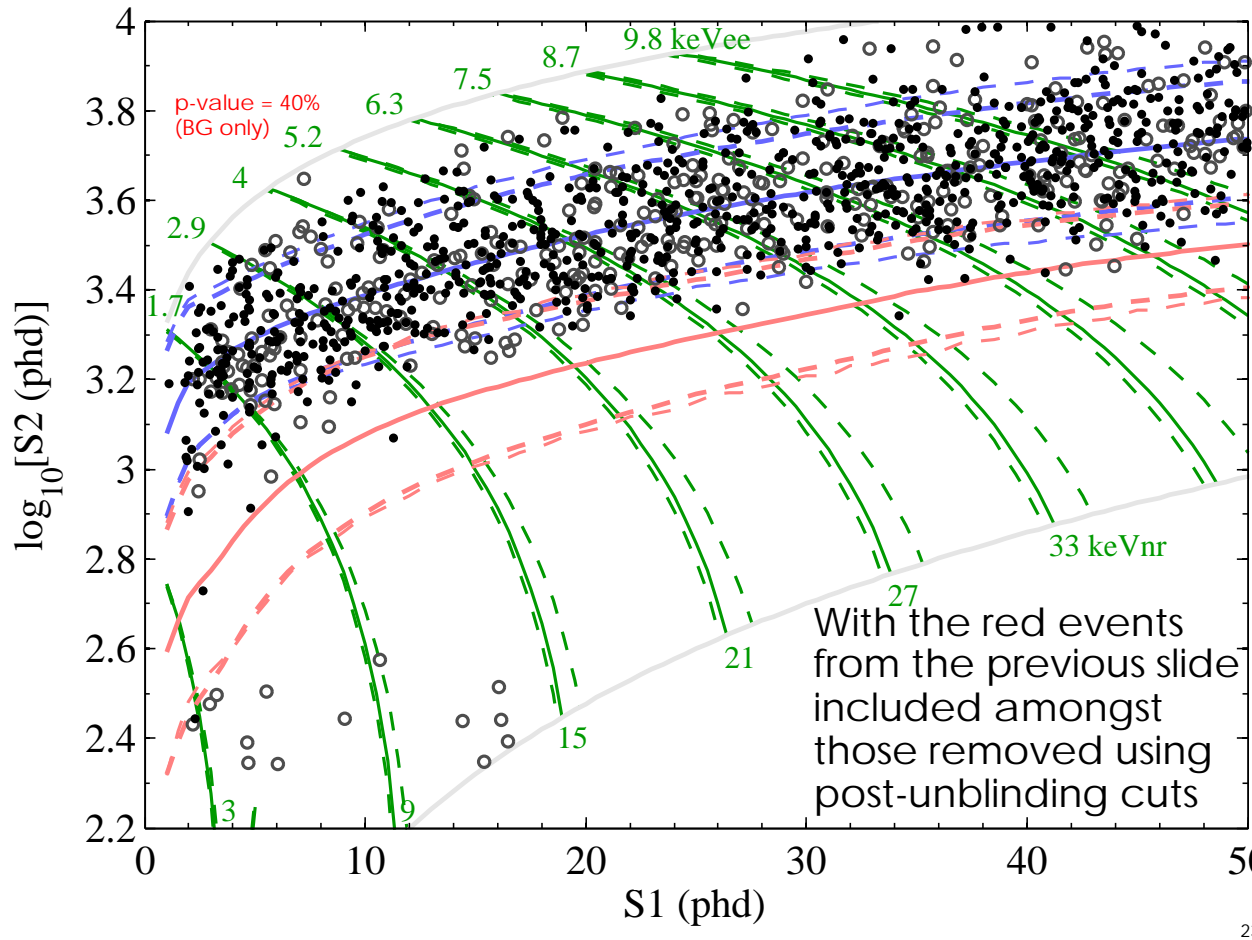
3.3×10^4 kg-day exposure
no dark matter candidates

PandaX, arXiv:1607.07400

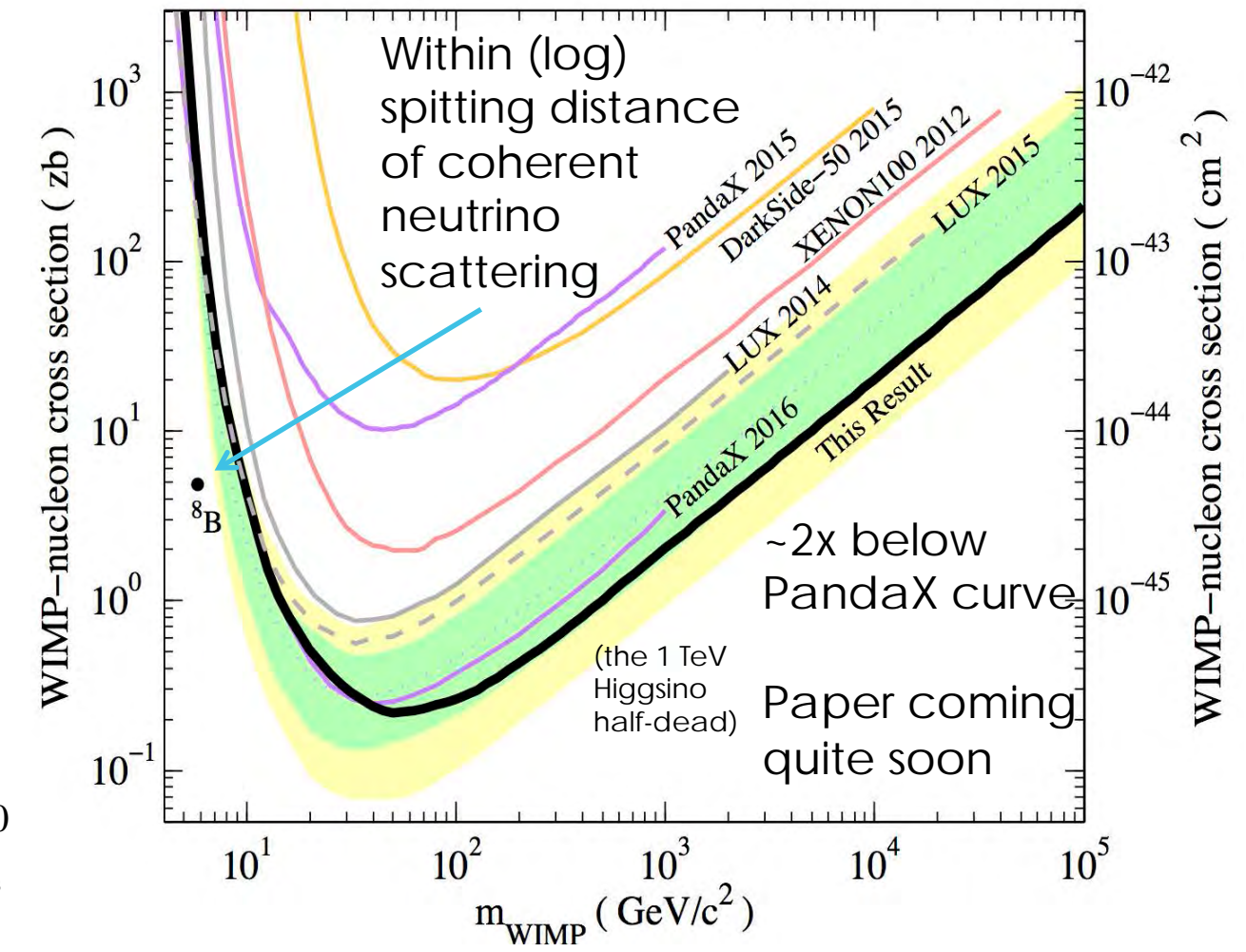


Liquefied noble gases recent results: xenon

LUX: dark matter data



LUX, paper in preparation

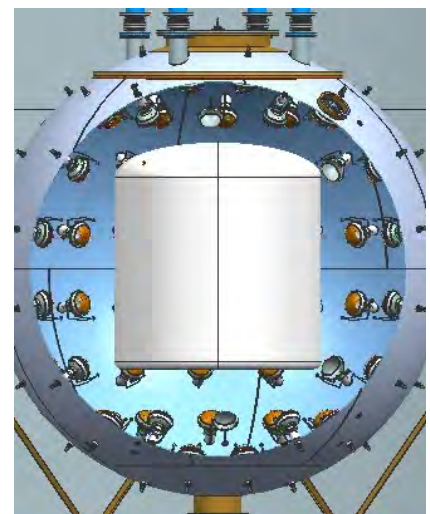


New and future noble liquid detectors

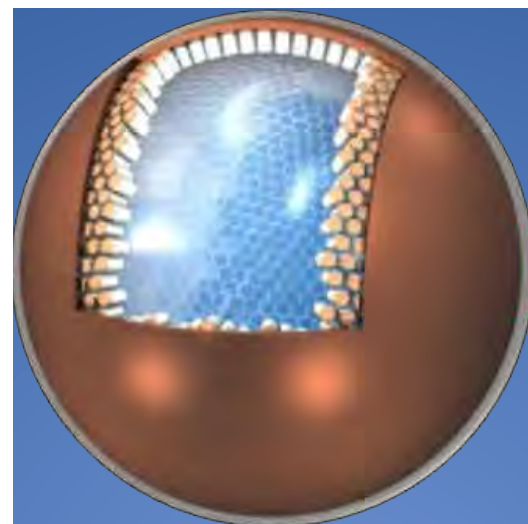
- Under commissioning: **XENON1T (3.5 t LXe) at Gran Sasso**
- Planned LXe: LUX-ZEPLIN 7t, XENONnT 7t, XMASS 6t
- Proposed LAr: DarkSide 20 t, DEAP 50 t
- Design & R&D stage: DARWIN 50 t LXe; ARGO 300 t LAr



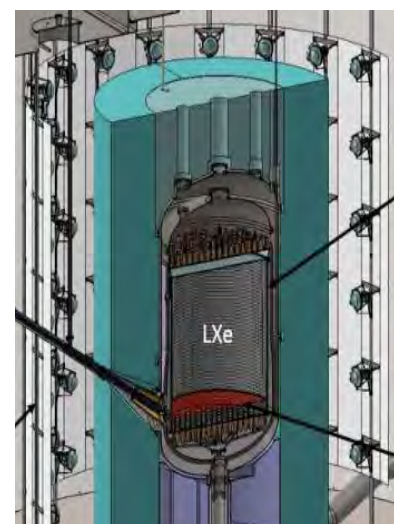
XENONnT: 7t LXe



DarkSide: 20 t LAr



XMASS: 6t LXe



LZ: 7t LXe



DARWIN: 50 t LXe

The XENON1T experiment

- Under commissioning at LNGS since January 2016
- Total (active) LXe mass: 3.5 t (2 t), 1 m electron drift, 248 3-inch PMTs in two arrays
- Background goal: $100 \times$ lower than XENON100 $\sim 5 \times 10^{-2}$ events/(t d keV)

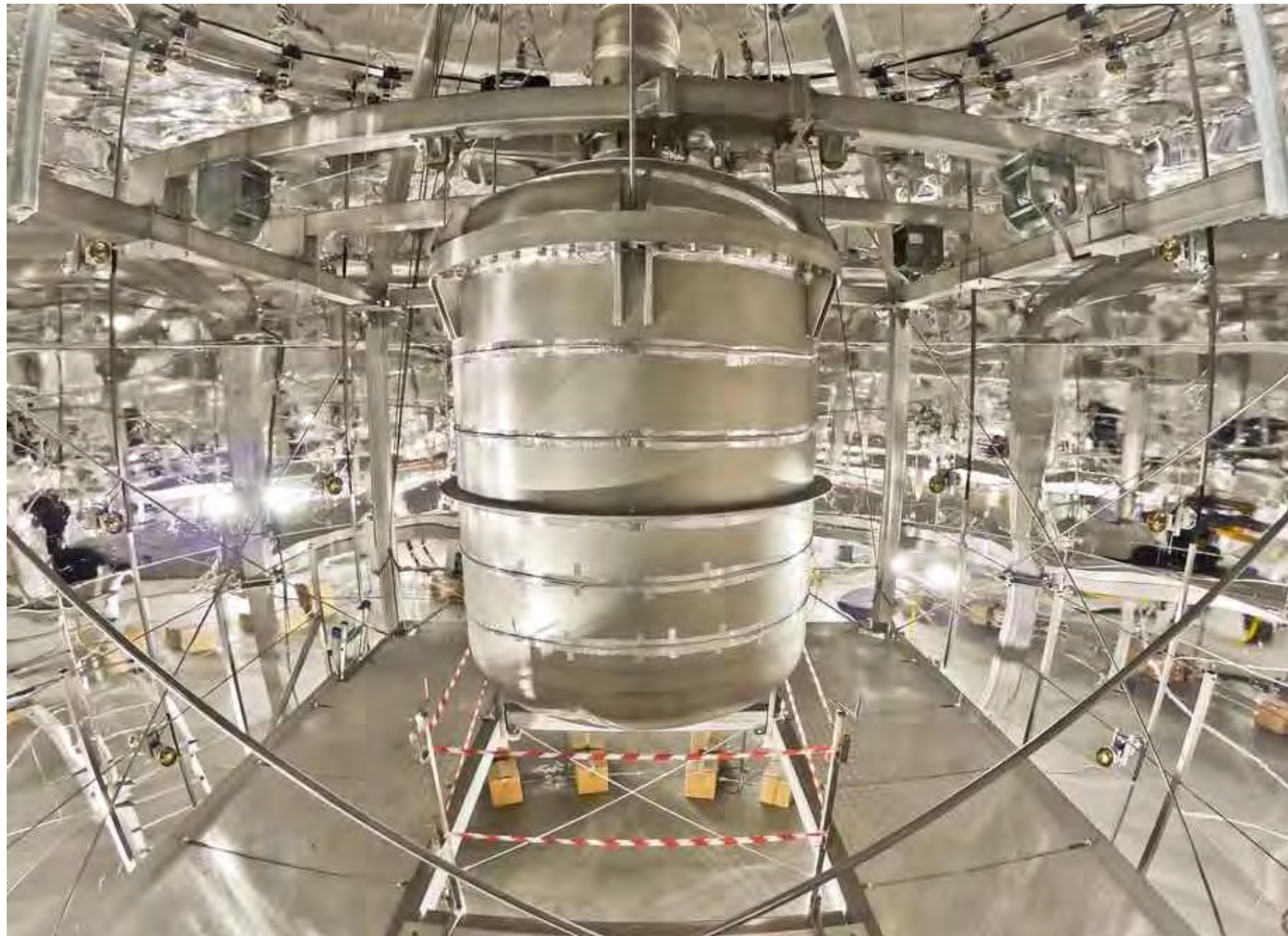


The XENON1T detector at LNGS



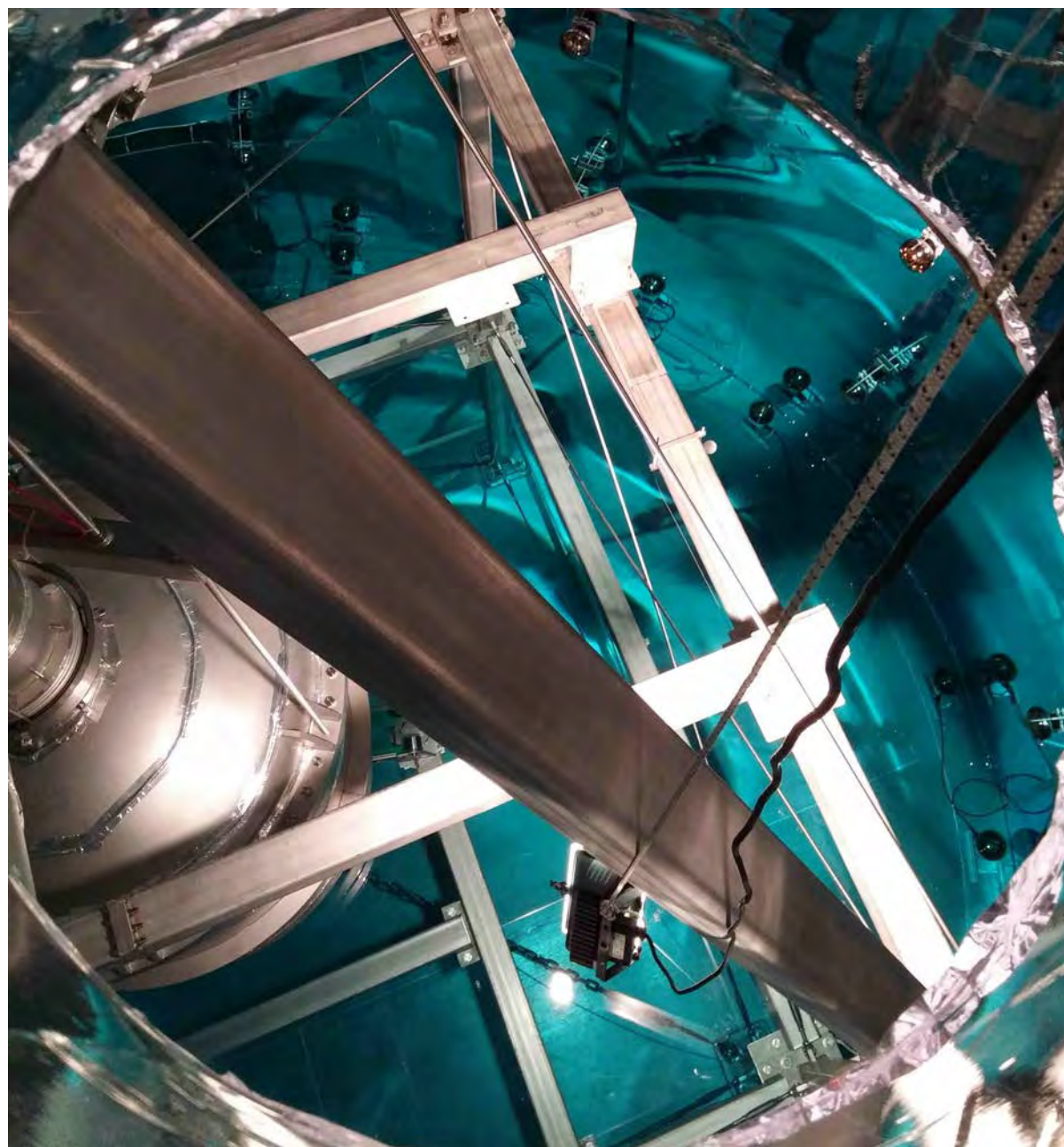
The XENON1T detector at LNGS

- Water Cherenkov shield, cryostat support, service building, electrical plant completed
- Cryostat, cryogenics, storage, purification, cables, fibres installed and commissioned



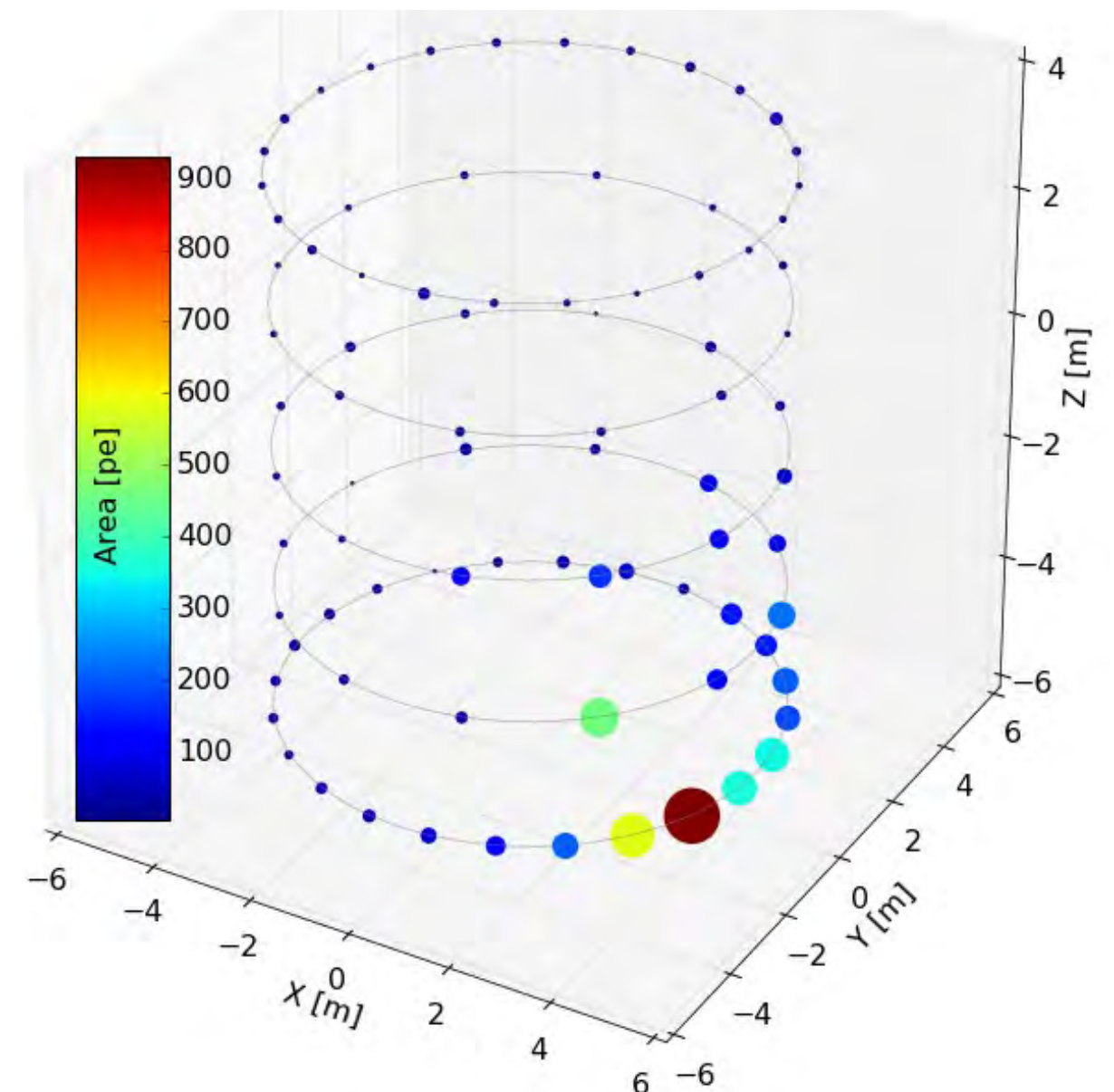
The XENON1T experiment: the muon veto

Water tank instrumented with 84 8-inch PMTs



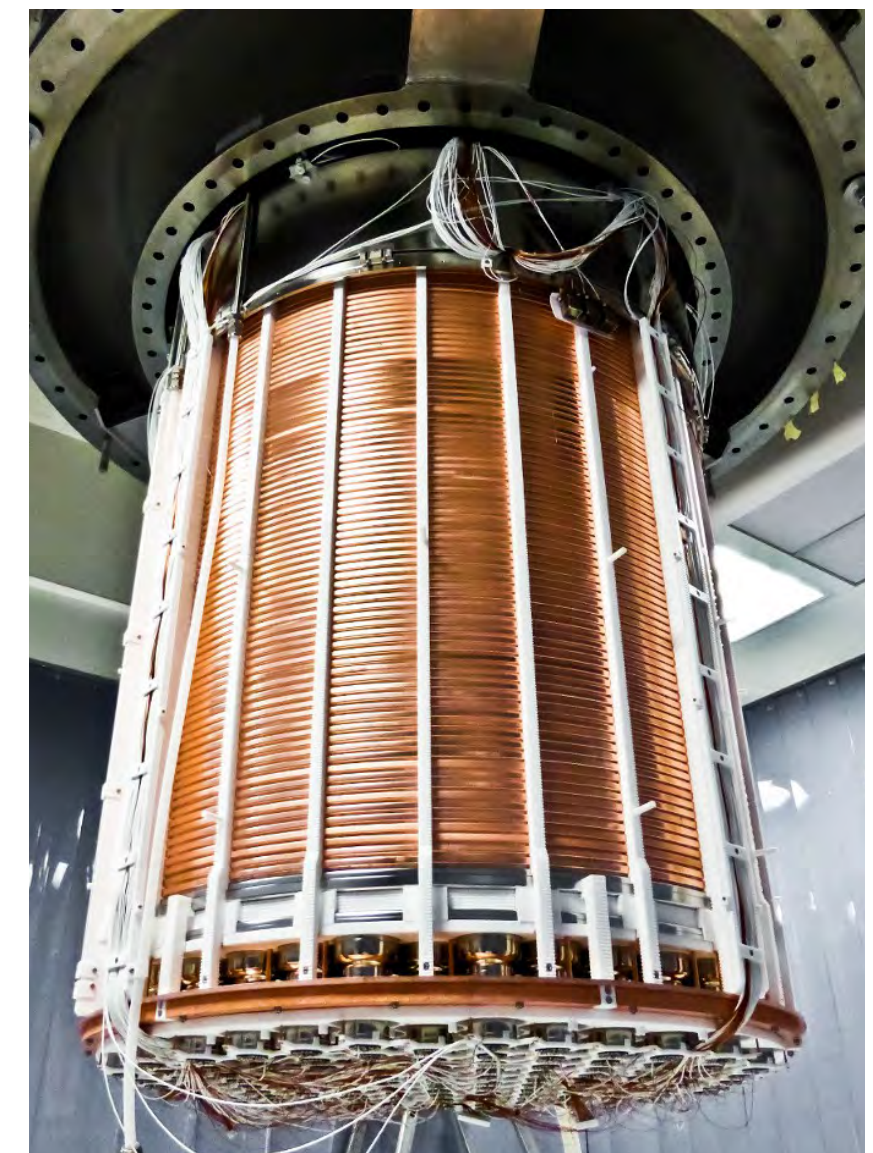
Tag > 99.5% of events where μ 's cross the water and
>70% of events with only n's (and showers)

One of the first muons seen in the XENON1T muon veto



The XENON1T experiment: inner detector

- Active liquid xenon volume observed by 248 3-inch, low-radioactivity PMTs
- **TPC installation at LNGS was completed in November 2015**



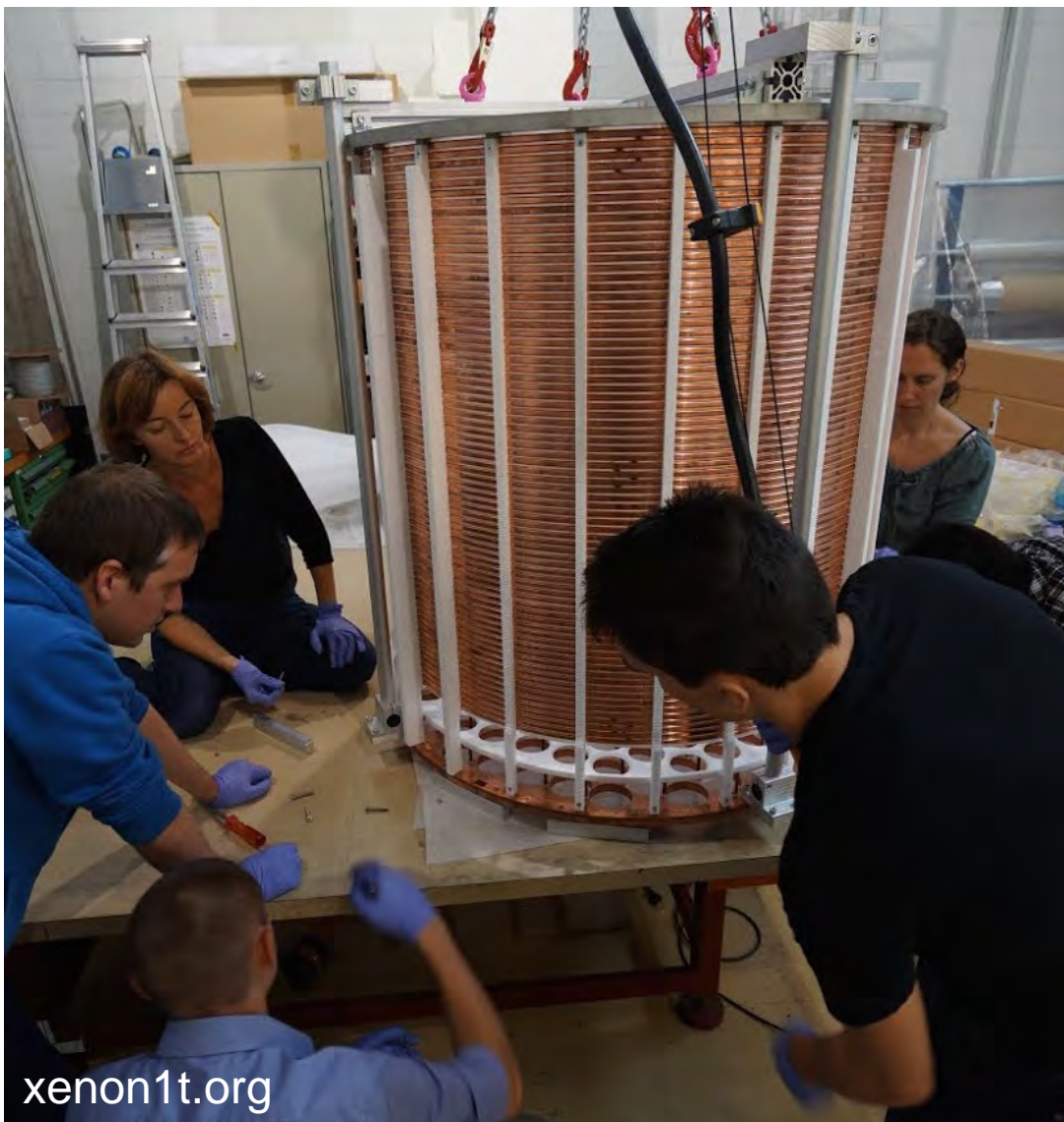
The TPC

PMT arrays

TPC installation underground

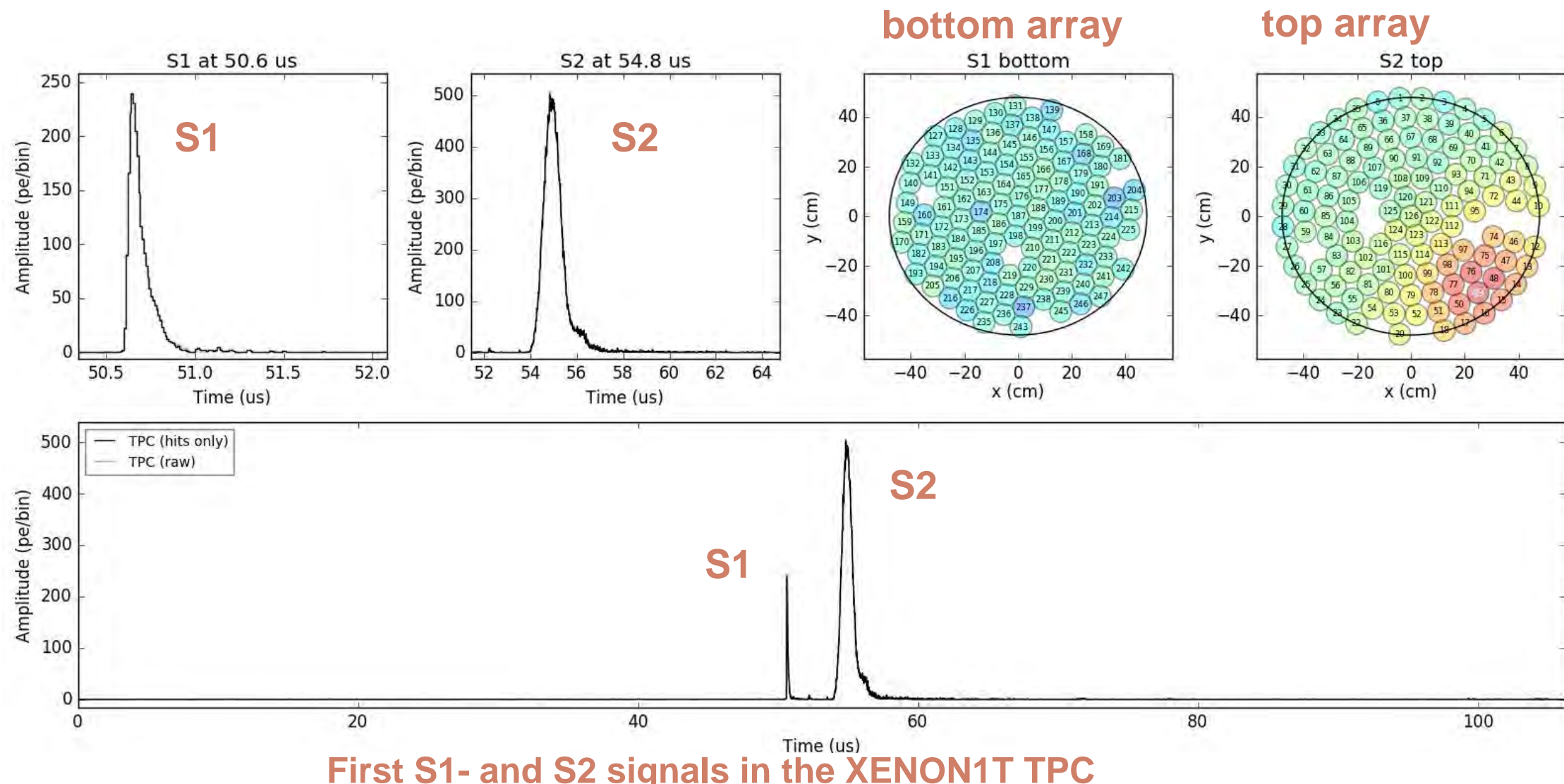
The XENON1T experiment: inner detector

- PMTs tested at cryogenic temperatures; arrays were assembled in October 2015
- TPC assembly and cold tests completed at UZH; installation at LNGS in November 2015

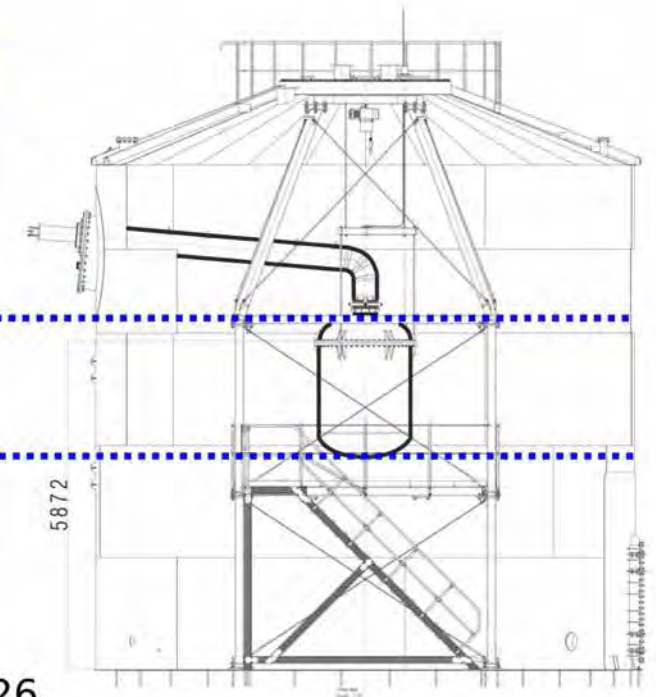
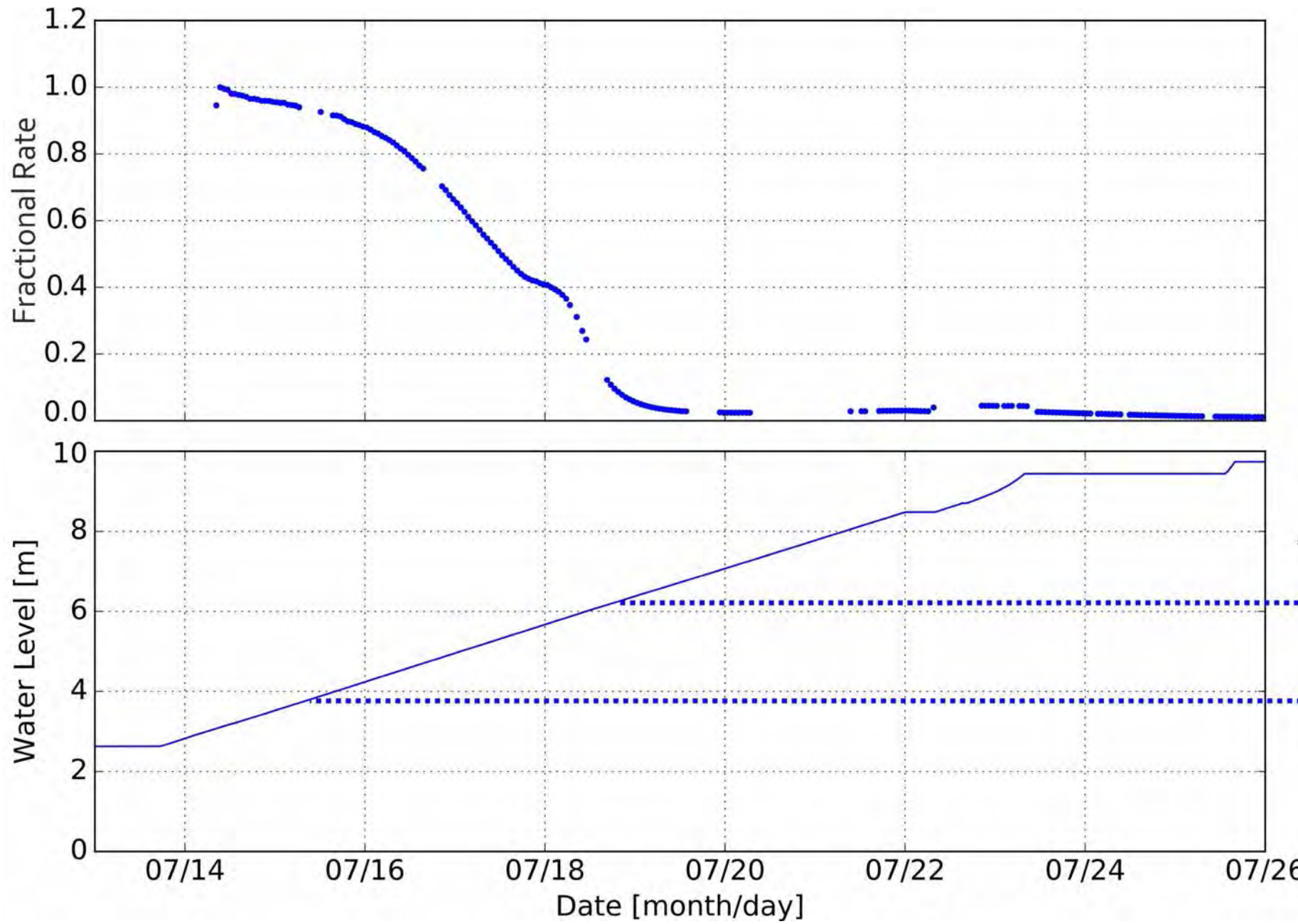


The XENON1T experiment: first light and charge

- The experiment is under commissioning (TPC, + optimisation of cryogenic system, DAQ, slow control, etc) & the calibration campaign is well underway
- **Water filling completed and Kr removal started last week**
- **First science run expected for autumn 2016**

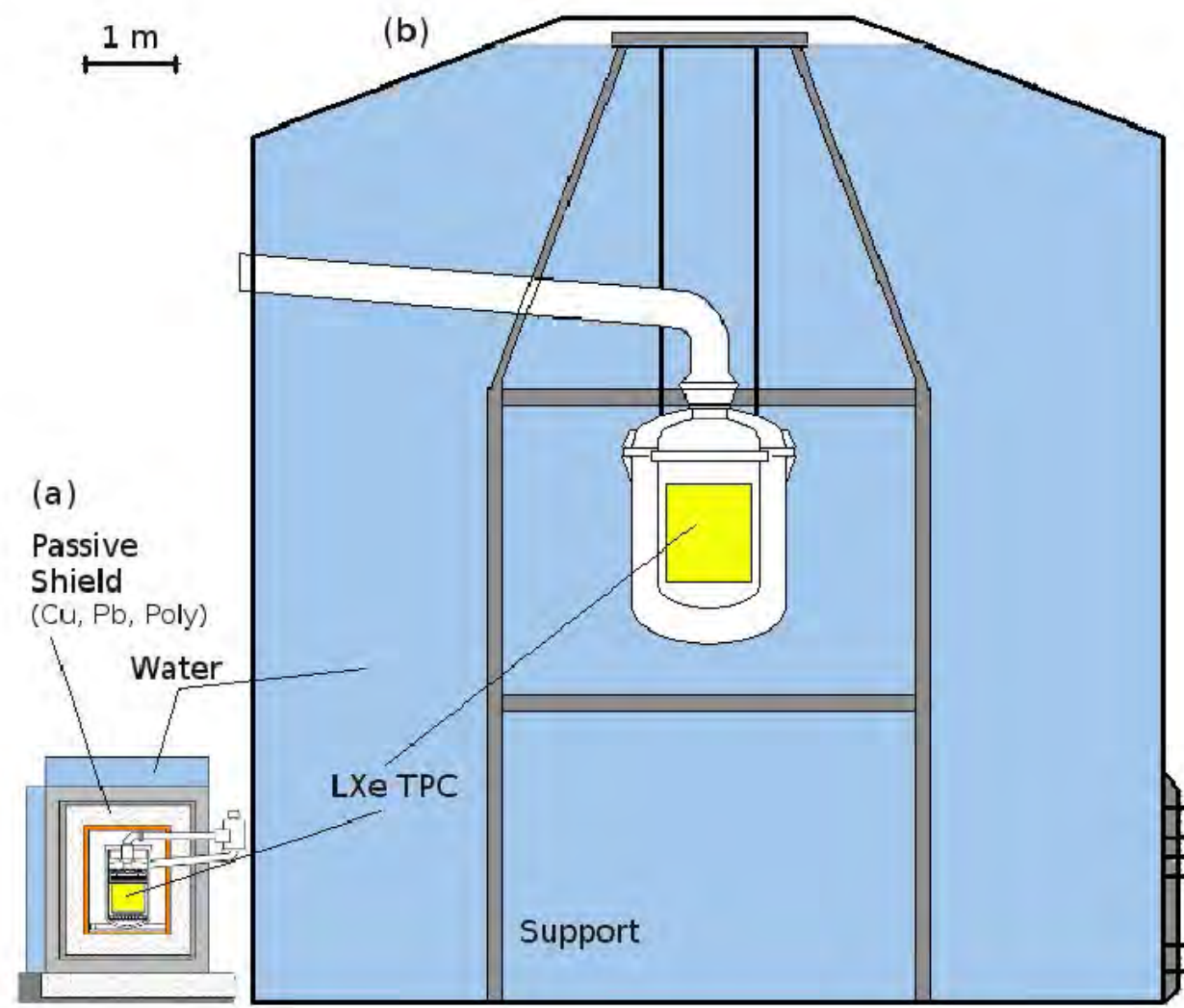


XENON1T: rate in the TPC versus water level



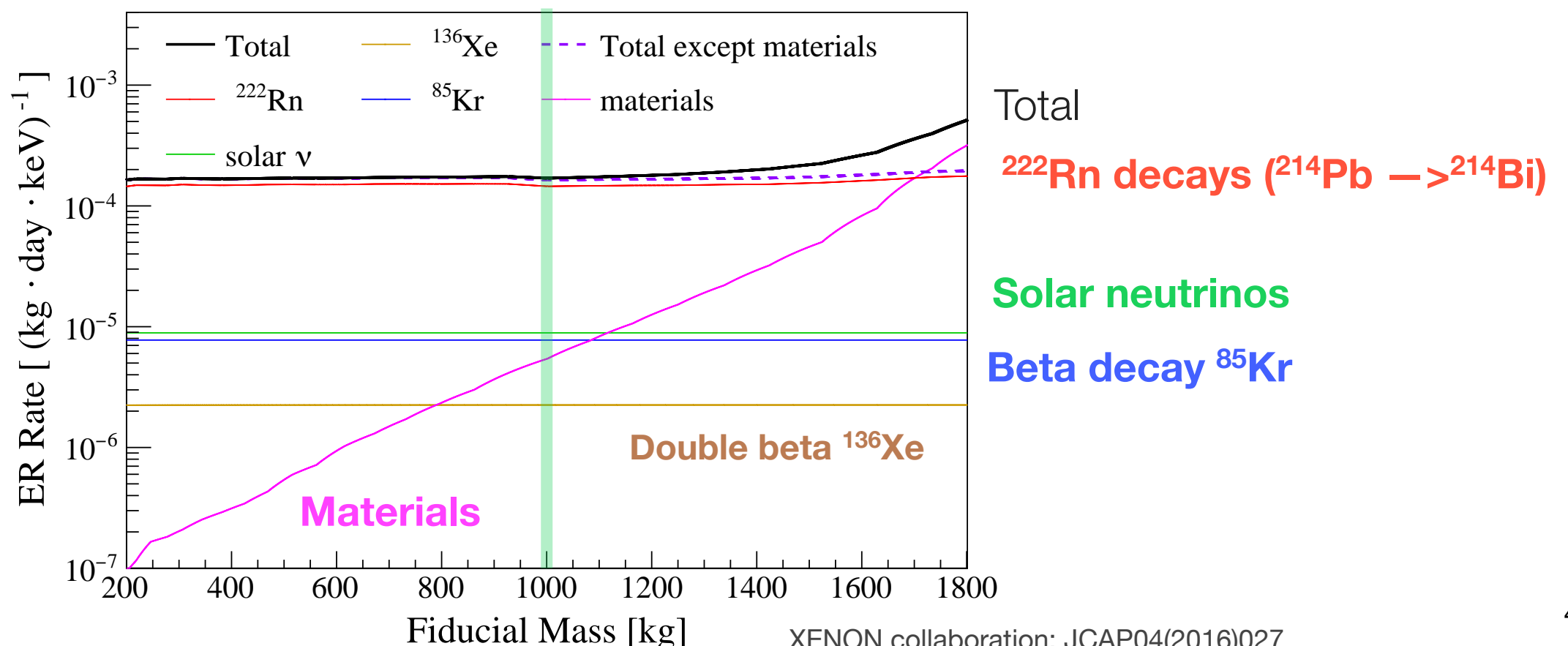
From XENON100 to XENON1T in numbers

	XENON100	XENON1T
Total LXe mass [kg]	161	3500
Background [dru]	5×10^{-3}	5×10^{-5}
^{222}Rn [$\mu\text{Bq/kg}$]	~ 65	~ 1
$^{\text{nat}}\text{Kr}$ [ppt]	~ 120	~ 0.2
e- drift [cm]	30	100
Cathode HV [kV]	-16	-100

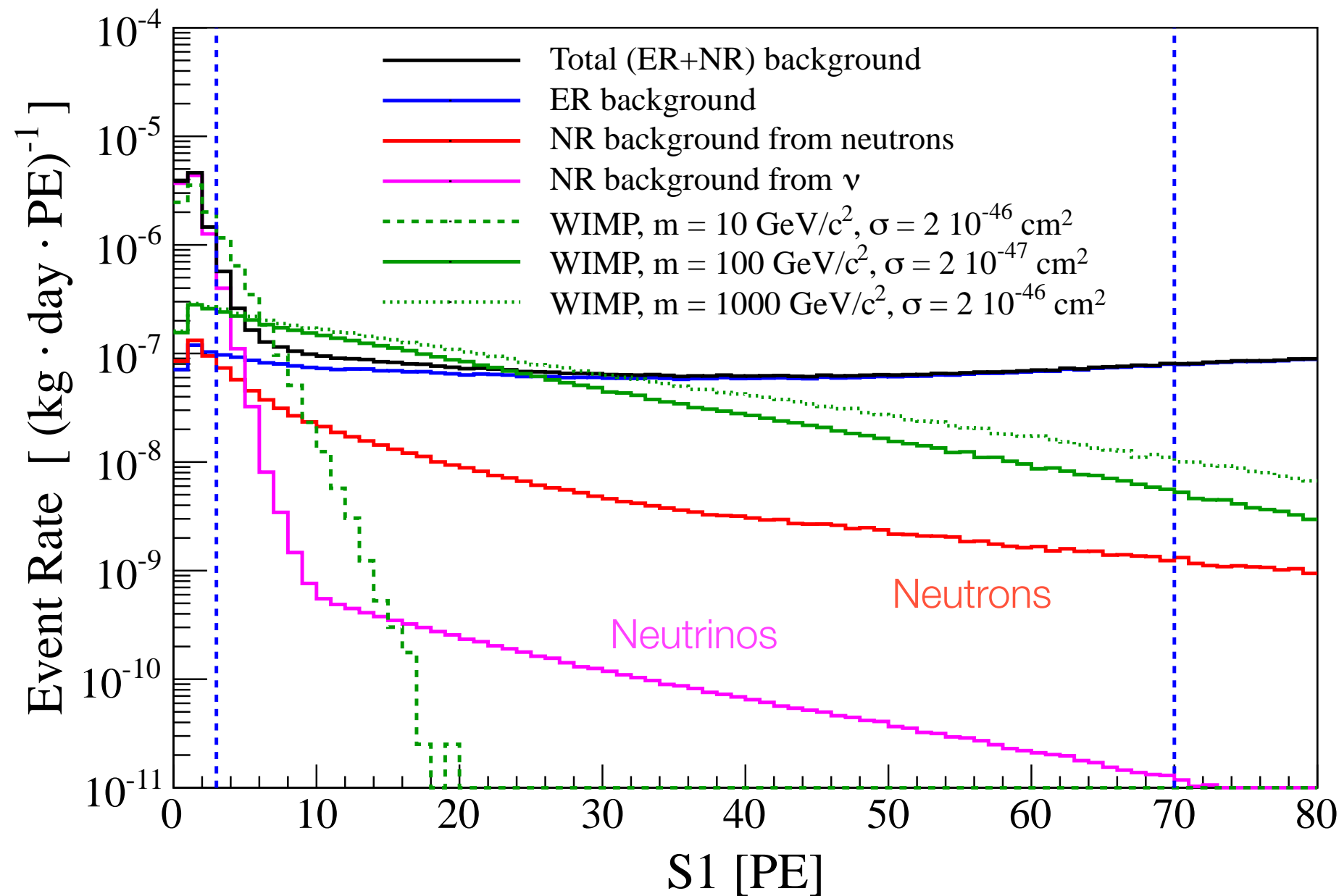


XENON1T background predictions

- Materials: based on screening results for all detector components
- ^{85}Kr : 0.2 ppt of $^{\text{nat}}\text{Kr}$ with $2 \times 10^{-11} \text{ }^{85}\text{Kr}$; ^{222}Rn : 10 $\mu\text{Bq}/\text{kg}$; ^{136}Xe double beta: $2.11 \times 10^{21} \text{ yr}^{-1}$
- ER vs NR discrimination level: 99.75%; 40% acceptance for NRs
 - **Total ERs: 0.3 events/year** in 1 ton fiducial volume, [2-12] keV_{ee}
 - **Total NRs: 0.6 events/year in 1 ton**, [5-50] keV_{nr} (muon-induced n-BG < 0.01 ev/year)



XENON1T backgrounds and WIMP sensitivity



Light yield = 7.7 PE/keV at 0 field

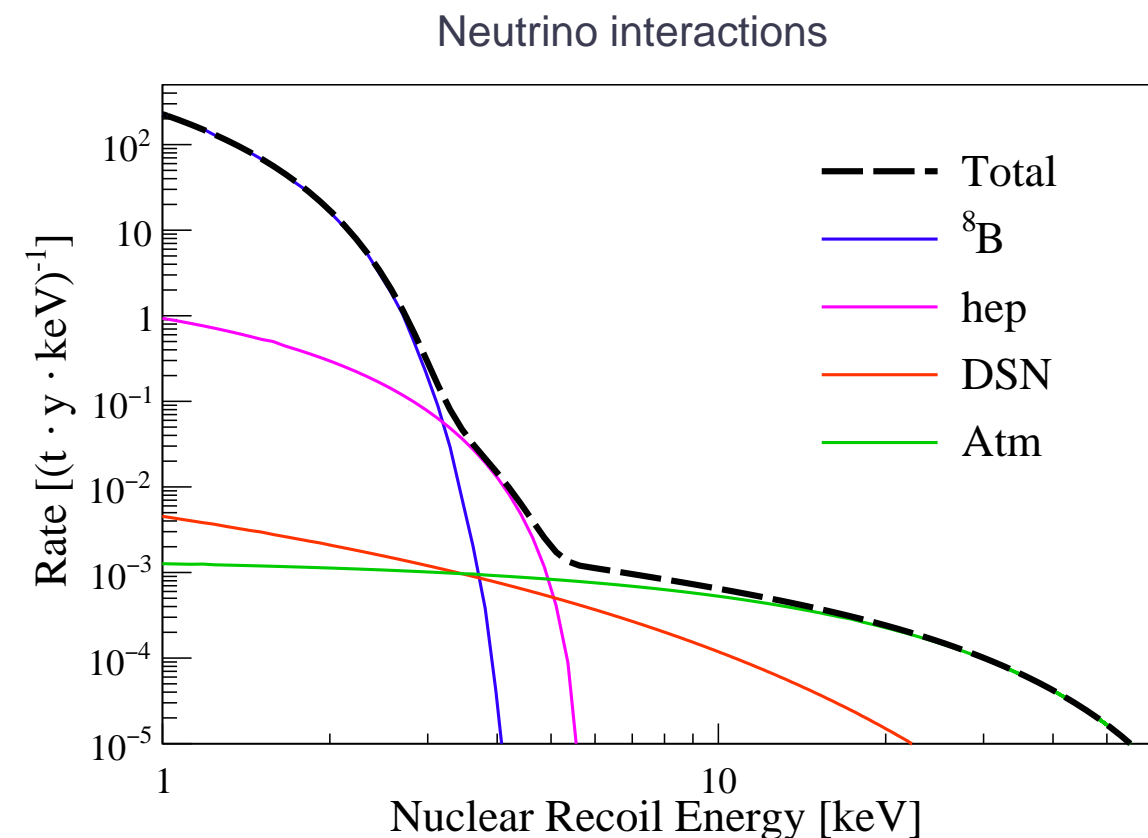
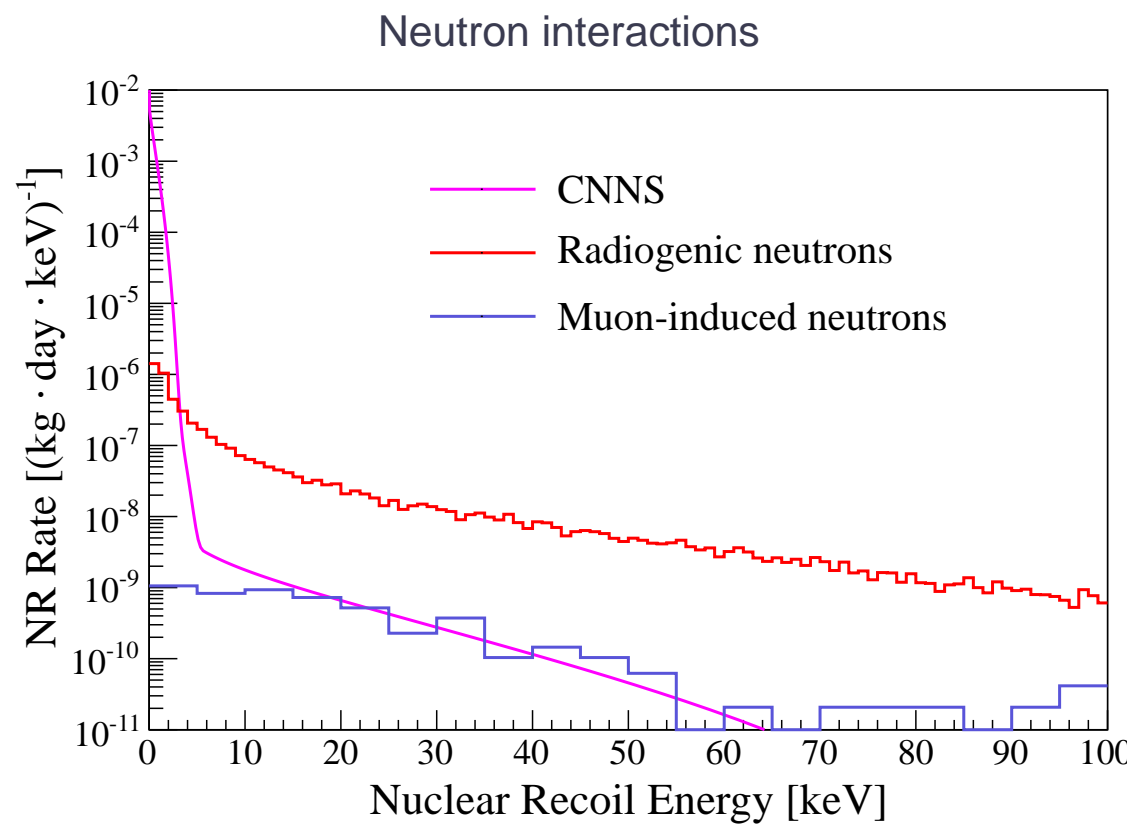
$L_{\text{eff}} = 0$ below 1 keVnr

99.75% S2/S1 discrimination

NR acceptance 40%

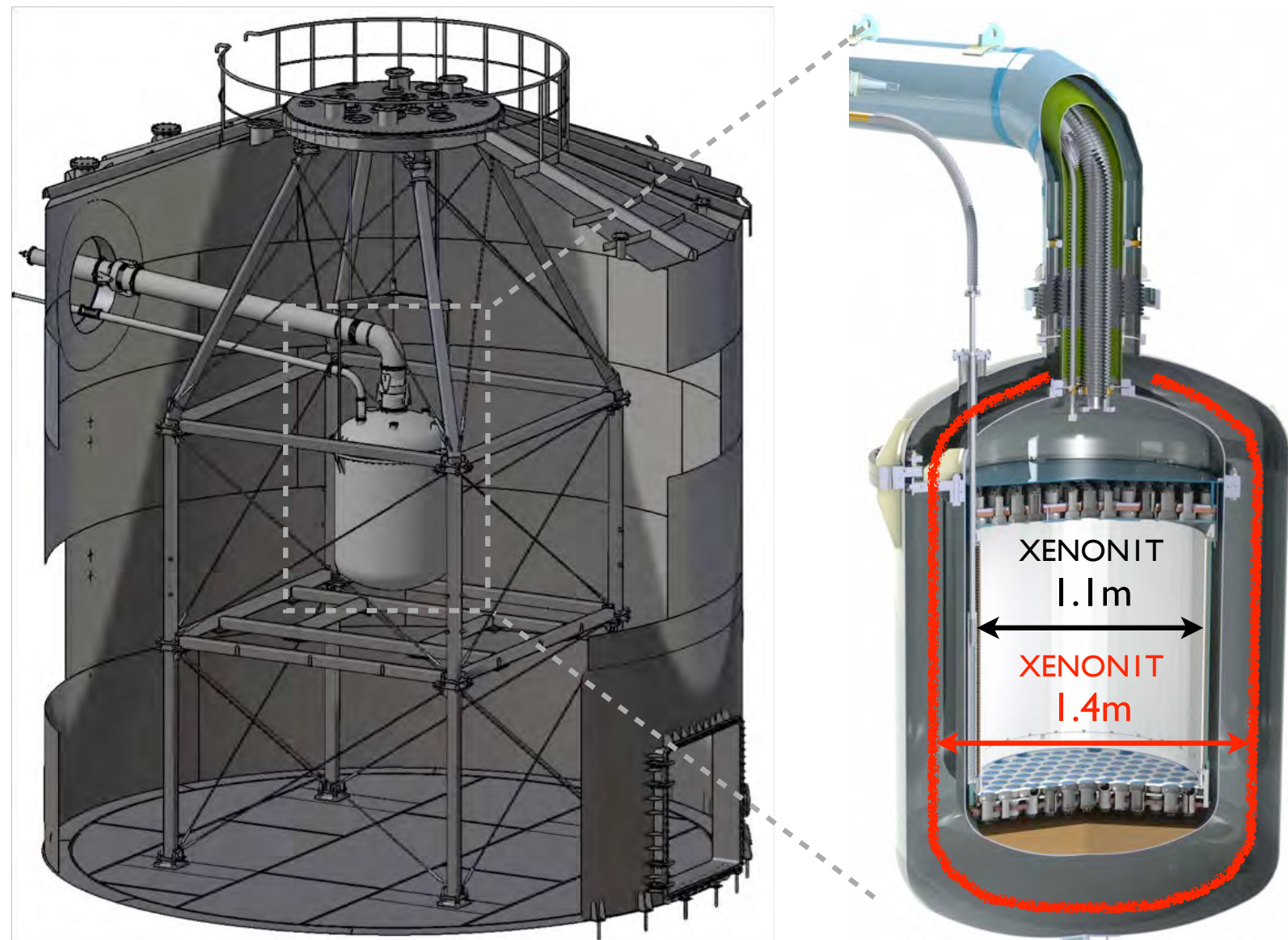
XENON1T NR background predictions

- Radiogenic neutrons: about 0.6 events/(ton x yr) in (5,50) keV
- Neutrinos: 1.8×10^{-2} events/(ton x yr) in (5,50) keV



XENONnT: 2018-2020

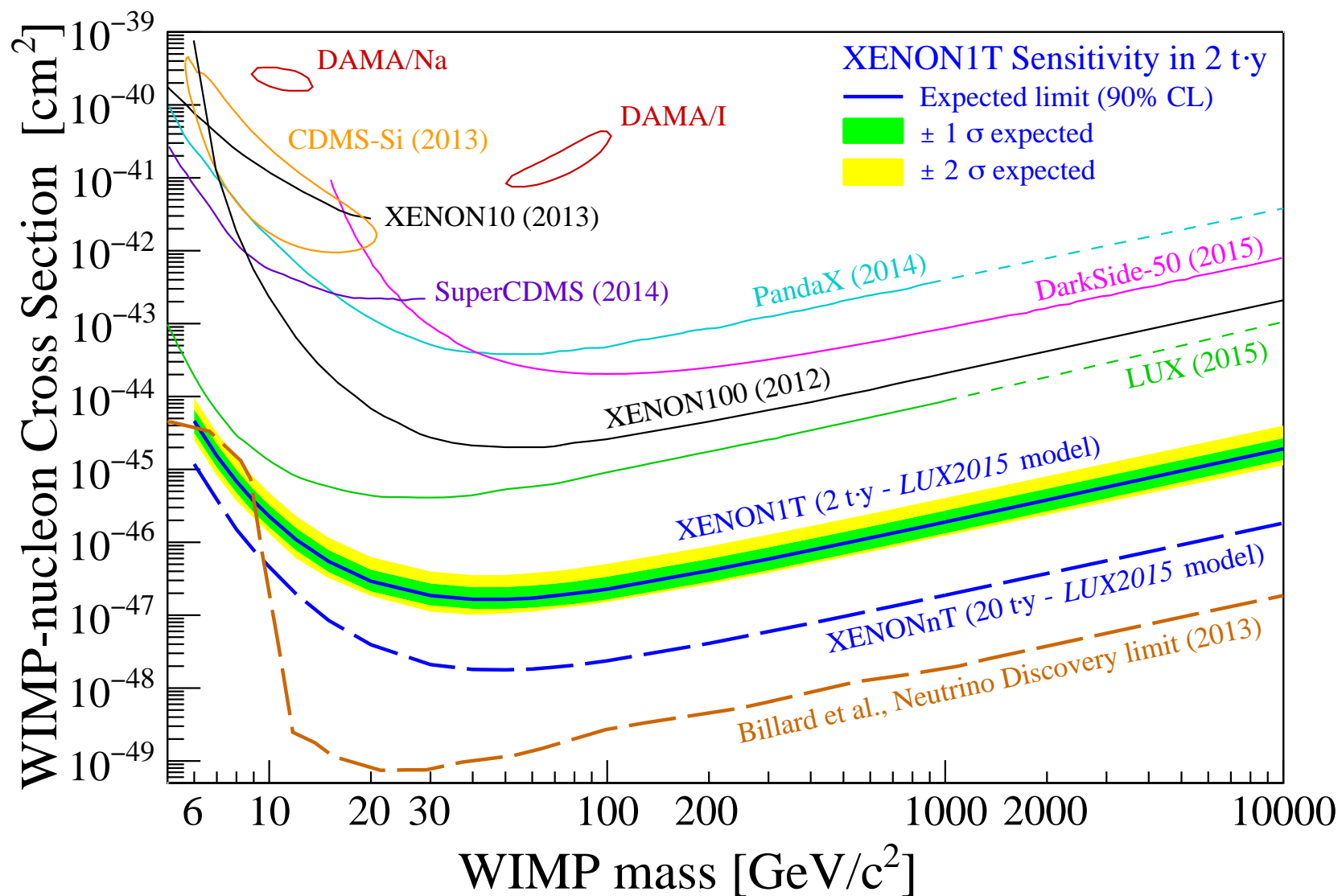
- Plan: double the amount of LXe (~7 tons), double the number of PMTs
- XENON1T is constructed such that many sub-systems will be reused for the upgrade:



- Water tank + muon veto
- Outer cryostat and support structure
- Cryogenics and purification system
- LXe storage system
- Cables installed for XENONnT as well
- + LXe, PMTs, electronics needed

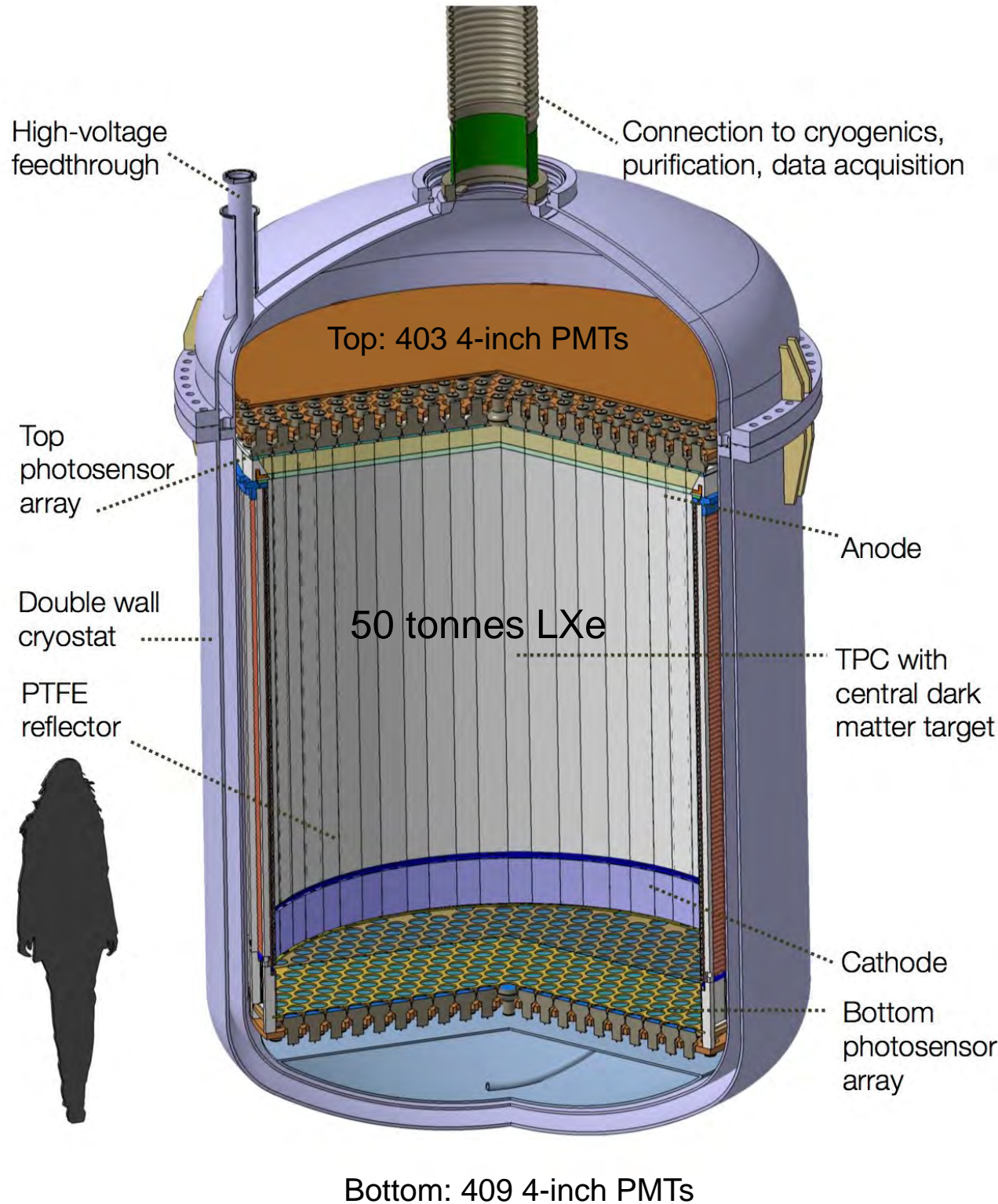
XENON1T (and XENONnT) sensitivity

- Exposure 2 years in 1 tonne fiducial volume
- Minimum probed cross section: $1.6 \times 10^{-47} \text{ cm}^2$ for a 50 GeV WIMP

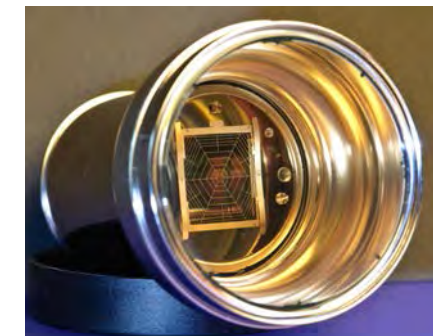


Events in 2 t·y exposure	
6 GeV WIMP $2 \times 10^{-45} \text{ cm}^2$	2.7
10 GeV WIMP $2 \times 10^{-46} \text{ cm}^2$	6.0
100 GeV WIMP $2 \times 10^{-47} \text{ cm}^2$	7.1
1 TeV WIMP $2 \times 10^{-46} \text{ cm}^2$	8.9
NR neutrons	1.1
NR neutrinos	5.4

DARWIN Dark matter WIMP search with noble liquids



- 50 t (40 t) LXe in total (in the TPC)
- $\sim 10^3$ photosensors
- 2.6 m drift length
- 2.6 m diameter TPC
- PTFE reflectors, Cu field shaping rings
- Background: dominated by neutrinos



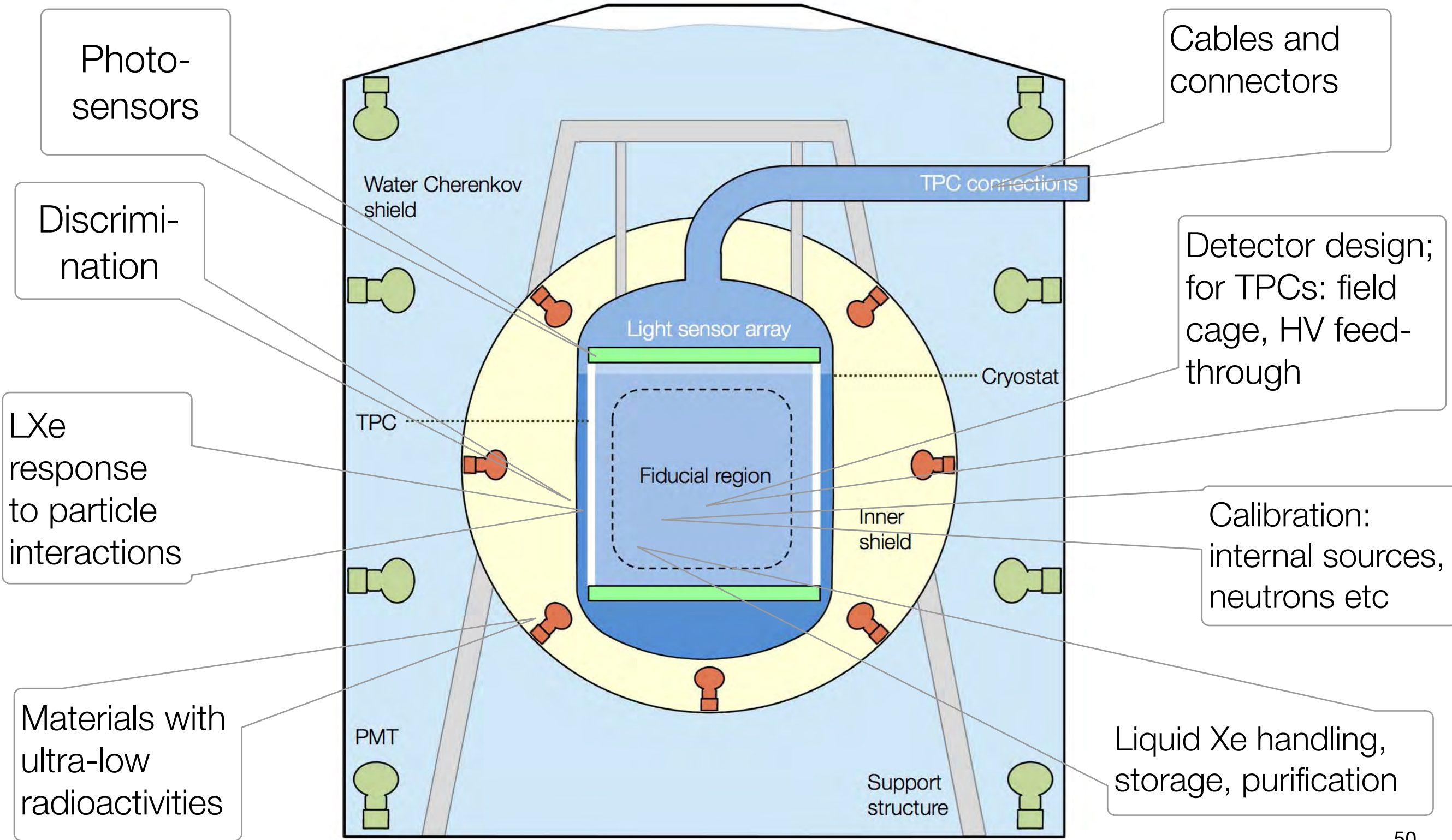
3-inch PMT, R11410-21



4-inch PMT

Strong R&D programme in place

DARWIN collaboration, arXiv:1606.07001

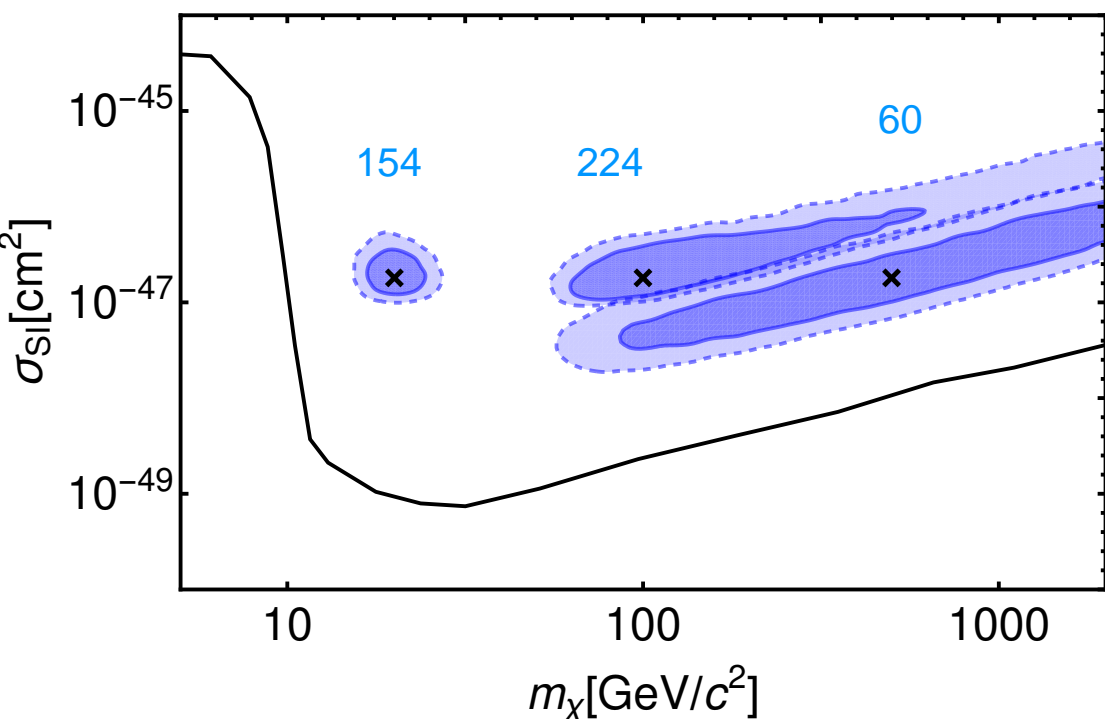


WIMP physics: spectroscopy

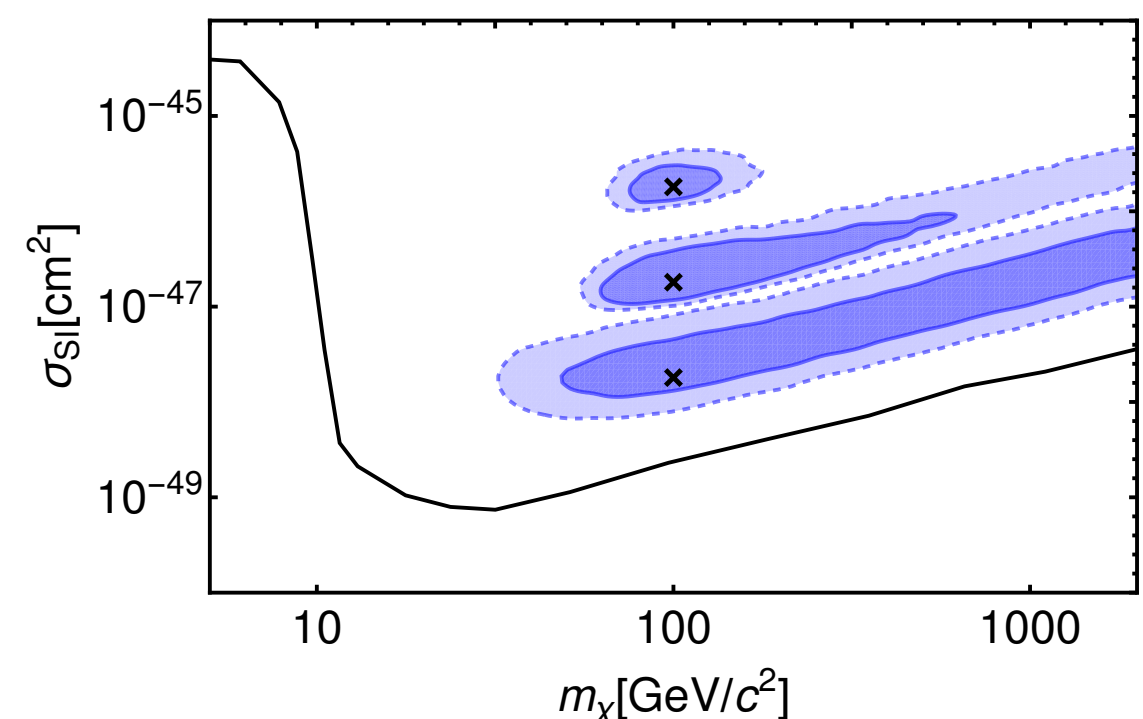
DARWIN collaboration, arXiv:1606.07001

- Capability to reconstruct the WIMP mass and cross section for various masses (**20, 100, 500 GeV/c²**) and cross sections

Exposure: 200 t y



Exposure: 200 t y



1 and 2 sigma credible regions after marginalising the posterior probability distribution over:

$$v_{\text{esc}} = 544 \pm 40 \text{ km/s}$$

$$v_0 = 220 \pm 20 \text{ km/s}$$

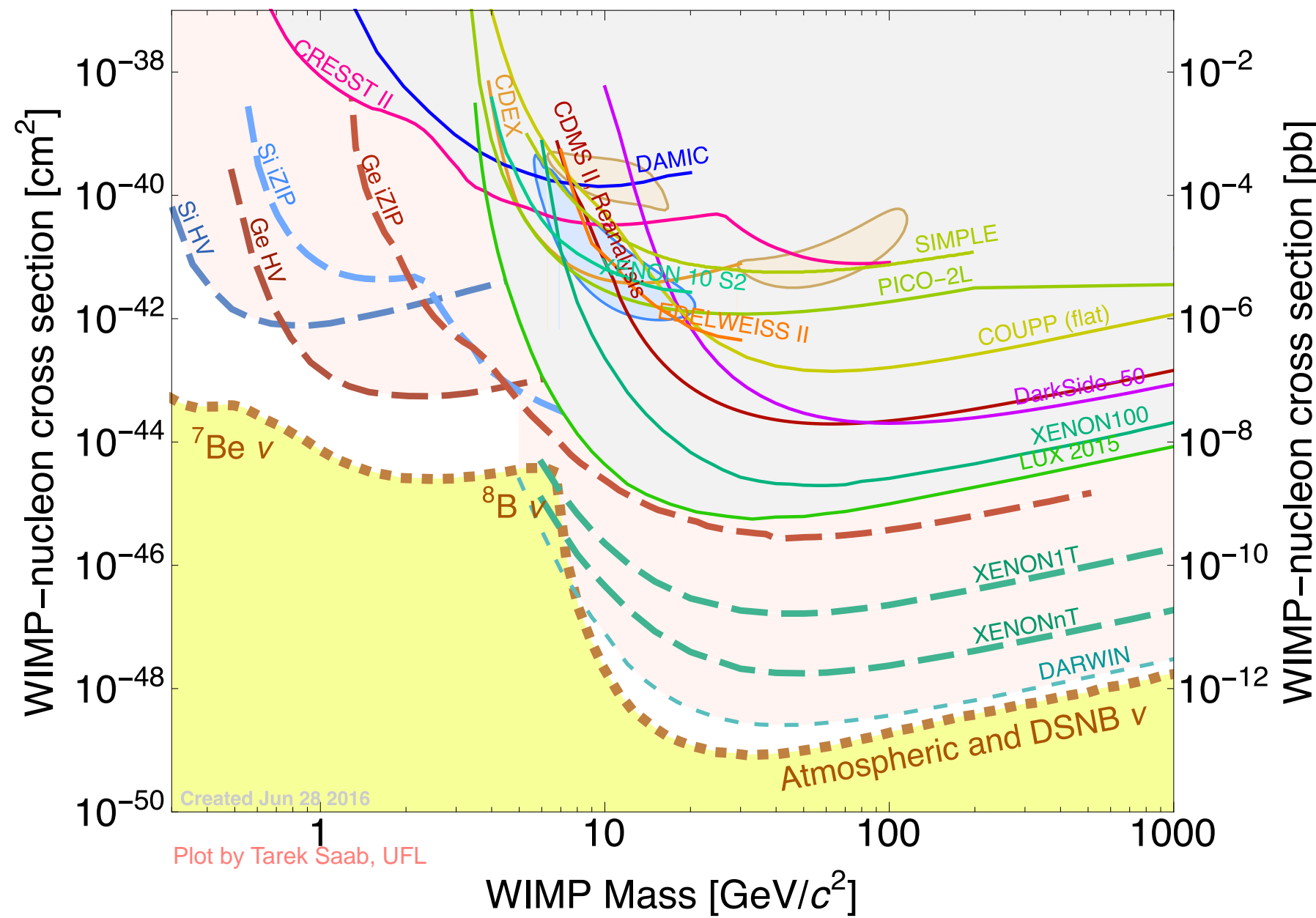
$$\rho_\chi = 0.3 \pm 0.1 \text{ GeV/cm}^3$$

Update: Newstead et al., PRD D 88,
076011 (2013)

WIMP physics

Of course, “the probability of success is difficult to estimate,
but if we never search, the chance of success is zero”

G. Cocconi & P. Morrison, Nature, 1959



Cryogenic Experiments at mK Temperatures

Cryogenic Experiments at mK Temperatures

- Principle: phonon (quanta of lattice vibrations) mediated detectors
- **Motivation:** increase the energy resolution + detect smaller energy depositions (lower the threshold); use a variety of absorber materials (not only Ge and Si)
- The energy resolution ($W = \text{FWHM}$) of a semiconductor detector ($N = \text{nr. of } e^-h \text{ excitations}$)

$$W_{stat} = 2.35 \sqrt{F\epsilon E} \quad \frac{\sigma(E)}{E} = \sqrt{\frac{F}{N}} = \sqrt{\frac{F\epsilon}{E}} \quad W_{stat} = 2.35 \sigma(E)$$

- E = deposited energy; F = Fano factor; $N = E/\epsilon$; in Si: $\epsilon = 3.6 \text{ eV}/e^-h$ pair (band gap is 1.2 eV! - where does 70% of the energy go?). $F \rightarrow$ the energy loss in a collision is not purely statistical ($=0.13$ in Ge; 0.11 in Si)
- Maximum phonon energy in Si: 60 meV
 - **many more phonons are created than e^-h pairs!**
- For dark matter searches:
 - **thermal phonon detectors (measure an increase in temperature)**
 - **athermal phonon detectors (detect fast, non-equilibrium phonons)**
- Detector made from superconductors: the superconducting energy gap $2\Delta \sim 1 \text{ meV}$
 - binding energy of a Cooper pair (equiv. of band gap in semiconductors); 2 quasi-particles for every unbound Cooper pair; these can be detected \rightarrow in principle large improvement in energy resolution

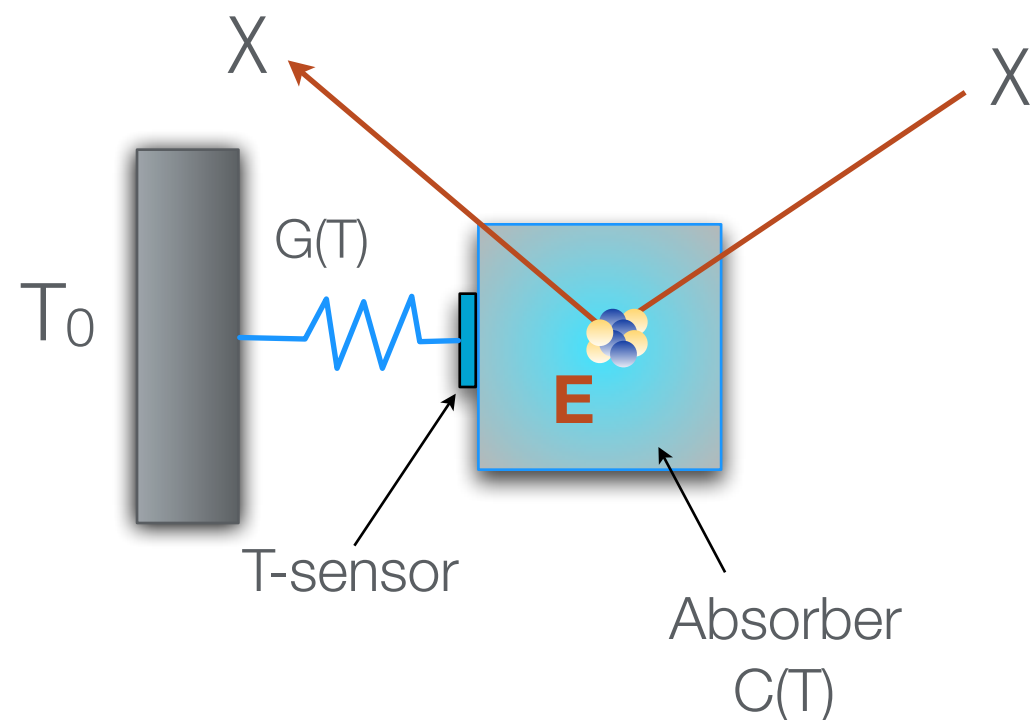
Basic Principles of mK Cryogenic Detectors

- A deposited energy E (ER or NR) will produce a temperature rise ΔT given by:

$$\Delta T = \frac{E}{C(T)} e^{-\frac{t}{\tau}} \quad \tau = \frac{C(T)}{G(T)}$$

$C(T)$ = heat capacity of absorber

$G(T)$ = thermal conductance of the link between the absorber and the reservoir at temperature T_0



Normal metals: the electronic part of $C(T) \sim T$, and dominates the heat capacity at low temperatures

Superconductors: the electronic part is proportional to $\exp(-T_c/T)$ (T_c = superconducting transition temperature) and is negligible compared to lattice contributions for $T \ll T_c$

Basic Principles of mK Cryogenic Detectors

- For pure dielectric crystals and superconductors at $T \ll T_c$, the heat capacity is given by:

$$C(T) \sim \frac{m}{M} \left(\frac{T}{\theta_D} \right)^3 \text{ J K}^{-1}$$

m = absorber mass

M = molecular weight of absorber

Θ_D = Debye temperature (at which the highest frequency gets excited) $\theta_D = \frac{h\nu_m}{k}$

- the lower the T, the larger the ΔT per unit of absorbed energy
- in thermal detectors E is measured as the temperature rise ΔT
- **Example:** at $T = 10$ mK, a 1 keV energy deposition in a 100 g detector increases the temperature by:

$$\Delta T \approx 1 \mu K$$

- this can be measured!

Thermal Detectors

- The intrinsic energy resolution (as FWHM) of such a calorimeter is given by (k_B is the Boltzmann constant):

$$W = 2.35\xi \sqrt{k_B T^2 C(T)}$$

$$\frac{C(T)}{k_B} = \text{number of phonon modes}$$
$$k_B T = \text{mean energy per mode}$$

$$\xi = 1.5 - 2$$

Info about the sensor, the thermal link and the T-dependance of $C(T)$

- Example for the theoretical expectation of the intrinsic energy resolution:

- a 1 kg Ge crystal operated at 10 mK could achieve an energy resolution of about 10 eV => two orders of magnitude better than Ge ionization detectors
- a 1 mg of Si at 50 mK could achieve an energy resolution of 1 eV => two orders of magnitude better than conventional Si detectors

Temperature Sensors

- **Semiconductor thermistor:** a highly doped semiconductor such that the resistance R is a strong function of temperature (NTD = neutron-transmutation-doped Ge - uniformly dope the crystal by neutron irradiation)
- **Superconducting (SC) transition sensor (TES/SPT):** thin film of superconductor biased near the middle of its normal/SC transition
- For both NTDs and TESs/SPTs, an energy deposition produces **a change in the electrical resistance $R(T)$** . The response can be expressed in terms of the logarithmic sensitivity:

$$\alpha \equiv \frac{d\log(R(T))}{d\log(T)}$$

Typical values:

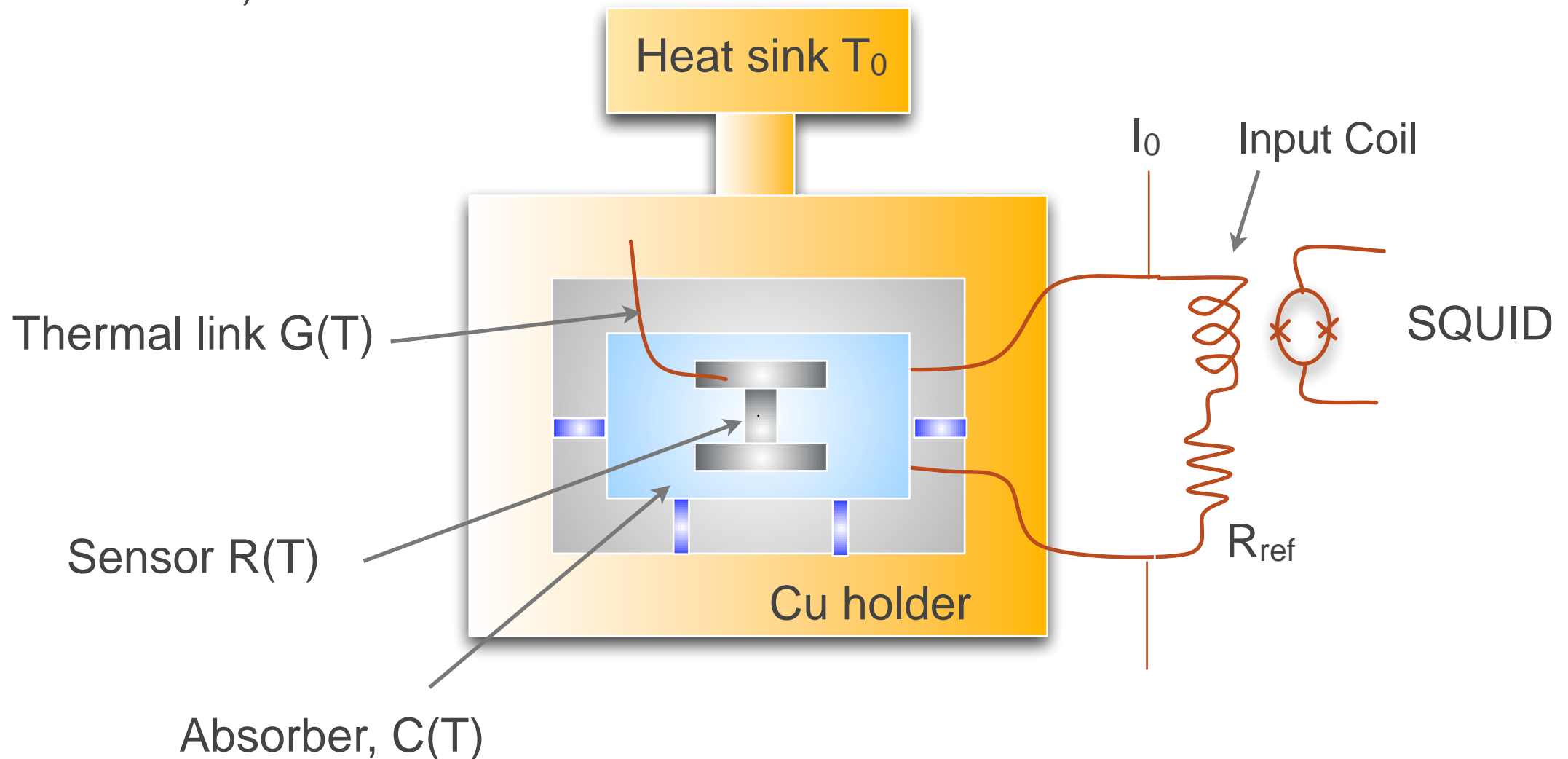
$\alpha = -10$ to -1 for semiconductor thermistors

$\alpha \sim +10^3$ for TES/SPT devices

- the sensitivity of TES/SPTs can be extremely high (depending on the width of the SC/normal transition)
- however, the temperature of the detector system must be kept very stable

Example: Thermal Detector with SPT-sensor

- The change of resistance due to a particle interaction in the absorber is detected by a superconducting quantum interference device (SQUID) (by the change in current induced in the input coil of the SQUID)



- Thermal detectors:** slow \rightarrow ms for the phonons to relax to a thermal distribution
- TES:** can be used to detect fast, athermal phonons \rightarrow how are these kept stable?

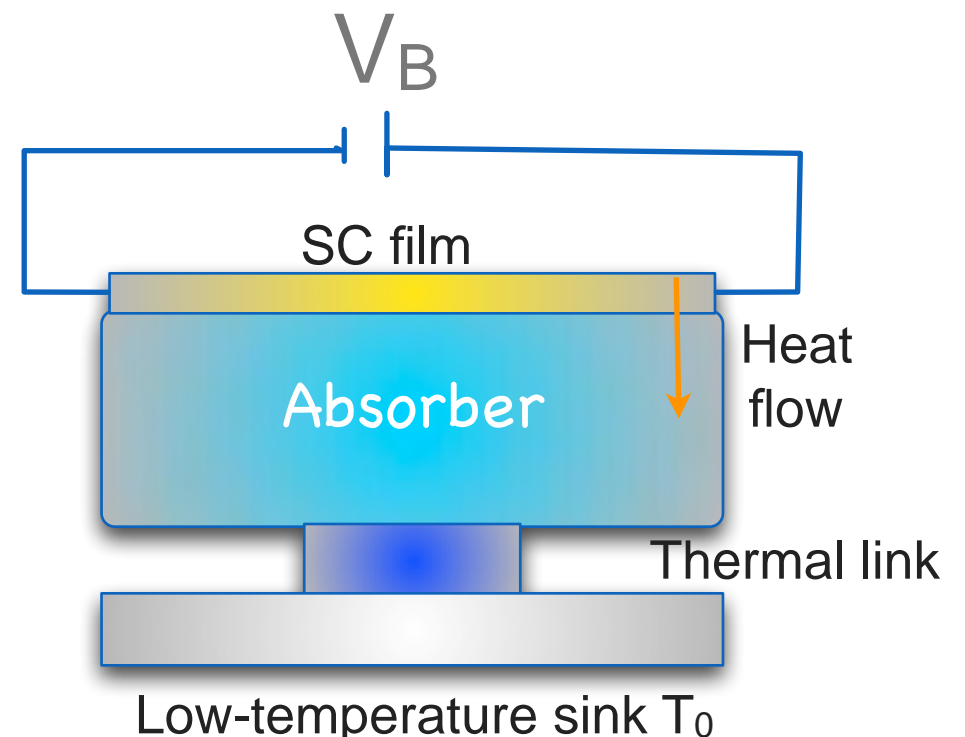
TES with Electrothermal-Feedback

- $T_0 \ll T_c$: substrate is cooled well below the SC transition temperature T_c

- A voltage V_B is placed across the film (TES)
and equilibrium is reached when ohmic heating of
the TES by its bias current is balanced by the
heat flow into the absorber

When an excitation reaches the TES

- the resistance R increases
- the current decreases by ΔI
- ⇒ this results in a reduction in the Joule heating



The feedback signal = the change in Joule power heating the film $P=IV_B=V_B^2/R$

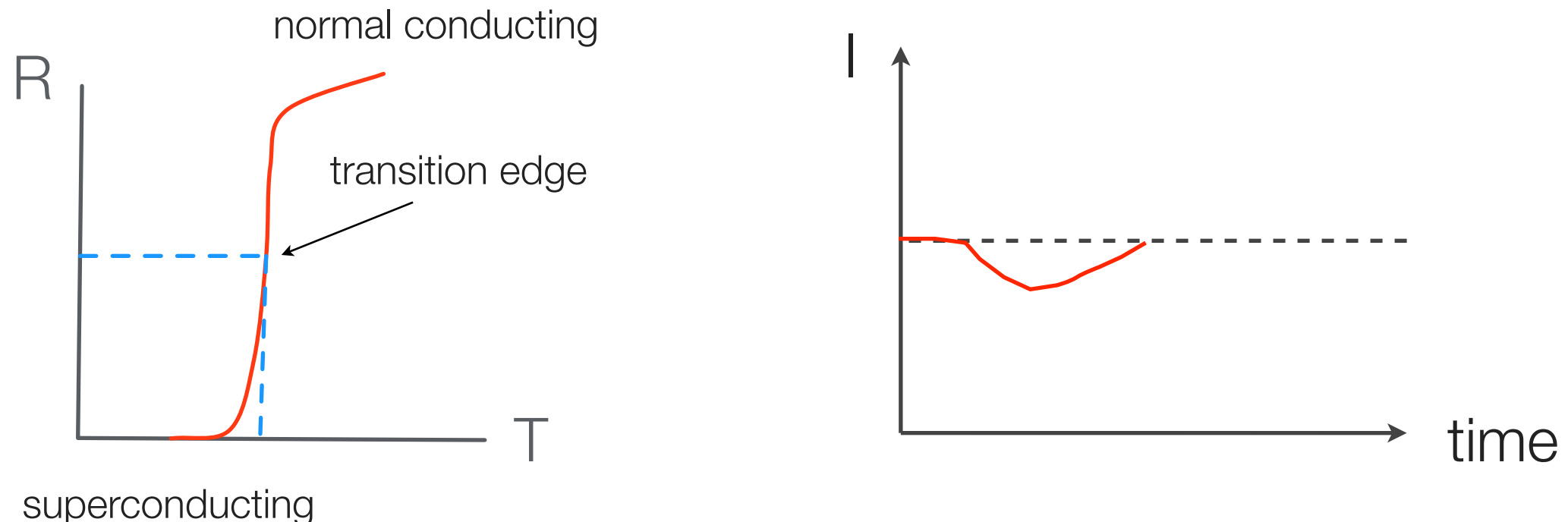
The energy deposited is then given by:

=> the device is self-calibrating

$$E = -V_B \int \Delta I(t) dt$$

TES with Electrothermal-Feedback

- By choosing the voltage V_B and the film resistivity properly
=> one achieves a stable operating T on the steep portion of the transition edge



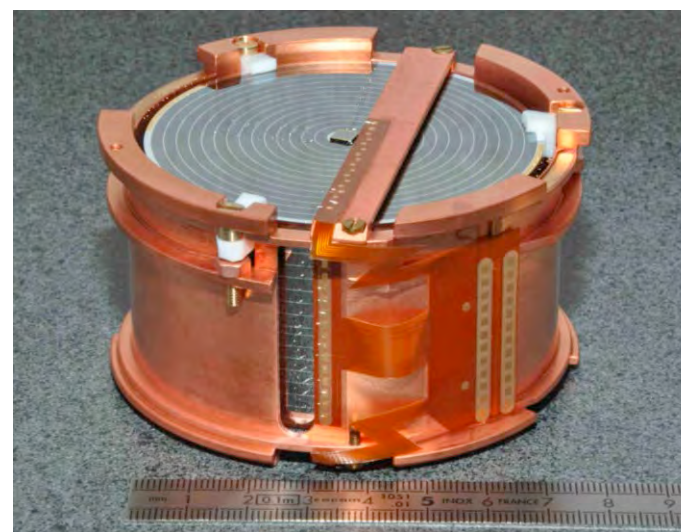
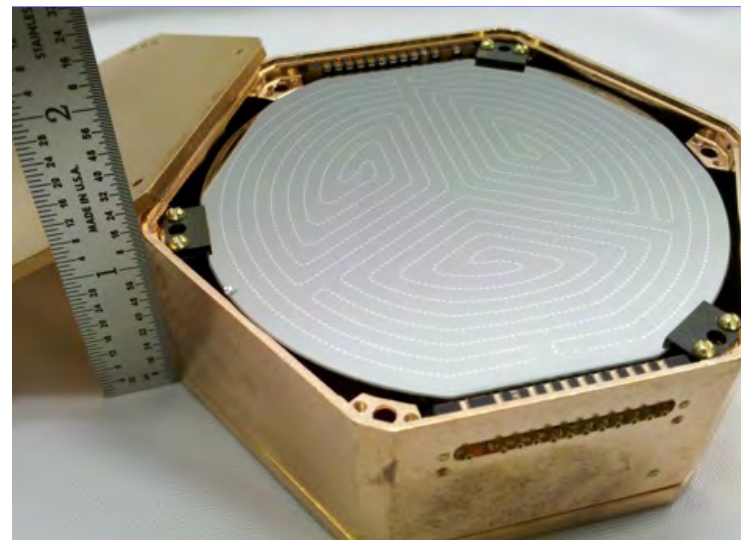
ET-feedback: leads to a thermal response time 10^2 faster than the thermal relaxation time
+ a large variety of absorbers can be used with the transition edge sensor

Experiments at ~mK temperatures

CDMS at Soudan
SuperCDMS at SNOlab
Ge/Si detectors at 30 mK
Detect phonons and charge

EDELWEISS at Modane
Ge detectors at 18 mK
Detect phonons and charge

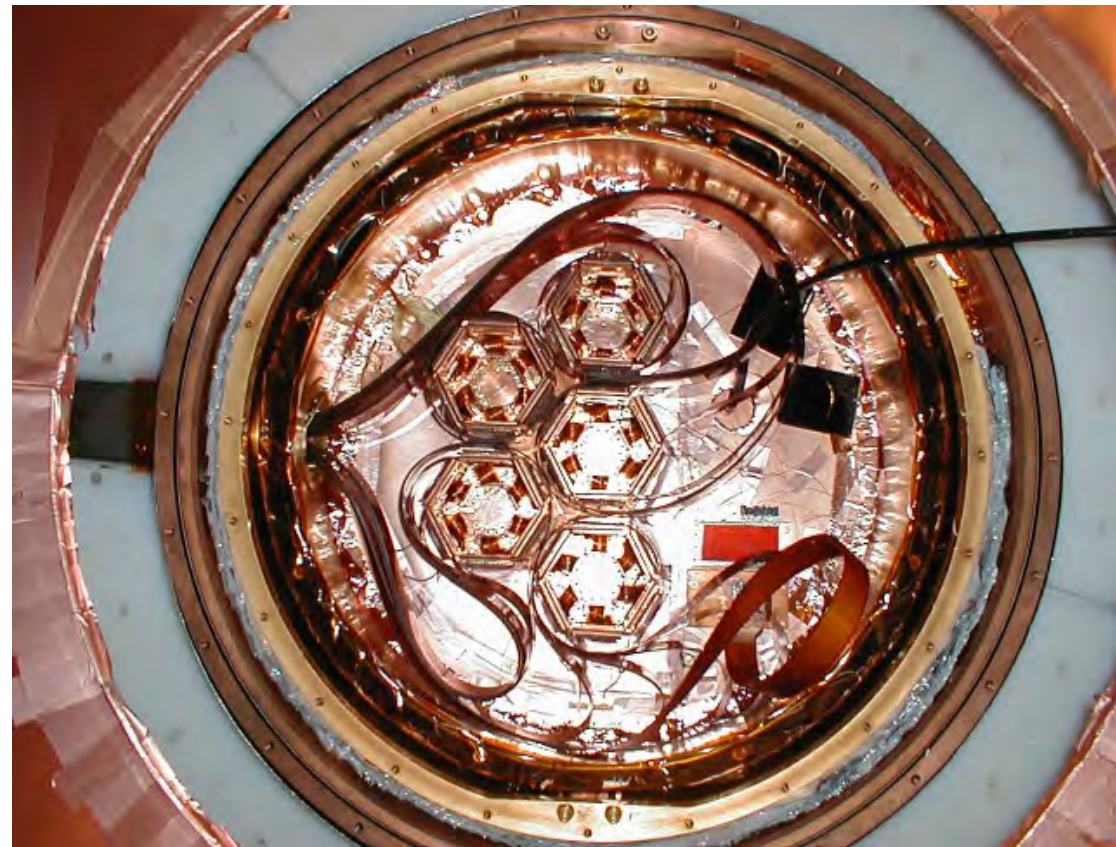
CRESST at LNGS
CaWO₃ detectors at 10 mK
Detect phonons and light



Example: the CDMS Experiment at the Soudan Mine

At the Soudan Lab in Minnesota:
neutron background reduced from
 $1/\text{kg/day} \rightarrow 1/\text{kg/year}$

5 towers a 6 Ge/Si detectors
in the ‘icebox’ were kept at $\approx 40\text{ mK}$



The Phonon Signal in CDMS

Particle interaction \Rightarrow THz (~ 4 meV) phonons

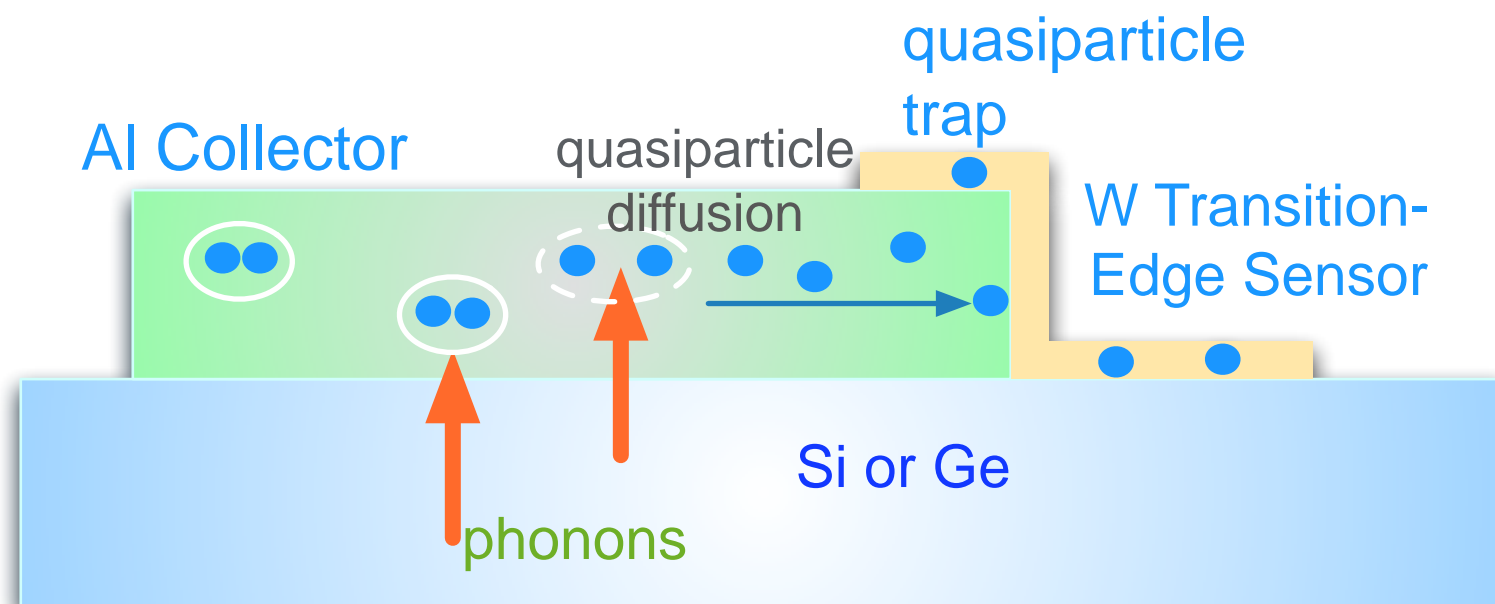
Phonons: propagate to SC Al-fins on the surface, break Cooper pairs \Rightarrow quasiparticles

Quasiparticles: diffuse in 10 μ s through the Al-fins and are trapped in the W-TES
 \Rightarrow release their binding energy to the W electrons

The electron system temperature is raised \Rightarrow increased resistance R

The TES is voltage biased and operated in the ETFB-mode

Current change is measured by SQUIDs

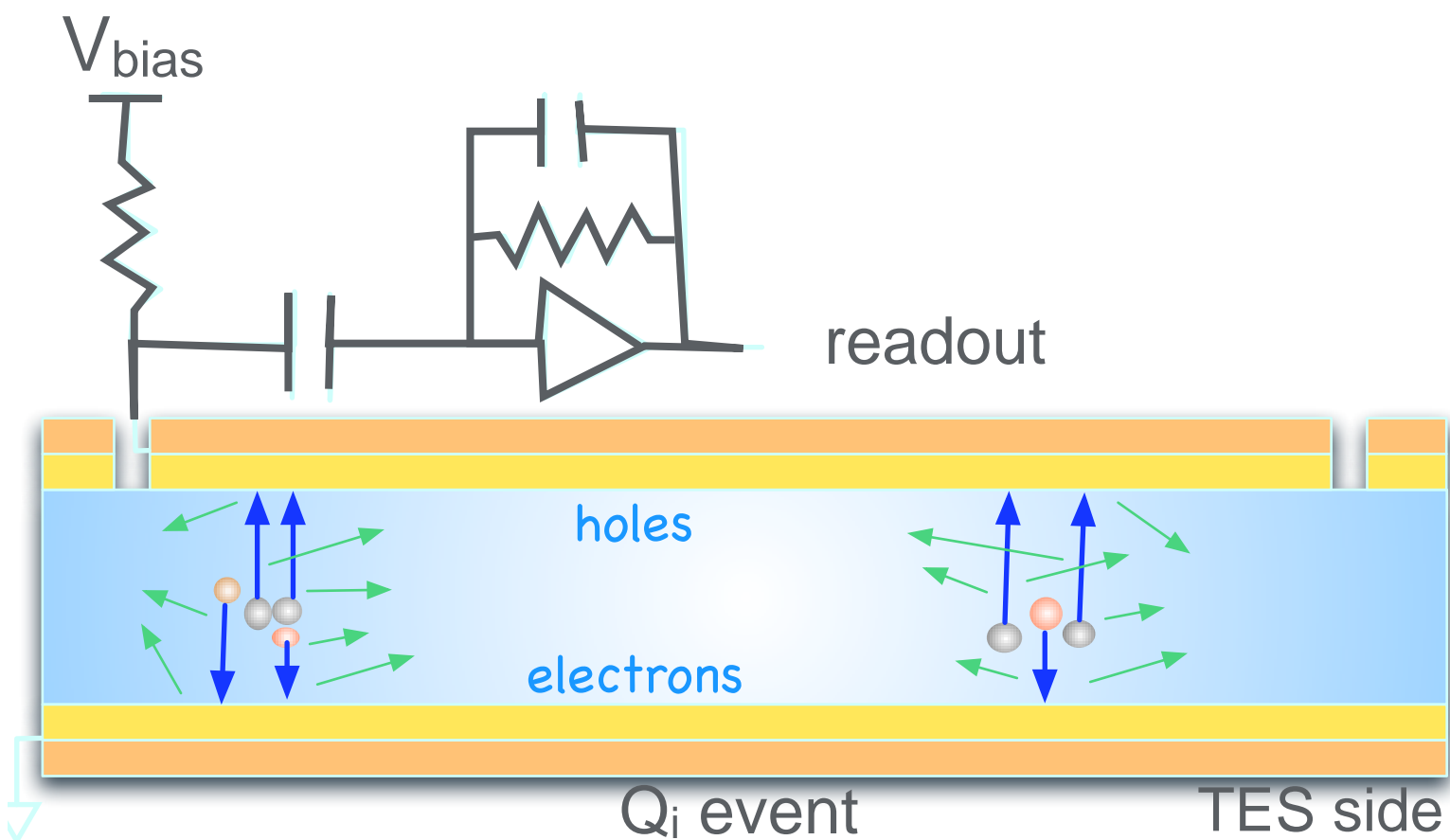


The Charge Signal in CDMS

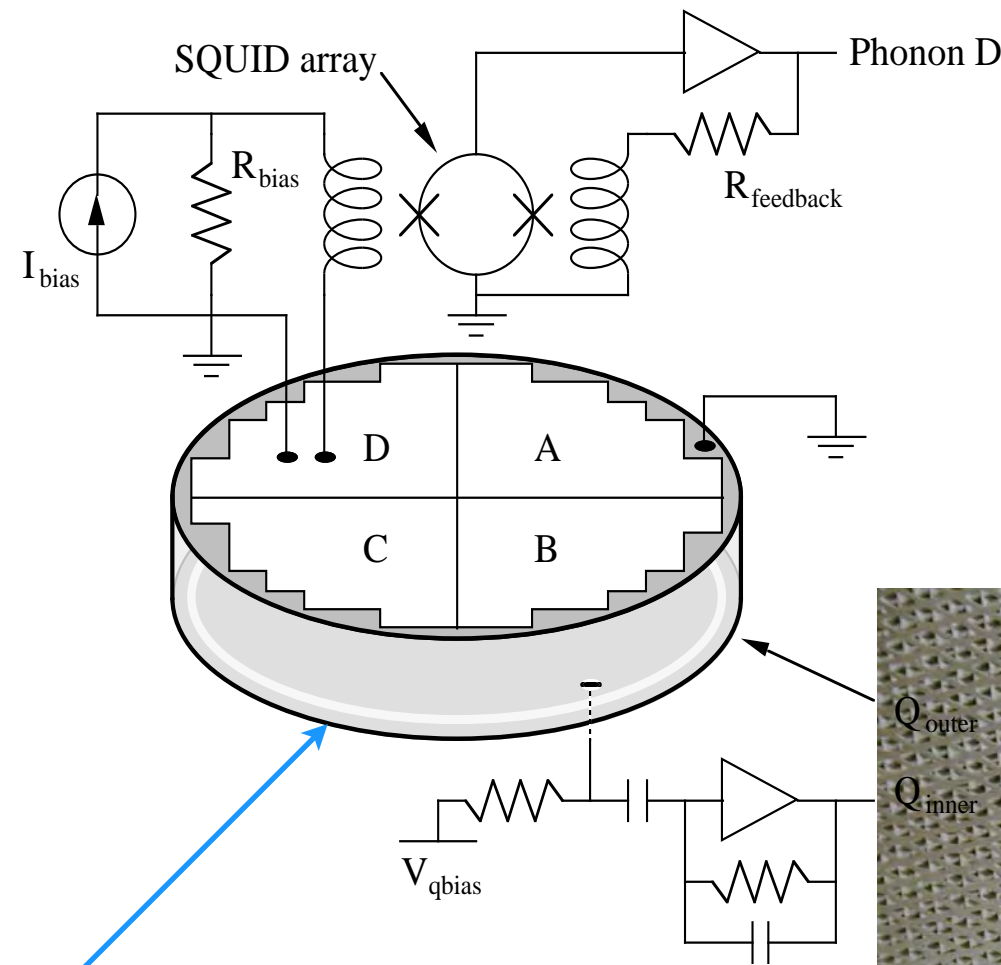
Interaction in the detector: breaks up the e-hole pairs in the crystal, separated by E-field
=> charge is collected by electrodes on the surface of the crystal

Two charge channels:

disk in the centre ($\approx 85\%$ of surface) + ring at the edge of the crystal surface
Events within few μm of the surface: deficit charge collection (“dead layer”)



CDMS Detectors: charge and phonon sensors

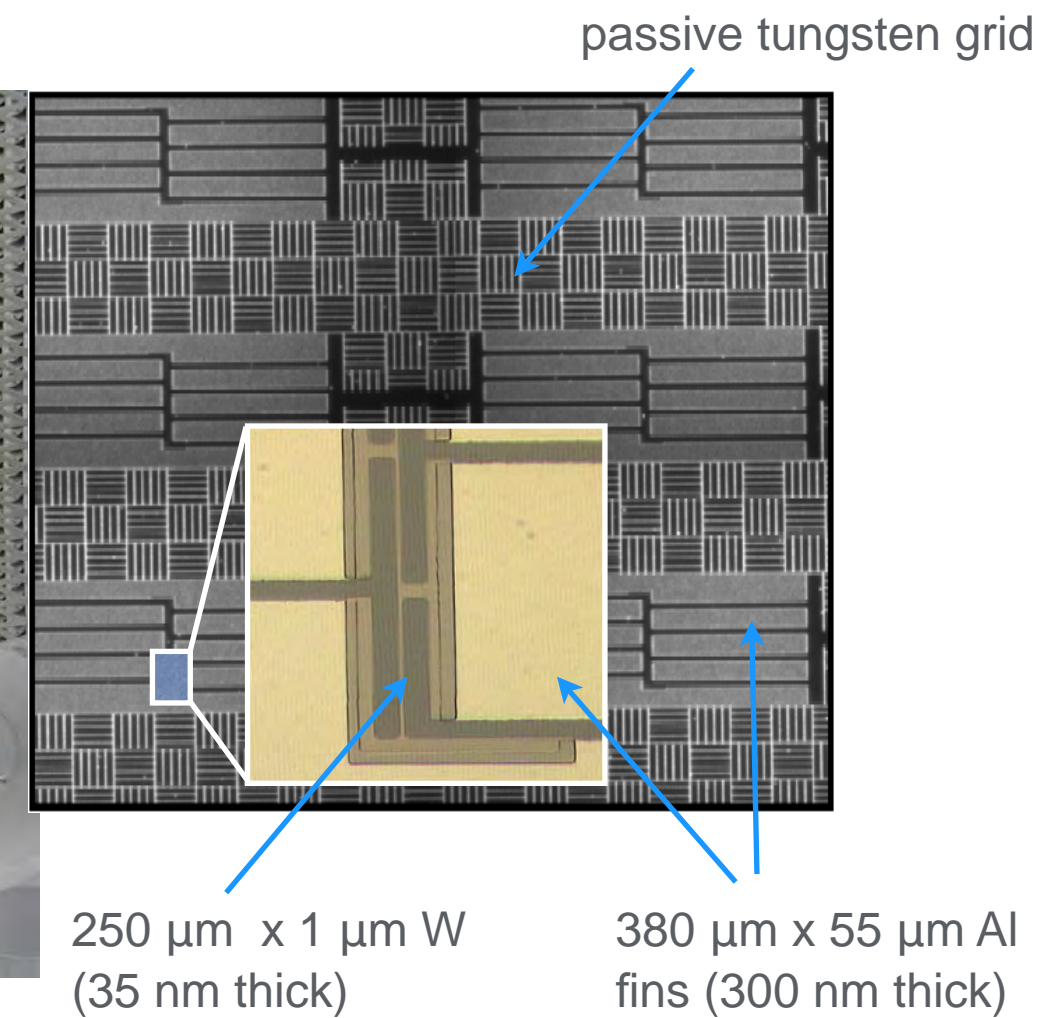
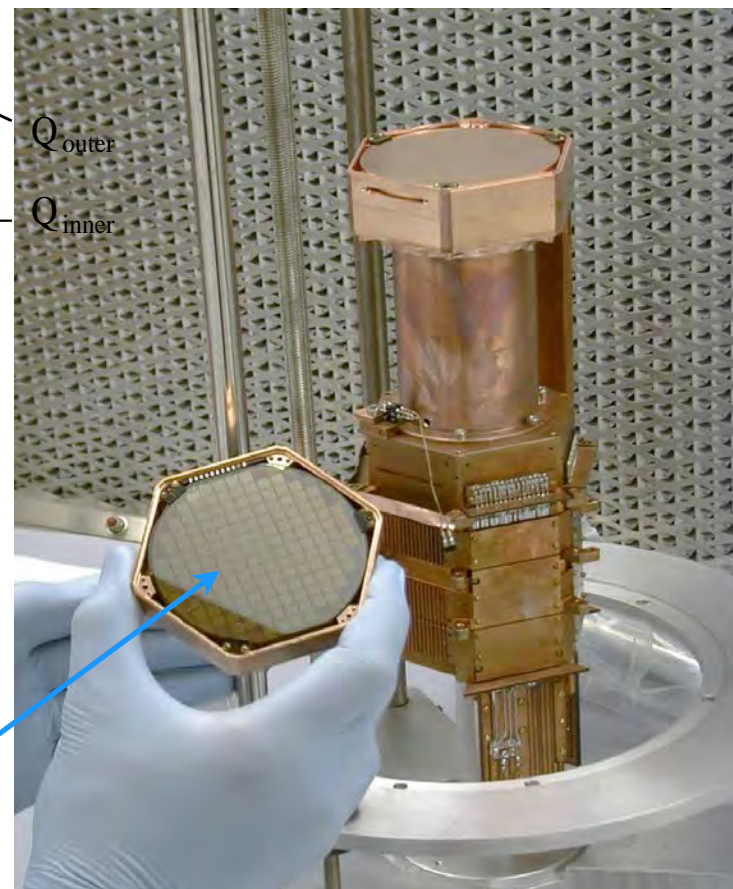


Absorber:

250 g Ge or 100 g Si crystals
1 cm thick x 7.5 cm diameter

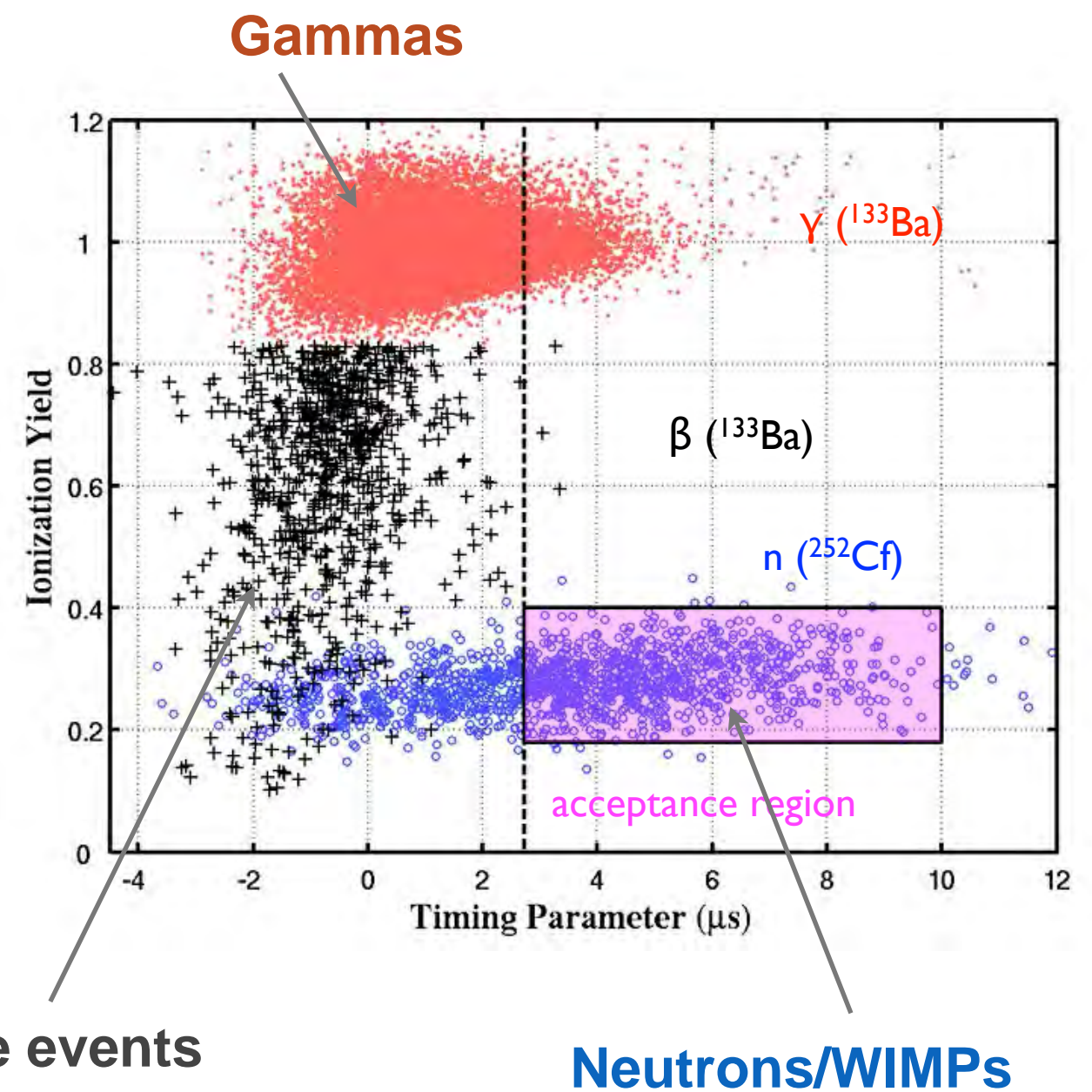
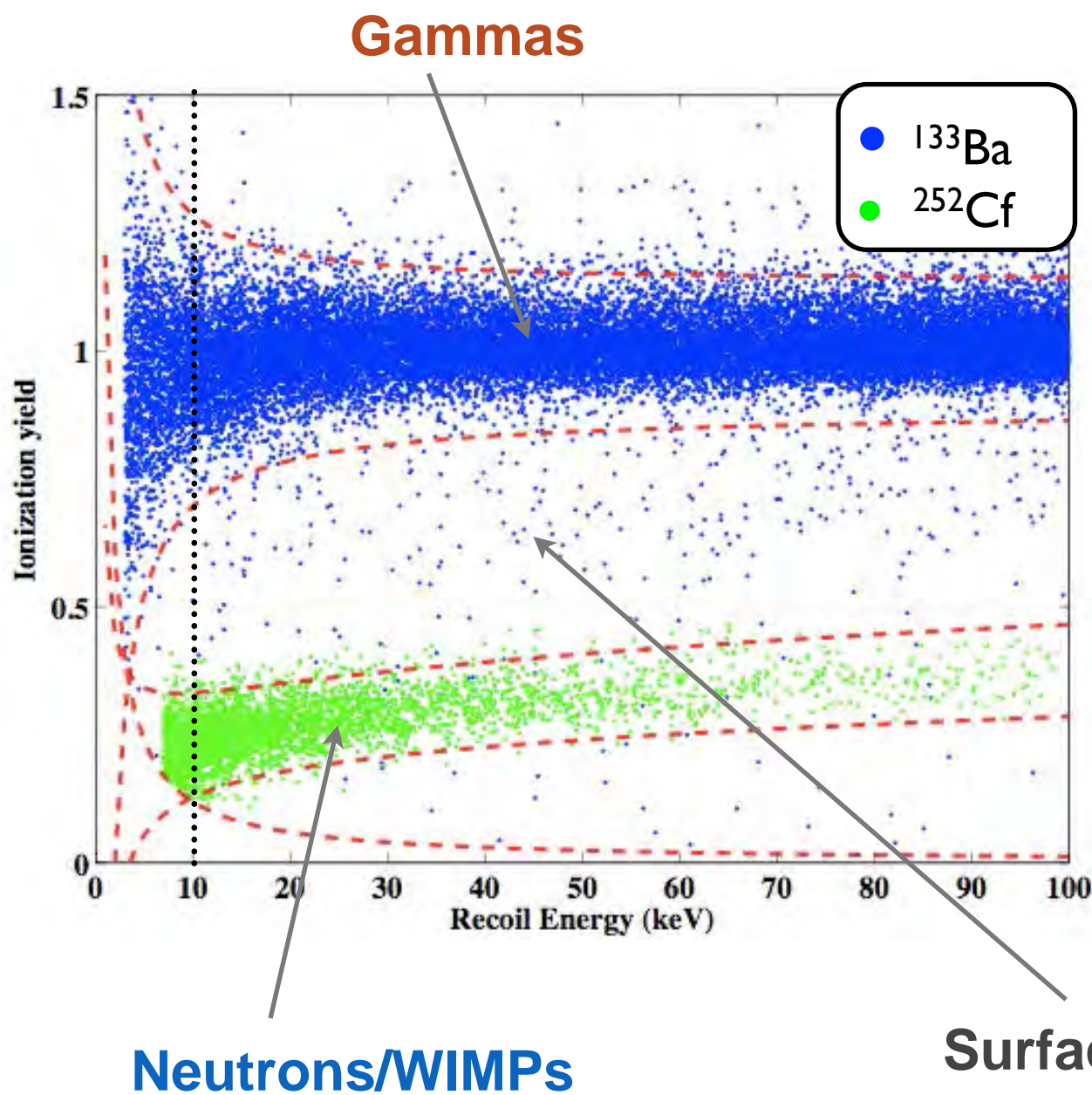
T-sensors:

photolithographically patterned thin films of Al +W, collecting athermal phonons

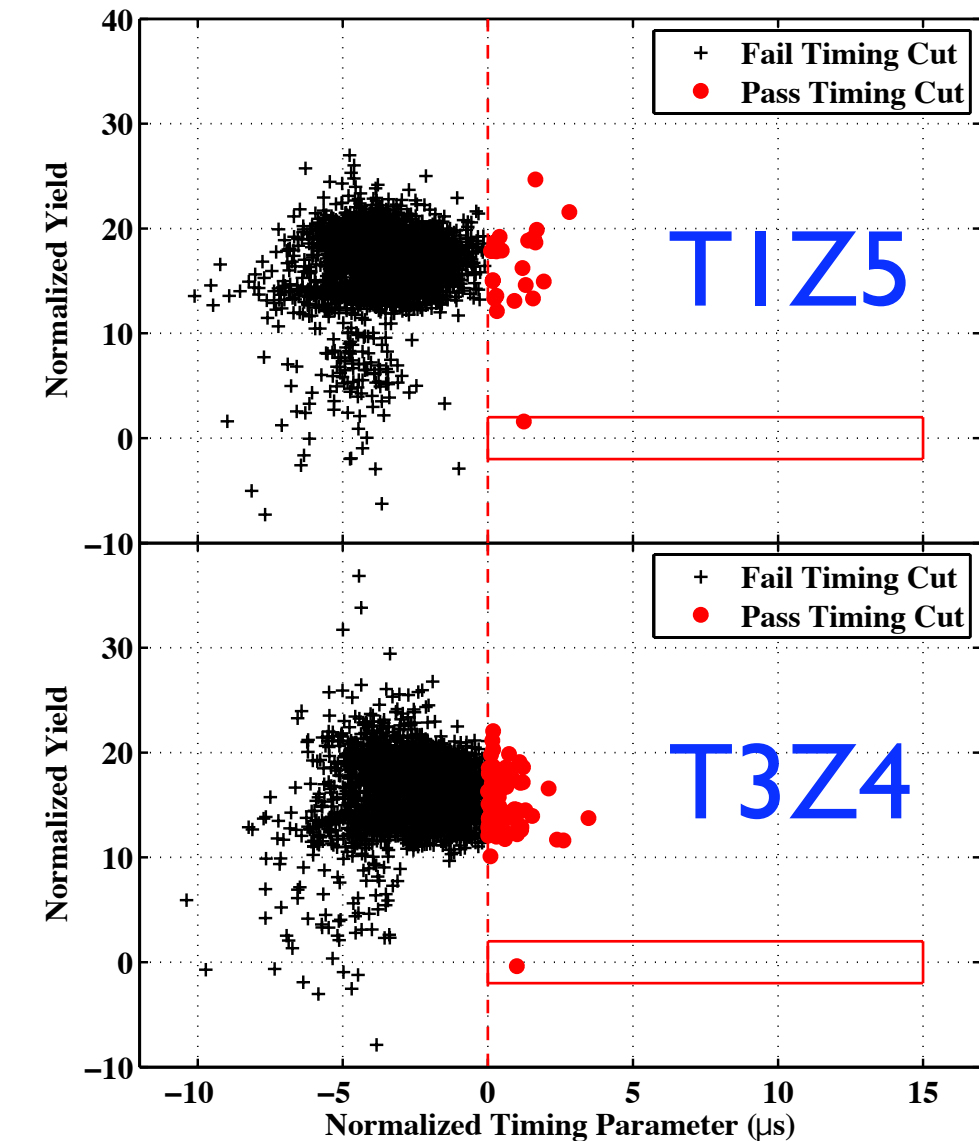
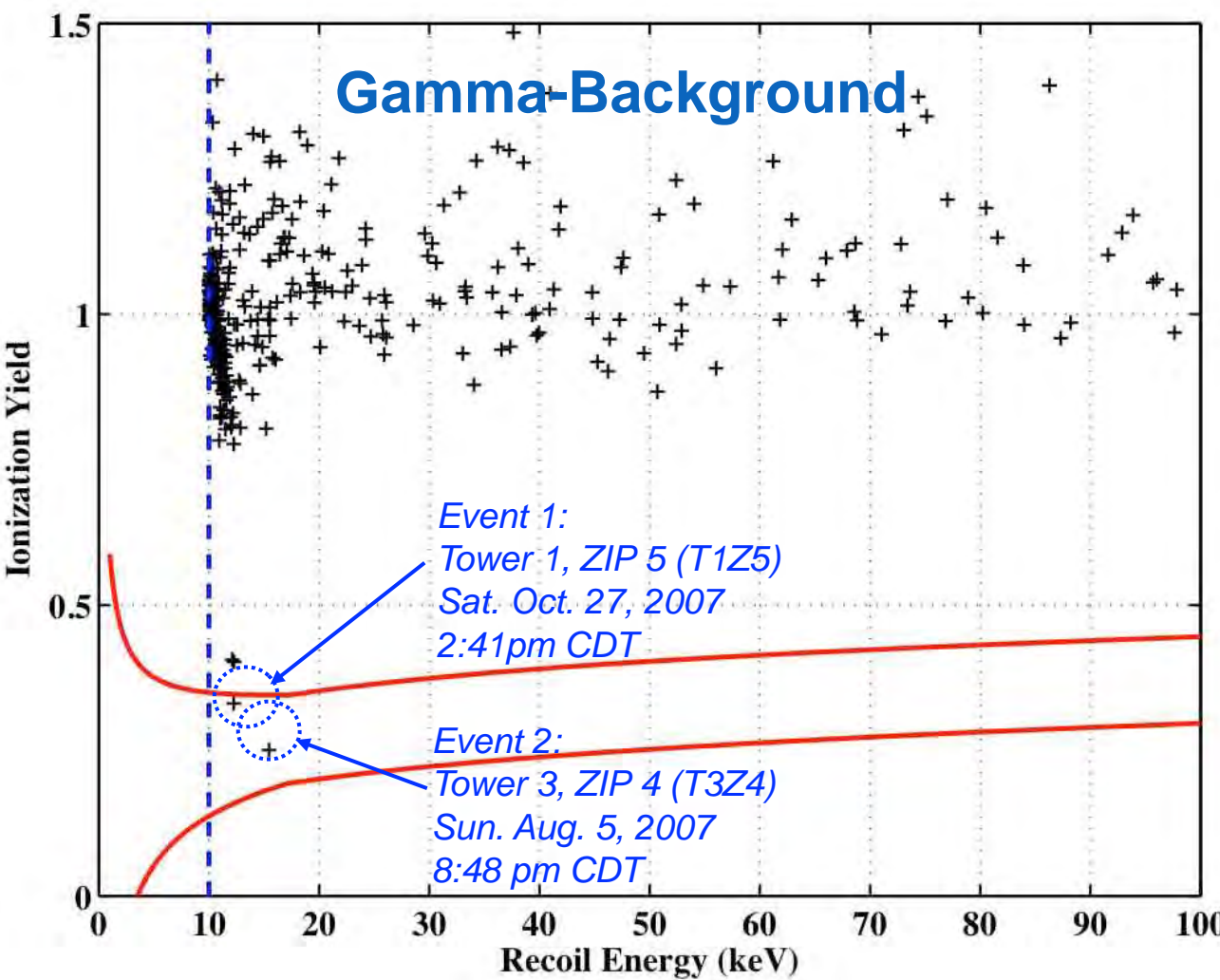


Background rejection

- Ratio of the charge/phonon-signal and time difference between charge and phonon signals => distinguish signal (WIMPs) from background of electromagnetic origin



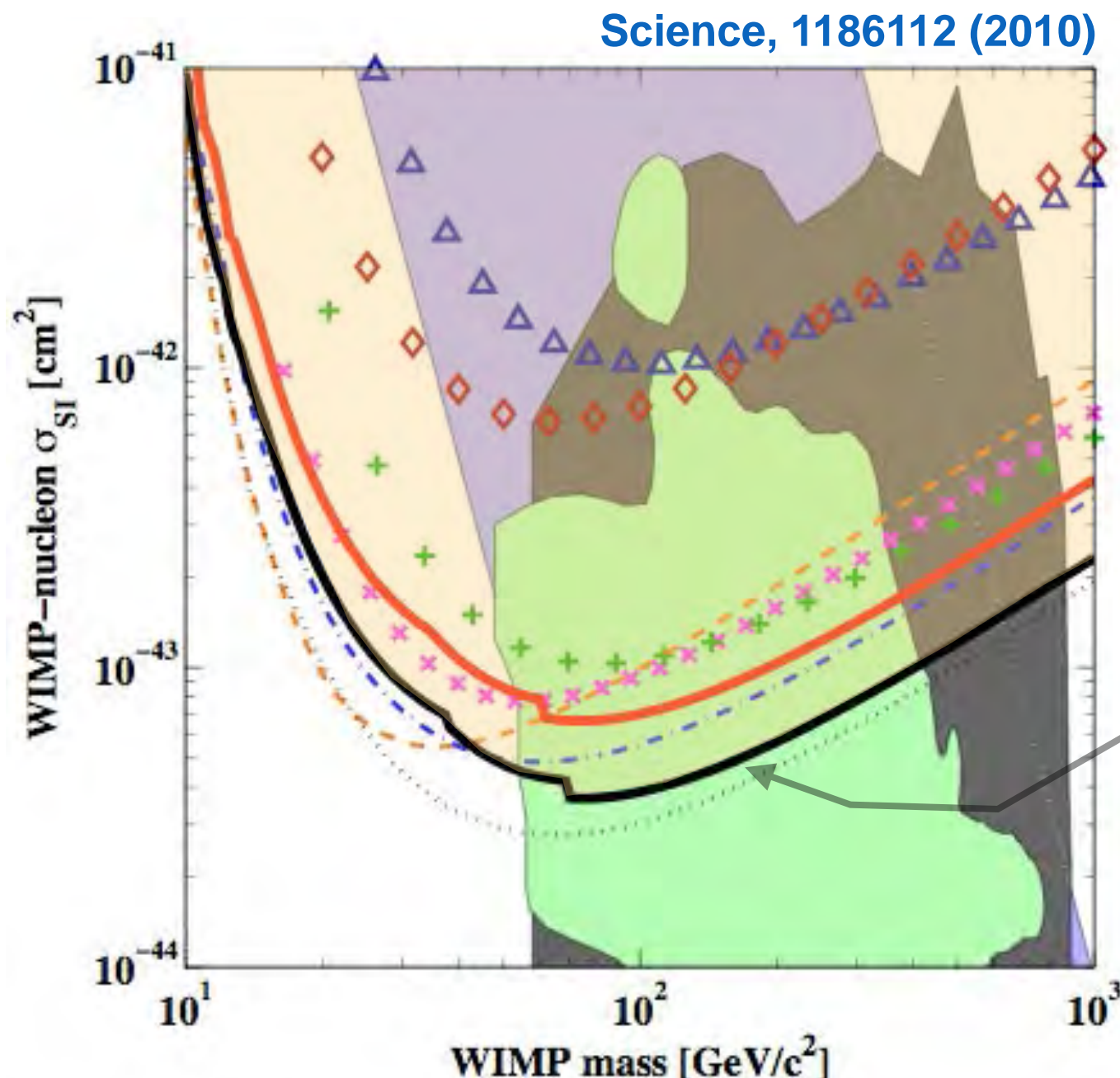
Example: CDMS WIMP Search Run of 191 kg days



Two events passing all cuts

(which were set based on calibration and background data outside the WS region = side-band events)

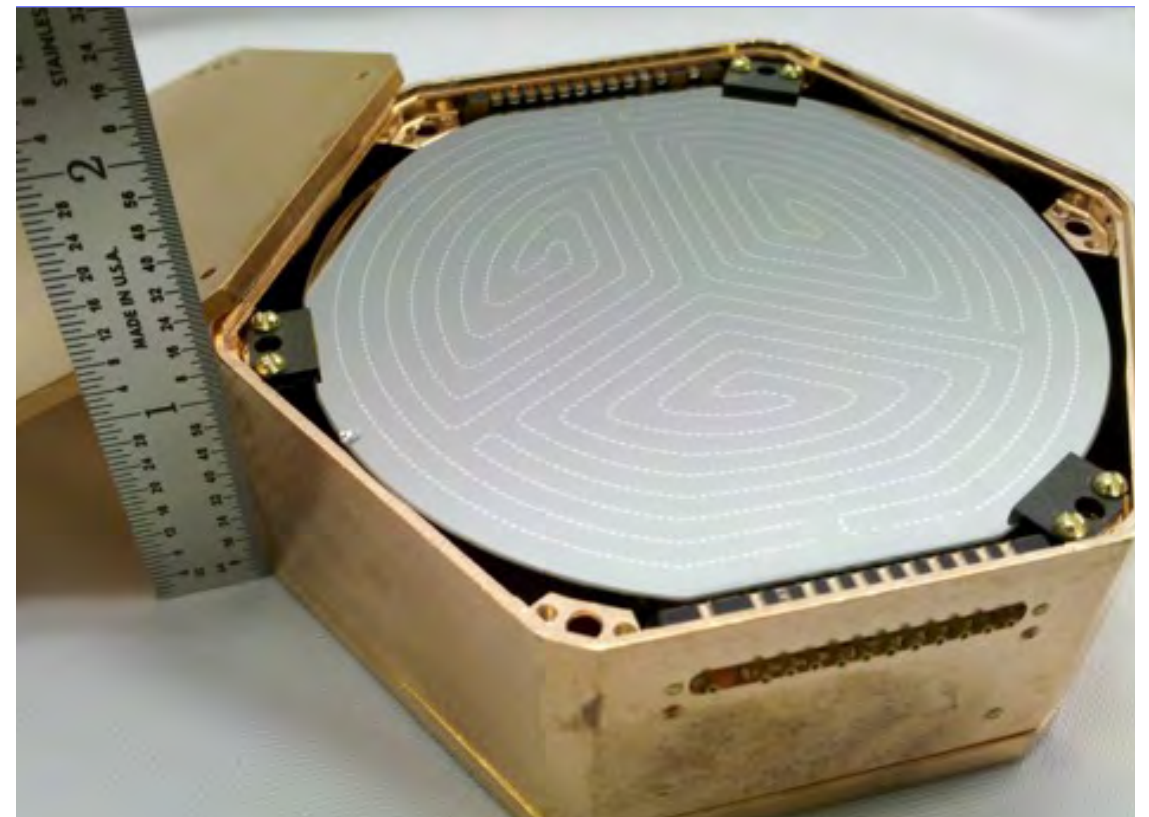
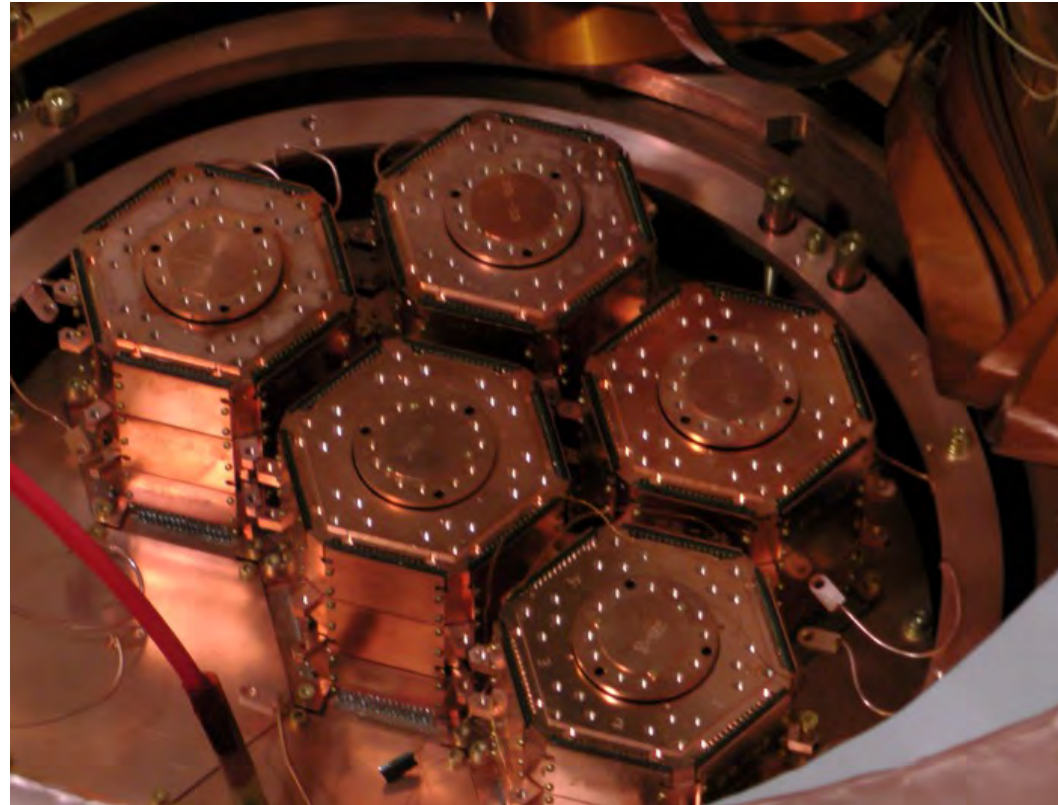
Example: the CDMS 90% Confidence Upper Limit



- **CDMS combined Soudan data:**
 - at a WIMP mass of 70 GeV, the limit on the spin-independent WIMP-nucleon cross section is: 3.8×10^{-44} cm² (90% C.L.)
- **Background estimate:**
- $0.8 \pm 0.1(\text{stat.}) \pm 0.2(\text{sys.})$ surface events
 - $0.04^{+0.04}_{-0.03}$ cosmogenic neutrons
 - $0.03 - 0.06$ radiogenic neutrons

Probability to observe 2 or more background events is 23%

The SuperCDMS experiment



Five super-towers had been installed at Soudan, each with 3 new, iZIP detectors, of 650 g

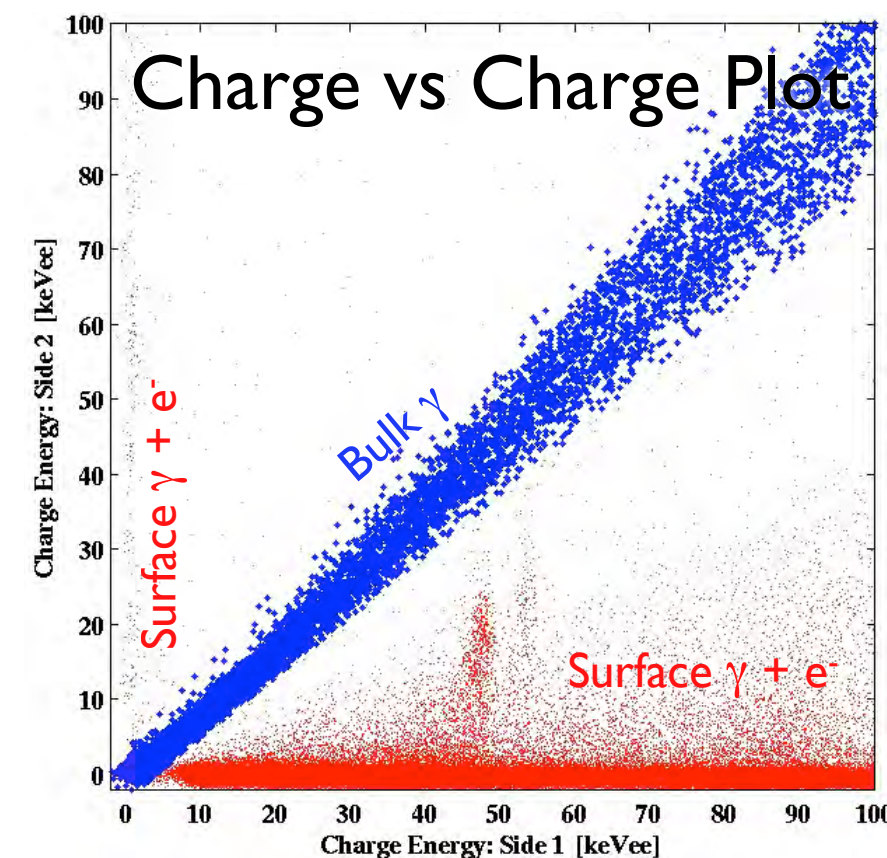
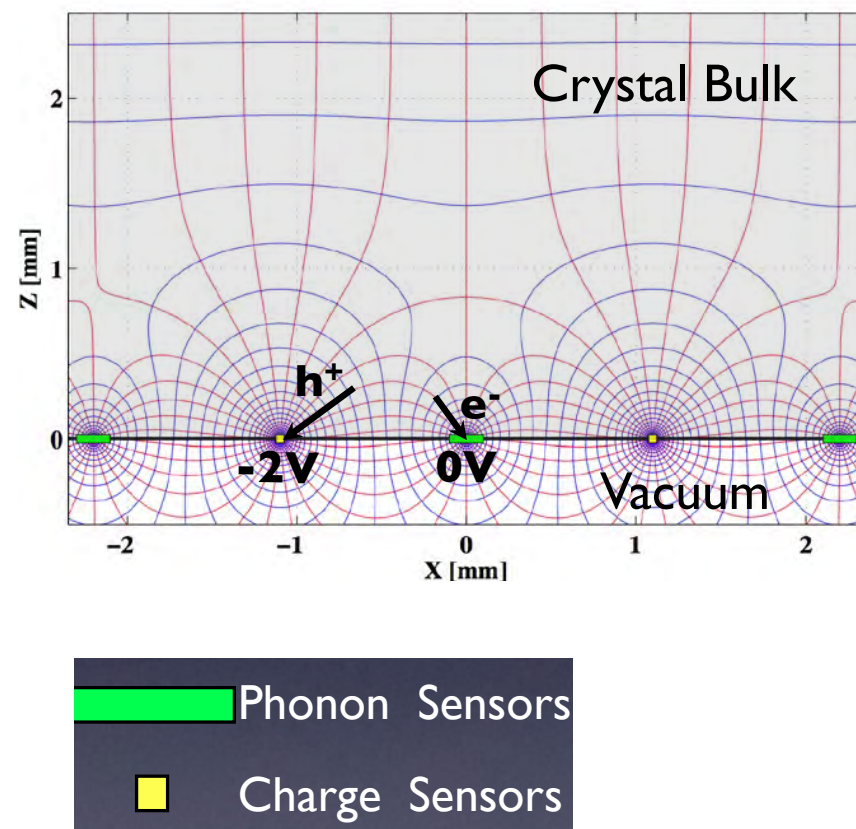
Total mass is 9 kg (\sim 6 kg fiducial mass)

The science run lasted for about 2 years

Sensitivity: between $5 - 8 \times 10^{-45} \text{ cm}^2$

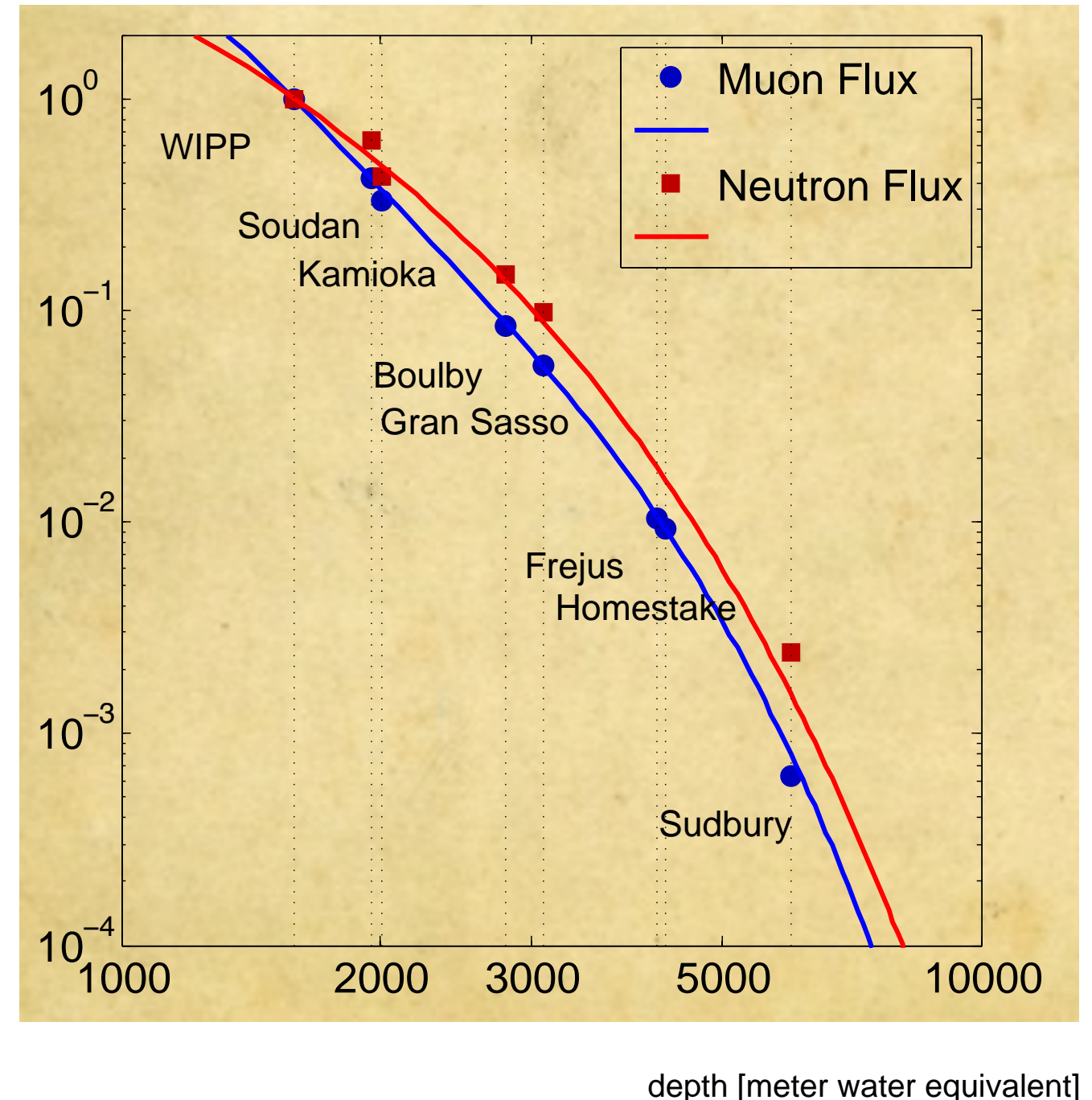
The SuperCDMS experiment: new detectors

- 3×10^{-5} surface event discrimination from charge signal alone
- additional discrimination power from phonon signal
- How?
 - when an event happens near the surface, the iZIP collects all the charge on one side only while bulk events (as expected also from WIMPs) create ionization signals on both sides



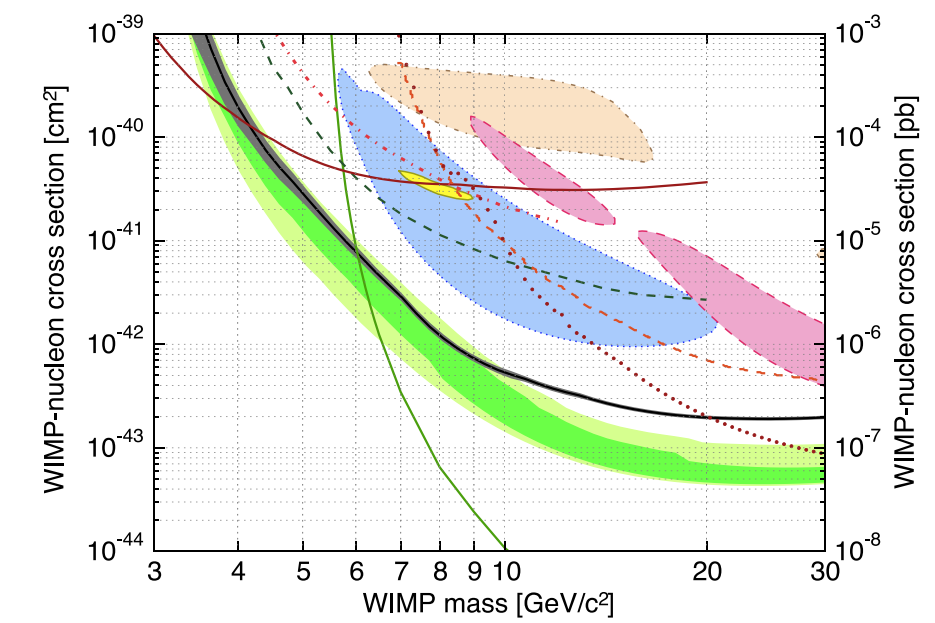
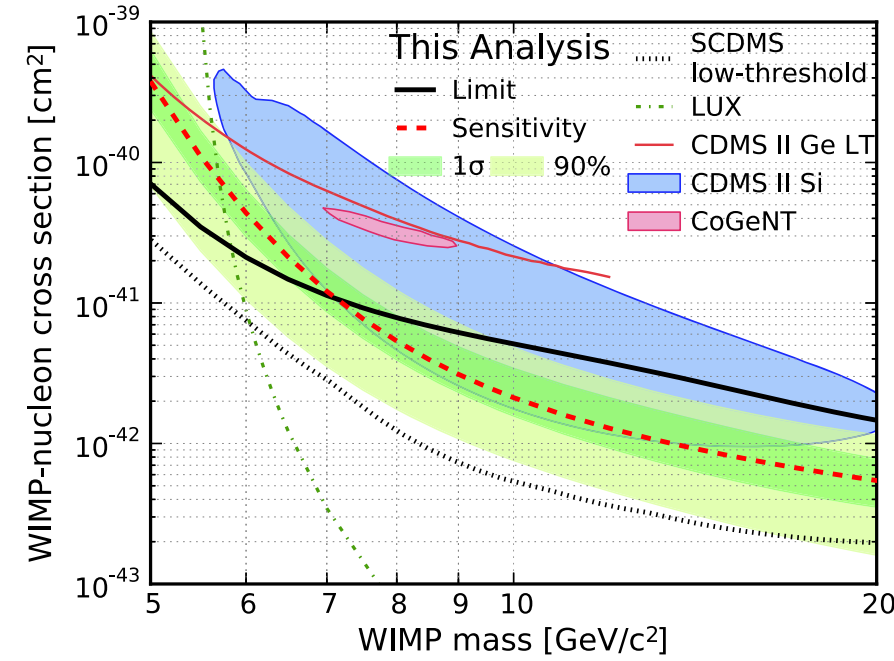
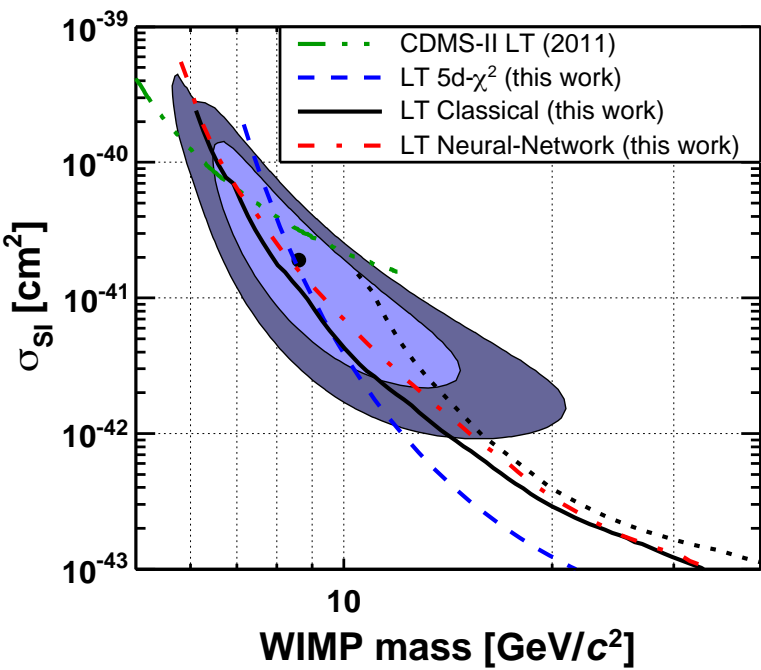
The SuperCDMS experiment: at SNOLAB

- SUF:
 - 17 mwe
 - 0.5 neutrons/(day kg)
 - 182.5 neutrons/(year kg)
- Soudan
 - 2090 mwe
 - 0.05 neutrons/(year kg)
- SNOLAB
 - 6060 mwe
 - 0.2 neutrons/(year ton)



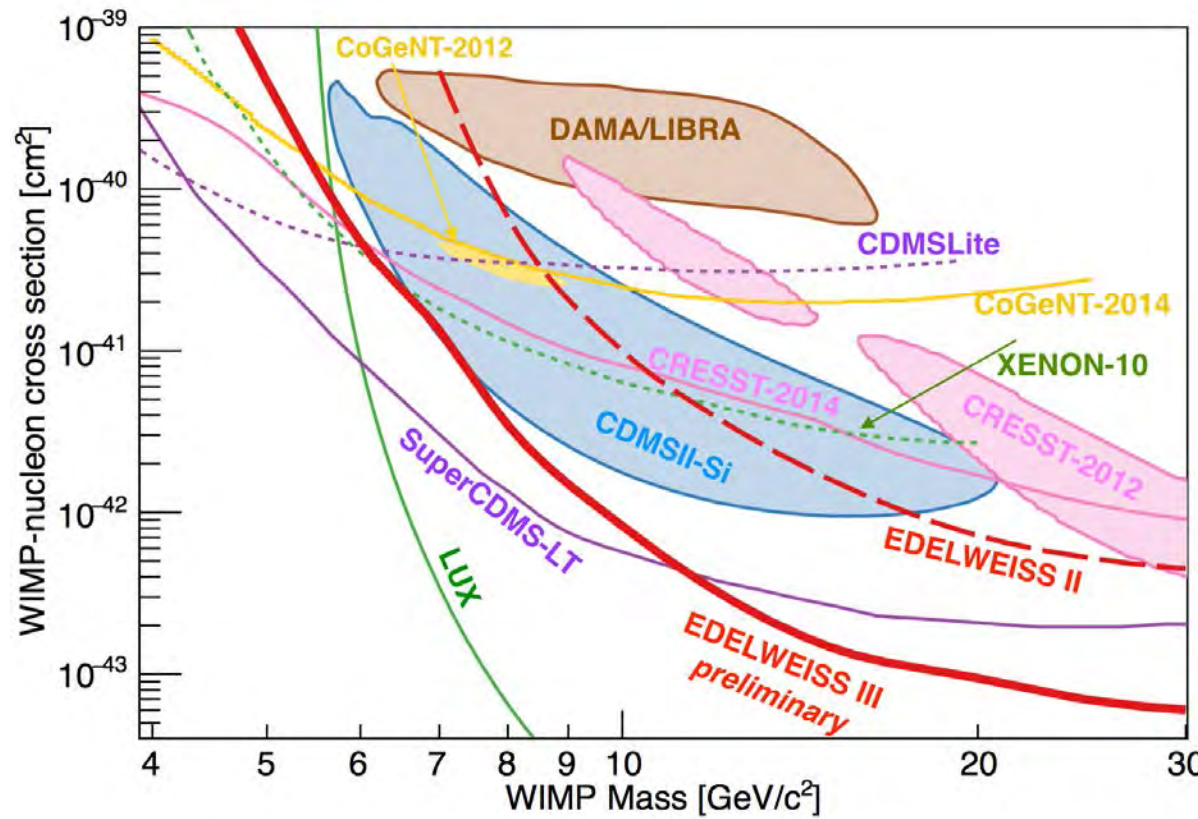
New CDMS results

- Meanwhile, a few new results from CDMS
- The current focus is on low mass WIMPs
- Energy threshold can be lowered at the cost of reduced background discrimination
- Several analyses of Ge and Si data from CDMS-II and first SuperCDMS run (at Soudan lab)

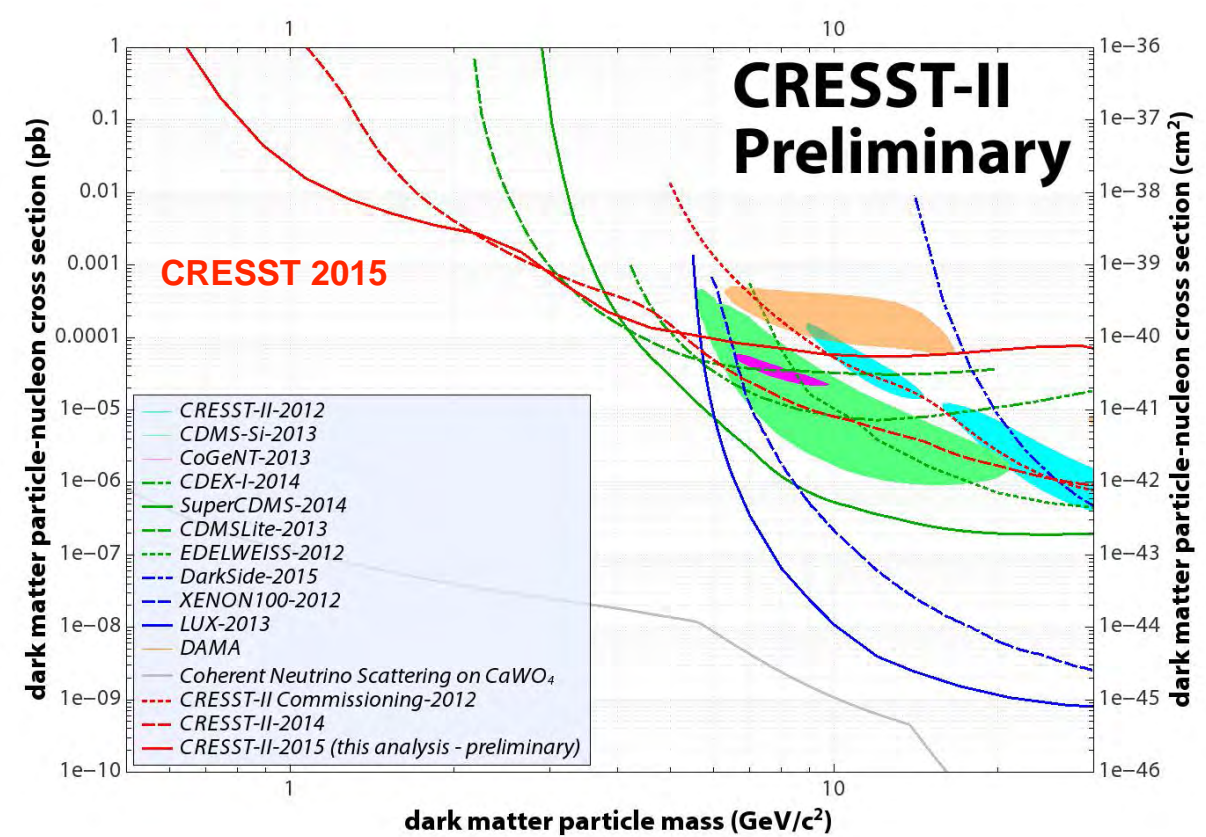


New EDELWEISS and CRESST Results

- Focus is also on low mass WIMPs



Edelweiss collaboration, arXiv: 1504.00820

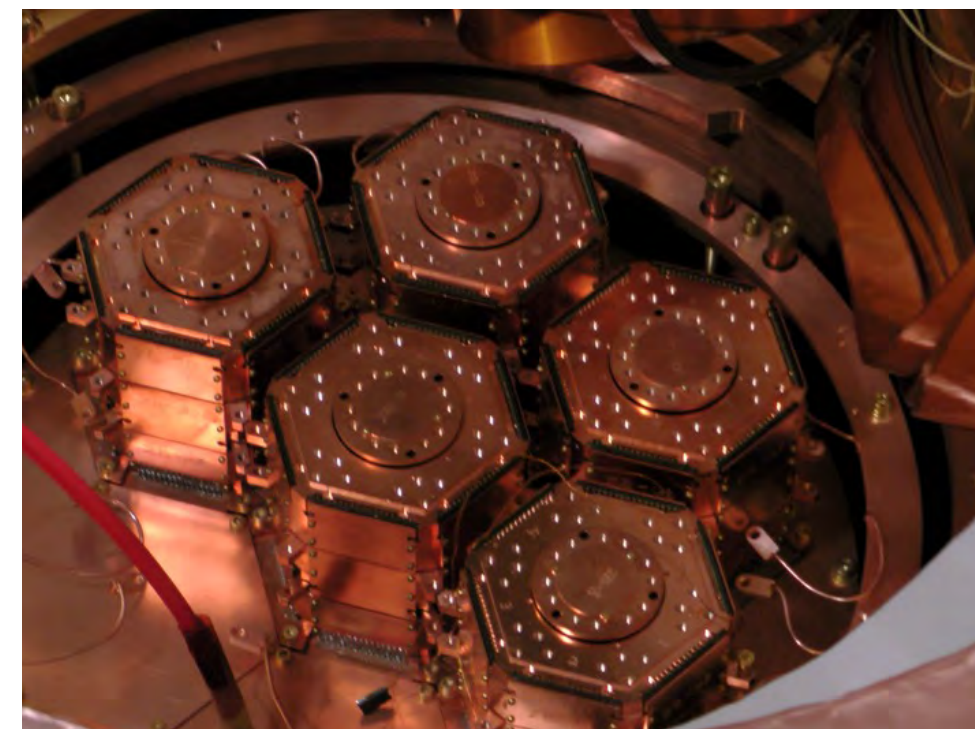
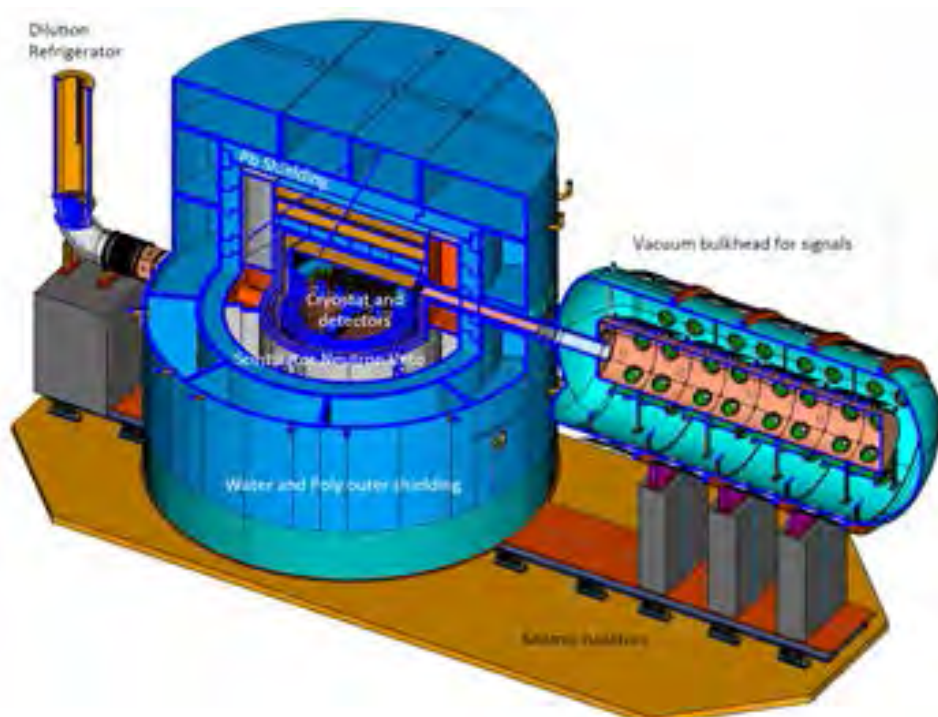


R. Strauss et al. JCAP 2015 06, 030 (2015)

Future: SuperCDMS/EURECA at SNOLAB

- Cooperation between **SuperCDM and EURECA** (CRESST+EDELWEISS) at SNOLAB
- SuperCDMS cryostat payload
 - initially 50 kg, up to 400 kg
- multi-target approach (Si, Ge, CaWO₃) to low-mass WIMP region

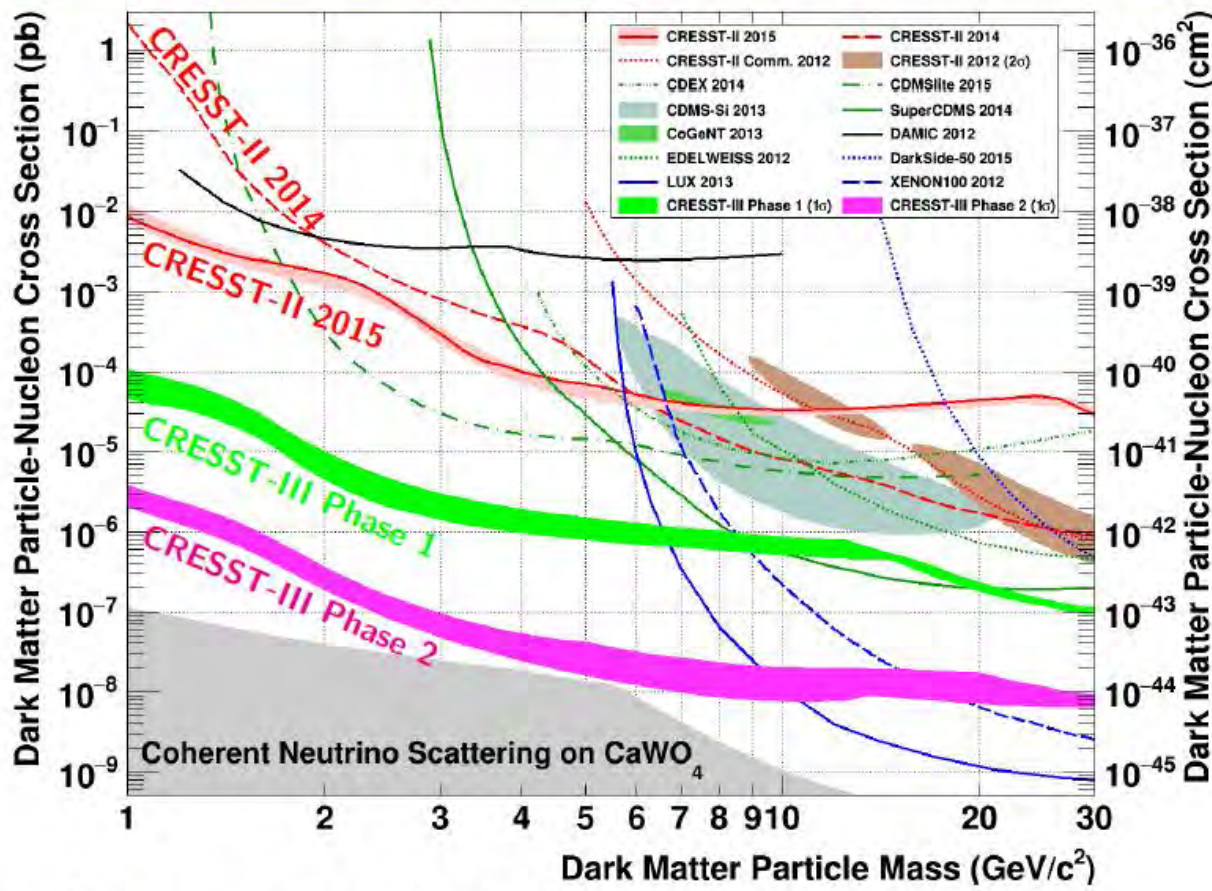
Start data taking in 2018



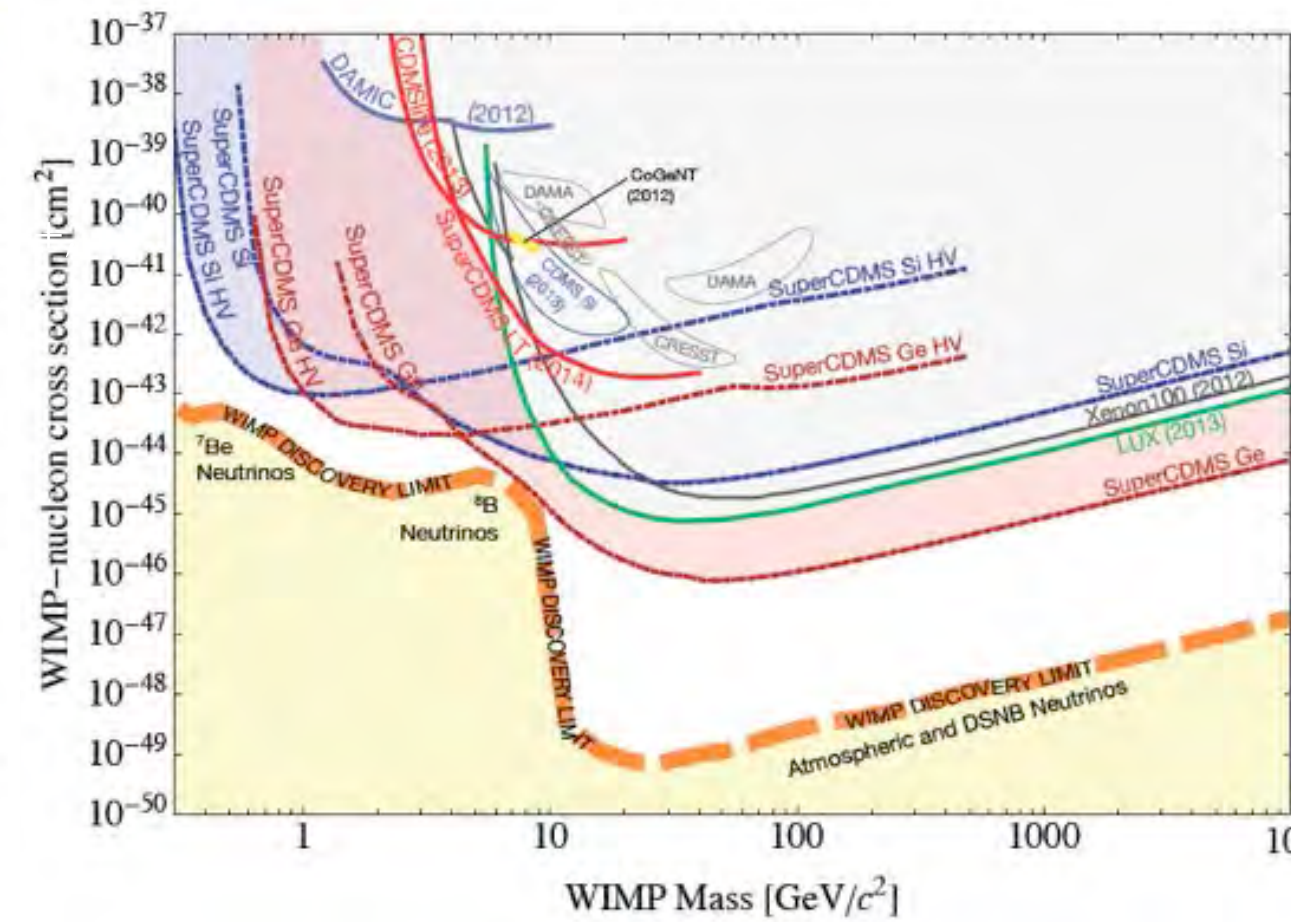
Cryogenic detectors at mK temperatures

- Goal: reach energy thresholds ≤ 100 eV
- Probe low-mass WIMP region (sub-GeV to few GeV)

CRESST-II and CRESST-III predictions



SuperCDMS and predictions



Conclusions

- Strong evidence for Cold Dark Matter in our Universe
- Cold Dark Matter: likely new, long-lived particles produced in the early Universe
- Neutral, massive and weakly interacting particles are independently predicted by physics beyond the standard model
- Dark matter particles of galactic origin can elastically scatter from nuclei in ultra-low background, low energy threshold terrestrial detectors
- The energy of the recoiling nucleus is transformed into a charge, light or phonon signal and could be detected with ultra-sensitive devices operated in underground laboratories
- A possible signal has to be consistent with a series of predicted ‘signatures’ in order to qualify as WIMP dark matter
- There were a few claims for a signal, not confirmed by other, independent experiments
- Existing experiments can probe WIMP-nucleon cross sections down to $\sim \text{few} \times 10^{-8}$ pb
- Experiments under construction and future, ton and multi-ton scale detectors should probe most of the theoretically interesting parameter space and reach the so-called “neutrino floor”

End
